Universidade de Lisboa

Faculdade de Farmácia

The links between membrane actin assembly by mycobacterial phagosomes and phagosome maturation, macrophage activation and pathogen killing

Maria Luísa Forte Marques Jordão

Doutoramento em Farmácia

(Biologia e Genética Molecular)

2007

Universidade de Lisboa

Faculdade de Farmácia

The links between membrane actin assembly by mycobacterial phagosomes and phagosome maturation, macrophage activation and pathogen killing

Maria Luísa Forte Marques Jordão

Doutoramento em Farmácia

(Biologia e Genética Molecular)

Tese orientada pela Professora Doutora Elsa Anes e co-orientada pelo Doutor Gareth Griffiths

2007

Dissertação de candidatura ao Grau de Doutor em Farmácia, apresentada à Faculdade de Farmácia, Universidade de Lisboa.

A presente dissertação foi realizada na Unidade de Retrovírus e Infecções Associadas da Faculdade de Farmácia de Lisboa (Portugal) e no Laboratório Europeu de Biologia Molecular (EMBL) em Heidelberg (Alemanha), sob a orientação da Professora Doutora Elsa Anes e co-orientação do Professor Doutor Gareth Griffiths.

O financiamento foi suportado pela Fundação para a Ciência e Tecnologia através das verbas atribuídas a dois projectos (FCT/FEDER POCTI/BCI/38983/2001 e POCI/BIA-BCM/55327/2004) e da bolsa de doutoramento com a referência SFRH / BD / 14284 / 2003.

Preface

The paradigm of mycobacteria infection is the fact that, in most cases, the host response is capable of controlling infection effectively: only a minority of infected individuals develops the active disease. Nevertheless tuberculosis remains one of the major infectious disease killers in the world.

Since the seminal studies of Armstrong and Hart, more than 30 years ago, is accepted in the field that pathogenic mycobacteria block phagosome maturation persisting in an immature phagosome. Although is not yet clear how this inhibition is achieved there is growing evidence that lipids and proteins secreted by the pathogens into the phagosomal membrane play a role. Phagosomes are complex organelles capable of a range of intricate functions after isolation even when they enclose an inert particle as a latex bead. Among its functions we can point acidification, nucleation of actin, binding to F-actin, binding and bi-directional motility along microtubules and fusion with early and late endosomes.

Taking advantage of the previous work done by Griffiths' group on latex bead phagosomes with the proposal of the actin track model for actin assembly and the knowledge of Anes group in the mycobacteria field a profitable collaboration started in the beginning of the present century. In the early years was possible to establish a relation between mycobacteria killing, phagosome maturation and actin assembly by the phagosome membrane. It was also shown that lipids are important modulators of the system. The present work is a follow up of these interesting results in which we try to contribute to the elucidation of the molecular mechanisms involved in mycobacteria killing and /or survival.

In the Introduction a general overview of the key aspects of mycobacteria/ macrophage interaction is given to the reader. The main goals of the work are also presented.

The second chapter presents a systematic study of J774 macrophages interaction with the non-pathogenic mycobacteria: *M. smegmatis*. This is an interesting model to identify the macrophage killer factors since *M. smegmatis* is cleared intracellularly within 48 h.

The third chapter is a follow up of the studies started with *M. smegmatis* now using different host macrophages and slow growing mycobacteria with different virulence profiles. The avirulent *M. bovis* BCG and the virulent *M. bovis* were used.
After the identification of some of the mechanisms involved in mycobacteria killing we modulate the system using lipids with different inflammatory properties. Since MAP kinase p38 plays an important role in pro-inflammatory response to bacterial infection its modulation by lipids was followed up in detail. A preliminary study of a lipid diet in animal models of intracellular pathogens infection was also conducted. All the results are presented in chapter 4.
In the final chapter the main conclusions are presented.

Part of the results obtained so far was presented in scientific meetings, published or submitted to publication.

A. Publications

1. Elsa Anes, Pascale Peyron, Leila Staali, Luisa Jordao, Maximiliano G. Gutierrez, Monica Hagedorn, Isabelle Maridonneau-Parini, Mhairi A. Skinner, Alan G. Wildeman, Stefanos A. Kalamidas, Mark Kuehnel and Gareth Griffiths, 2006, Dynamic life and death interactions between *Mycobacterium smegmatis* and macrophages, *Cell Microbiol.*, 8:939-960
2. Luisa Jordao, Gareth Griffiths and Elsa Anes, 2006, Understanding Host-pathogen interactions during macrophage infection with *Mycobacterium bovis*. *Int J Infect Dis* 10(S1):S313(66018)
3. Luisa Jordao, Christopher K. E. Bleck, Luis Mayorga, Gareth Griffiths and Elsa Anes, On the killing of mycobacteria by macrophages, *Accepted for publication in Cell Microbiol.*.
4. Luisa Jordao, Carlos Guzman, Pablo D. Becker, Andreas Lengeling, Yann Bordat, Frederic Boudou, Brigitte Gicquel, Olivier Neyrolles, Gareth Griffiths and Elsa Anes, Lipid regulation of inflammatory states during macrophage infection with *Mycobacterium*, *Submitted*.
5. Maximiliano Gabriel Gutierrez, Bibhuti B. Mishra, Luisa Jordao, Edith Elliot, Elsa Anes and Gareth Griffiths, NF-κB activation is required for the late endosome/lysosome fusion mediated-killing of *M. smegmatis* by macrophages, *In preparation*.

B. Communications in scientific meetings

1. Luisa Jordao, Pascale Peyron, Leila Staali, Maximiliano Gutierrez, Monica Hagedon, Mark Kuehnel, Gareth Griffiths and Elsa Anes. 2004. A role for p38 MAP kinase in the dynamic life and death interactions of *Mycobacterium smegmatis* in macrophages. Euresco conference Frontiers of Cellular Microbiology and Cell Biology: Spacial and temporal dynamics of the endomembrane system, San Féliu de Guixols, 2004. (Poster and Invited Conference by Gareth Griffiths).

2. Gareth Griffiths, Mark Kuehnel, Pascale Peyron, Leila Staali, Maximiliano Gutierrez, Luisa Jordao and Elsa Anes. Phagosome Biology : from a Latex Bead model to mycobacteria. EMBO/ Novartis Foundation Workshop on Innate Immunity in the Lung, Cape Town, South Africa, 2005. (Plenary Conference by Gareth Griffiths)

3. Luisa Jordao, Gareth Griffiths and Elsa Anes. Cell Biology of Mycobacterium bovis interaction with macrophages. Sixth International Conference on the Pathogenesis of Mycobacterial Infections, Saltsjobaden, Sweeden, 2005 (Poster)

4. Luisa Jordao, Gareth Griffiths and Elsa Anes. Cell Biology of *Mycobacterium bovis* interaction with macrophages. Workshop Cryo Methods in Analytical and Immuno-Electron Microscopy. Sociedade Portuguesa de Microscopia Electronica e Biologia Celular, Lisbon, Portugal, 2005 (Oral communication)

5. Luisa Jordao, Gareth Griffiths, and Elsa Anes. Cell Biology of *Mycobacterium bovis* interaction with macrophages The EMBO Practical Course on Electron Microscopy and Stereology in Cell Biology. Ceske Budejovice, Czech Republic, 2005 (Oral communication)

6. Luísa Jordão, Gareth Griffiths, and Elsa Anes. Cell Biology of *Mycobacterium bovis* interaction with macrophages. EMBO/ University of Cape Town Practical Course Functional Microscopy of host pathogen interactions. Cape Town, South Africa, 2005 (Oral communication)

7. Elsa Anes, Mark Kuehnel, Luisa Jordao, Pascale Peyron, Leila Staali, Maximiliano Gutierrez, Mónica Hagedorn and Gareth Griffiths. Lipids and P38 MAP kinase signalling for actin assembly on phagosomal membranes: implications on phagosome maturation and mycobacterial killing in macrophages. "Tuberculosis: Integrating Host and Pathogen Biology" Keystone Symposia, Whistler, British Columbia, 2005 (Poster)

8. Luisa Jordao, Gareth Griffiths and Elsa Anes. *Mycobacterium bovis* interaction with macrophages. 2nd Workshop on host-pathogen interactions and cell signalling. Faculty of Pharmacy, University of Lisbon, Portugal, 2006 (Oral communication)

9. Luisa Jordao, Pascale Peyron, Leila Staali, Maximilliano Gutierrez, Mark Kuehnel, Gareth Griffiths and Elsa Anes, A role for p38 MAP kinase in the dynamic life and death interactions of Mycobacterium smegmatis in J774 macrophages. FEBS 15th Protein Kinase Meeting- Spatial and Temporal Regulation of Signalling. Oslo, Norway, 2006 (Poster)

10. Luisa Jordao, Gareth Griffiths and Elsa Anes, 2006, Understanding Host-pathogen interactions during macrophage infection with *Mycobacterium bovis*. 12th International Congress on Infectious Diseases, Lisbon, Portugal, 2006 (Poster)

11. Luisa Jordao, Gareth Griffiths and Elsa Anes, Dietary lipids and host response to tuberculosis. "Tuberculosis: From Lab Research to Field Trials" Keystone Symposia, Vancouver, British Columbia, 2007 (Poster)

12. Luisa Jordao, Gareth Griffiths and Elsa Anes. Role of sphingolipids in MAP kinase signalling during *Mycobacterium spp* infections. Lipid signalling pathways: from cell biology to novel drug targets, FEBS Advanced Course, Ortona, Itália, 2007 (Poster and selected oral communication)

Acknowledgments

I would like to thank Elsa Anes and Gareth Griffiths for having supervised my research in the last years. I'm also grateful to URIA-CPM (Faculty of Pharmacy, University of Lisbon) and EMBL (Heidelberg) for the use of their facilities to develop the work presented in this thesis.

I would like to acknowledge Prof Aida Duarte and her group for the open access to her laboratory equipment in FFUL; Prof Cecilia Rodrigues and her group for technical support and use of their facility in FFUL; Prof Isabel Portugal for molecular characterization of *Mycobacterium* strains; Drª Rosário Cidadão for providing access to and help in collecting blood from bovine cattle; Prof Carmo Fonseca for the use of the confocal facility at IMM and her team for technical advise and support; Prof António Pedro for the use of the electron microscopy facility at Hospital Curry Cabral and the laboratory at the Faculty of Dental Medicine as well as the technical support provided by Mena; everybody in the FFUL that contributed with blood samples and reagents for this work. I'm also grateful to everyone mentioned in the acknowledgment sections of the different chapters of this thesis. Finally I thank the people that formerly shared the laboratory with me (Zita and Ana), my colleagues from the neighbouring laboratories specially Alexandra Silva, Ana Rodolfo and Filipa Grosso, my present laboratory colleague Marta Simões and all the people working in URIA-CPM and the Animal and Vegetal Biology sub-group for their support.

I'm also grateful to the members of Griffiths' group, ALMF and EM facility for technical support during my stay in EMBL. I would like to particularly acknowledge Birgit, Daniela, Leila, Sabrina, Sonja and Uta not only for their technical advices but also for their friendship that help me to overcome a lot of difficult situations. To Leila and Sabrina I would also like to thank for their availability to analyse my data and for sharing with me their comments and ideas.

I also thank all the people that showed interest for the data I presented in several meetings and contribute for the present work with their comments and suggestions.

I thank my parents, my brother and my friends specially Sandra Lopes and Cláudia Valente for all the support. I'm sure that without the support of all these people I would have never finished this work.

Finally I thank FCT for the financial support.

Resumo

A infecção pelo *Mycobacterium tuberculosis* e por outra micobactérias pertencentes ao complexo *Mycobacterium tuberculosis* (MTC) é eficazmente controlada pelo sistema imunitário do hospedeiro em 90% dos casos. Contudo, embora os mediadores do sistema imunitário envolvidos neste processo estejam devidamente identificados e se saiba que o γ-IFN desempenha um papel central é dificíl prever o desfecho de uma infecção por micobactérias. Por esta razão é premente estudar a interacção micobactéria-hospedeiro ao nível molecular de forma a identificar potenciais alvos terapêuticos para o controlo da tuberculose.

As micobactérias são microrganismos intracelulares facultativos que sobrevivem nos macrófagos alveolares ao nível dos fagossomas. Os macrófagos são células fagocíticas profissionais com capacidade para eliminar invasores através da resposta imune inata. Esta inclui mecanismos como a produção de espécies radicalares de oxigénio e azoto, a maturação do fagossoma em fagolisossoma, produção de quimiocinas e a apresentação de antigénios micobacterianos ao sistema imunitário que resulta no desenvolvimento de uma imunidade adaptativa. As micobactérias patogénicas não só forçam a sua entrada nos macrófagos como são capazes de persistir intracelularmente resistindo aos vários mecanismos bactericidas dos macrófagos. A inibição da maturação do fagossoma em fagolisossoma pelas micobactérias patogénicas é apontada, à mais de três décadas, como a principal razão para o sucesso destes patogenes.

Uma vez que a capacidade de subverter os mecanismos bactericidas dos macrófagos é característica das micobactérias patogénicas iniciamos este estudo com um parente distante do *M. tuberculosis*, o *M. smegmatis*. Nesta parte do trabalho pretendemos identificar os mecanismos bactericidas do macrófago activados por uma micobactéria não patogénica no decorrer da infecção que resultam na eliminação da mesma. Utilizando macrófagos de ratinho (J774 e BMM) verificamos que o *M. smegmatis* apresenta um perfil de sobrevivência intermédio entre o de uma micobactérias de crescimento lento como o *M. tuberculosis* e o apresentado por bactérias de crescimento rápido como a *E. coli* ou o *Streptococcus*. Estas últimas são eliminadas pelos macrófagos em 4 h, enquanto que o *M. smegmatis* sobrevive intracelularmente até 48 h apresentando mesmo ciclos de multiplicação intracelular.

Para verificar se este perfil de sobrevivência se deve apenas à micobactéria ou se o hospedeiro também desempenha um papel importante no desfecho da infecção usámos macrófagos de vários hospedeiros . Em macrófagos de ratinho Raw e em macrófagos isolados do sangue periférico de voluntários saudáveis (HMDM) verificamos que o *M. smegmatis* era eliminado de uma forma contínua ao longo de 48 h.

Assim, tomando partido da capacidade de replicação de *M. smegmatis* em J774 e das vantagens técnicas proporcionadas por uma linha celular de rato iniciámos uma abordagem sitemática dos mecanismos envolvidos na eliminação desta micobactéria não patogénica de crescimento rápido pelos macrófagos ao longo de 24 h.

O sistema estudado revelou-se extremamente dinâmico envolvendo um período inicial de morte (1-4 h), seguido de um período de replicação (4-8 h) e dois períodos de morte (8-12 h e 12-24 h). A síntese de óxido nítrico (NO) constitui o primeiro mecanismo de defesa dos macrófagos mas a sua acção está circunscrita à primeira fase de morte. A organização de uma rede de actina e a fusão com organelos endocíticos tardios coincidem com a primeira e última fase de morte. A reciclagem de marcadores de fase fluida e membranar do fagossoma coincidem com a fase de replicação micobacteriana (4-8 h). A acidificação e a aquisição de sub-unidades da bomba protónica (V-ATPase) pelo fagossoma apresentam um perfil diferente e coincidente com as fases tardias de morte. Além do mais, a colocalização da V-ATPase não é coincidente com a dos marcadores característicos de endossomas tardios e lisosomas. A MAP cinase p38 é crucial para a regulação de todos os processos investigados, excepto a produção de NO, funcionando alternadamente a favor do hospedeiro ou do patogene. Um modelo matemático suporta a hipótese de que períodos alternados de actividade bactericida da célula são mais eficazes para a elimição total de parasitas intracelulares do que uma actividade contínua.

Umas vez definidos os perfis de sobrevivência/ morte intracelular de uma micobactéria não patogénica de crescimento rápido resolvemos estender a mesma abordagem a micobactérias de crescimento lento avirulentas (*Mycobacterium bovis* BCG) ou virulentas (*M. bovis*). Neste estudo foram utilizados macrófagos de ratinho (J774, Raw e BMM) e de dois hospedeiros naturais de *M. bovis*. Os macrófagos humanos utilizados foram isolados a partir do sangue periférico ou da linha celular THP-1. Os macrófagos de bovino foram isolados a partir do sangue periférico de animais saudáveis (BMDM). O estudo dos perfis de sobrevivência demonstrou que o BCG é eliminado de uma forma

contínua em todos os macrófagos excepto nos HMDM onde após um ciclo de replicação atinge um estádio estacionário ao fim de 3 dias de infecção. Os perfis de sobrevivência observados para o *M. bovis* são distintos dos do BCG. A micobactéria virulenta permanece num estado de latência ou consegue replicar-se activamente em todos os macrófagos estudados. Em nenhum dos casos se observou a eliminação desta micobactéria pelos macrófagos.

Os macrófagos de ratinho J774 e os HMDM foram escolhidos para a realização de estudos mais detalhados. A nossa escolha recaiu nestas células porque apresentam perfis de sobrevivência distintos para as duas micobactérias utilizadas. O facto de serem de hospedeiros distintos (rato e Homem) permitiu avaliar a importância do hospedeiro no desfecho da infecção.

A produção de NO pelos macrófagos de ratinho desempenha um papel importante no controlo das infecções por estas micobactérias. À semelhança do anteriormente observado com *M. smegmatis*, a acção do NO e dos radicais reactivos de azoto (RNI) está limitada aos estádios precoces da infecção (3h-3dias) embora seja possível detectar a produção de NO até ao sétimo dia de infecção. Em nenhum momento da infecção foi possível detectar uma associação entre a membrana do fagossoma micobacteriano e a sintetase inductível do óxido nítrico (iNOS).

Nas células humanas não foi possível detectar a produção de NO ao longo da infecção o que pode, pelo menos parcialmente, explicar a diferença observada nos perfis de sobrevivência.

As micobactérias patogénicas são conhecidas por bloquearem a fusão do fagossoma com o lisossoma evitando desta forma a exposição a alguns dos agentes bactericidas mais potentes do macrófago. Por esta razão, a acidificação do fagossoma contendo *M.bovis spp* e a sua fusão com vesículas endocíticas tardias e/ou lisossomas foi seguida ao longo de 7 dias. Os resultados obtidos demonstram que as duas micobactérias são capazes de interferir com a maturação do fagossoma. O fagossoma micobacteriano não adquire marcadores de maturação de fase tardia como a V-ATPase ou o ácido liso-bis-fosfatídico (LBPA), não acidifica o suficiente para acumular o corante acidotrópico lysotracker ou fundir com endossomas tardios e/ou lisossomas. Contudo, o mais surpreendente nestes resultados é o facto de duas micobactérias com perfis de sobrevivência distintos apresentarem perfis de aquisição de marcadores de maturação semelhantes. Embora, não nos seja possível apresentar evidências experimentais directas uma diferente sensibilidade das duas estirpes de micobactérias à acção de

efectores como os RNI e o hidrogenião podem explicar estes resultados. *In vitro* a estirpe virulenta de *M. bovis* revelou ser mais resistente à acção do pH ácido e do NO do que o BCG. A realização de estudos em culturas de macrófagos com inibidores da bomba protónica e da iNOS confirmaram os resultados obtidos *in vitro*.

A última parte do trabalho consistiu na modulação da resposta inflamatória dos macrófagos e no estudo do seu impacto nas infeções por micobactérias. A modulação do sistema foi efectuada através da adição de lípidos. A nossa escolha recaiu sobre estas substâncias porque (i) existem estudos epidemiológicos que suportam a associação entre uma dieta rica em lípidos omega-3 e uma elevada incidência de tuberculose, (ii) estudos anteriores em culturas celulares infectadas com o bacilo da tuberculose demonstraram que o tratamento com estes lípidos provocam efeitos semelhantes, (iii) os lípidos são importantes para a regulação da nucleação da actina e consequentemente para a maturação do fagossoma em fagolisossoma.
O tratamento das culturas de macrófagos com ácido eicosopentaenoico (EPA), ácido araquidónico (AA) e ceramida (Cer) produziram efeitos distintos. O lípido omega-3 (EPA) estimula a sobrevivência do bacilo da tuberculose enquanto que o omega-6 (AA) e a ceramida exercem o efeito contrário. A ceramida foi incluída neste estudo por estar intimamente ligada com as vias biosintéticas do AA.
A MAP cinase p38 é importante na sinalização pró-inflamatária durante as infecções bacterianas. Neste contexto resolvemos estudar o efeito dos diferentes lípidos na actividade desta cinase. Uma vez mais o EPA apresentou efeitos distintos do AA e da ceramida. O primeiro lípido não estimula a activação da p38 ao contrário do AA e da ceramida. A infecção das culturas de macrófagos com o bacilo da tuberculose altera radicalmente a sinalização para a p38. O bacilo é capaz de bloquear a activação desta cinase nos estádios precoces da infecção. A sinalização para a p38 é modificada pelo tratamento com os lípidos e condiciona a sobrevivência do *M.smegmatis* nesta linha celular.

O conjunto dos nossos resultados demonstra que no decorrer das infecções por micobactéria o hospedeiro utiliza de uma forma faseada os vários mecanismos de defesa de que dispõe. Numa fase inicial a produção de NO e de RNIs desempenha um papel primordial. A fusão do fagosoma micobacteriano com o fagolisossoma constitui um importante mecanismo de defesa do hospedeiro, contudo a eliminação da

micobactéria pode ocorrer num fagosoma imaturo. A eliminação das micobactérias no compartimento precoce é mais lenta. Finalmente, a modulação do sistema com lípidos afecta dramaticamente o desfecho da infecção, contudo, devido à complexidade dos mecanismos activados é difícil extrapolar os resultados obtidos em linhas celulares para animais de experiência e para o Homem.

Palavras chave: *Mycobacterium spp*, macrófago, interacção patogéne-hospedeiro, lípidos, mecanismos bactericidas

Abstract

Non pathogenic mycobacteria are cleared from macrophages within 24 - 48 h while pathogenic mycobacteria can persist in the same cells for long periods of time. Using the non-pathogenic fast growing *Mycobacterium smegmatis* and two slow growing mycobacteria with distinct virulence (*M. bovis BCG* Pasteur and *M. bovis*) we start a systematic study to elucidate the role of different killing mechanisms during mycobacteria infection. Although all mycobacteria reside in phagosomes the acquisition of maturation markers were distinct for *M. smegmatis* and *M. bovis spp*. Thus different mycobacteria live and are killed in distinct compartments. Nevertheless, macrophage control of mycobacteria infections seems to follow a well established program where different killing mechanisms play a role at different times of infection. NO production is the first killing mechanism involved then phagossome maturation resulting in acidification of phagosome content and acquisition of lysosomal enzymes are also involved. Since inhibition of phagosome maturation plays a central role in mycobacteria pathogenesis we try to identify key regulators of this process. Previous studies shown that actin nucleation plays an important role in this process. In the present study we provide evidence that MAP kinase p38, a central player in the pro-inflamatory response to bacteria infection, regulates actin assembly by non-pathogenic mycobacteria containing phagosomes at early stages of infection. This kinase is a key regulator of all killing mechanisms except NO production.

In the last part of the work we studied the modulation of the host defense mechanism by lipid treatment. This approach is supported by (i) the well established link between particular diets and tuberculosis incidence and (ii) recent results by Anes group showing that omega-3 and omega-6 lipids had opposite effects in *M. tuberculosis* survival in macrophages mediated probably by their ability to regulate actin nucleation and phagosome maturation. At the macrophage level, in general, the effects of Cer and/or AA were opposite to those of EPA, but in many infection stages these pro- and anti-inflammatory lipids were capable of reversing the signalling states between killing and survival. The effects of Cer and EPA were in part regulated by p38 MAP Kinase. These results argue against the idea of considering a simple recommended lipid-based diet against mycobacteria.

Keywords: *Mycobacterium* spp, macrophages, pathogen-host interaction, lipids

Abbreviations

AA	Arachidonic acid
AhpC	Alkyl hydroperoxide redutase subunit C
AIDS	Acquired immune deficiency syndrome
ARP	Actin related proteins
BCG	Calmette-Guérin bacillus
BMDM	Bovine monocyte derived macrophages
BMM	Bone marrow macrophages
BSA	Bovine serum albumin
CDV	Cardiovascular
CEMOVIS	Cryo electron microscopy of vitrified sections
Cer	Ceramide
CFU	Colony forming unit
COPASI	Complex pathway simulator
COX	Ciclooxygenase
EEA1	Early endosome antigen 1
EM	Electron microscopy
EPA	Eicosapentaenoic acid
ERM	Ezrin, radixin, moesin
ERK	Extracellular signal-reculated kinases
HIV	Human immunodeficiency virus
HMDM	Human monocyte derived macrophages
IFN	Interferon
IL	Interleukin
iNOS	Inducible nitric oxide synthase
JAK/STAT	Janus kinase/ signal transducer and activator of transcription
JNK	c-Jun-N-terminal kinase
LAM	Lipoarabinomannan
LAMP-1	Lysosomal associated membrane protein 1
LBPA	Lysobisphosphatidic acid
LB	Latex bead
LBP	Latex beads phagosomes
LDL	Low density lipoproteins
L-NAME	N-(G)-nitro-L-arginine methyl ester hydrochloride
5-LOX	5-Lipoxygenase

LPS	Lipopolisaccharides
LT	Leukotrienes
LYAAT	Lysosomal amino acid transporter
MAP	Mitogen activated protein
MOI	Multiplicity of infection
NF-κB	Nuclear factor κB
NFP	Nucleation-promoting factor
NO	Nitric oxide
OD	Optical density
PA	Phosphatidate
PBS	Phosphate buffer saline
PC	Phosphatidylcholine
PG	Prostaglandins
PI	Post-infection
PIP_2	Phospatidylinositol biphosphate
PIP-3P	Phosphatidylinositol 3-phosphate
PPAR	Peroxisome proliferator activactor receptor
PPR	Pattern recognition receptor
PUFAs	Polyunsaturated fatty acids
RNI	Reactive nitrogen intermediates
Sph	Sphingosine
S1P	Shingosine-1-phosphate
ROI	Reactive oxygen intermediates
TB	Tuberculosis
TfRs	Transferrin receptors
TLR	Toll like receptor
WASP	Wiskott –Aldrich syndrome protein
WAVE	WASP family verpolin homologus protein
XDR	Extensively drug resistant

Figures Index

Tables Index

Table of contents

Chapter 1

Introduction

TUBERCULOSIS: THE NEW OLD DISEASE

Tuberculosis (TB) is one of the oldest infectious diseases affecting the human kind. Bone TB was identified in skeletons, from Europe and Middle East, as the cause of death showing that 4000 years ago this disease was a widespread health problem. In recorded history, Hippocrates writes of patients with consumption (the old definition of TB), i e, wasting away associated with chest pain and coughing, frequently with blood in sputum. The frequency of descriptions of patients with these symptoms indicated that the disease was already well entrenched.

The explosion of European population and the growth of large urban centres made this continent the epicentre of many TB epidemics during the 16th and 17th centuries. Although, during the first half of the 19th century the incidence of TB peaked causing death to approximately one quarter of European population, in the second half of this century TB mortality decreased due to improving sanitation and housing. The 20th century brought a steadily drop of morbidity and mortality due to TB, in developed world, due to better public health practices, massive vaccination with Calmette-Guérin bacillus (BCG) vaccine and the advent of antibiotics. This downward trend ended in the mid-1980s triggered by emergence of acquired immunodeficiency syndrome (AIDS) and an increase in homeless and poverty in the developed word. This fact pointed the important role played by the immune system in this disease and also the importance of socio-economical factors. More recently the identification of multi-drug resistant (MDR) and extensively drug resistant (XDR) strains of mycobacteria turned this disease even more frightening [1,2].

Actually more than one-third of the world's population is infected with *Mycobacterium tuberculosis* (*M. tuberculosis*). One in every ten of these individuals will develop TB at some point in their lifetime and around 2 million people die of this disease every year [3]. New drugs, better vaccines and new diagnostic methods are desperately needed to change and revert this situation. Despite the big effort made in order to develop new tools to fight this plague the successful candidate has not been found. In the present work we favour the hypothesis of boosting the host natural defence mechanisms to contribute to solve the problem. The first step towards this goal will be a better understanding of the host-pathogen relationship.

THE CAUSAL AGENT

The *Mycobacterium tuberculosis* complex includes strains from five species- *M. tuberculosis*, *M. canettii*, *M. africanum*, *M. microti* and *M. bovis* and two subspecies – *M. caprae* and *M. pinnipedii* [4]. These mycobacteria are characterized by 99,9% similarity at nucleotide level and virtually identical 16S rRNA sequences [5-8] but differ widely in terms of host tropisms, phenotypes and pathogenicity [4,9,10].

The most notable member of the complex is *Mycobacterium tuberculosis* the causative agent of human tuberculosis which has an exclusive tropism for this host. In contrast, *M. bovis*, the etiologic agent of bovine tuberculosis, cause only 5 -10% of human tuberculosis cases and has a wide host spectrum. The impact of *M. bovis* in human health declined sharply after the advent of pasteurization but there are records of new cases among immunocompromised individuals and re-activation in elderly individuals.

Although in some countries eradication of bovine tuberculosis was possible due to programs based on a test and slaughter strategy it still constitutes an economic burden in developed countries as New Zealand and England [11,12]. The persistence of *M. bovis* among wildlife that can serve as a reservoir for domestic animals is the aim of the problem. The disease in wild and domestic animals presents a wide spectrum of manifestations that mimic the progression of tuberculosis in humans. These animals when experimentally infected can serve as useful models of human disease since they are outbred, natural host of disease, allow experimental challenge in vaccine trials and is possible to monitor the immune response through the progression of the disease[13,14]. The major limitation of the model is the use of *M. bovis* instead of *M. tuberculosis* and the relative high cost.

THE PATHOGENESIS OF TUBERCULOSIS

The infectious bacilli are inhaled as droplets from the atmosphere. In the lung, the bacteria are phagocytosed by the alveolar macrophages. The interaction of mycobacteria components with macrophage receptors as the Toll-like receptors (TLR) results in chemokines and cytokines production [15] that serve as signals of infection. The bacteria enter the parenchyma and replicate within the alveolar or lung resident macrophages.

The signals induced results in migration of monocyte derived macrophages and dendritic cells from the blood stream to the site of infection in the lung. The dendritic cells that engulf bacteria mature and migrate to the lymph nodes [16-18]. Once there, CD4 and CD8 T cells are primed against mycobacterial antigens. Primed T cells expand and migrate back to the focus of infection in the lungs, probably in response to mediators produced by infected cells. This phenomenon of cell migration towards the infection focus culminates in formation of a granuloma the wall mark of tuberculosis. The granuloma is formed by T cells, macrophages, B cells, dendritic cells, endothelial and epithelial cells among others in a proportion that varies with the age of the structure. The granuloma walls the bacilli resident within macrophages preventing spreading and generating an immune microenvironment which facilitates the interaction between cytokines secreted by macrophages and T cells. However, the granuloma also provides housing for *M. tuberculosis* during a long period of time. The latent bacilli could be released if the cytokine balance is broken and originate a reactivation of the disease.

ENTRY OF MYCOBACTERIA INTO HOST CELLS

M. tuberculosis entry into macrophages is mediated by receptor binding and phagocytosis. Although the majority of studies indicate that the bacilli favour interaction with complement and mannose receptors, which are benign because they trigger minimal superoxide production, experimental data suggest that the receptor type has little impact on the intracellular survival of the bacteria [19,20]. Selective receptor blockade during phagocytosis does not alter the survival and growth in human macrophages [20] although differential use of receptors may affect the invasion of different phagocytes populations.

For instance the macrophage mannose receptors are expressed on mature macrophages and allow uptake of virulent *M. tuberculosis* H37Rv but not the avirulent H37Ra. The interaction between the receptor and the mycobacteria is mediated at least by terminal residues present in mycobacteria lipoarabinomannam (LAM) [21,22] that are also involved in CD14 interaction. Since the expression of these receptors is downregulated by γ-IFN their role in mycobacteria ingestion is circumvented to early stages in infection and in individuals with compromised cellular immunity [23]. In addition to mannose and complement receptor other receptors such as surfactant protein A receptors [24] and class

A scanveger receptors [20] are involved in mycobacteria uptake associated with a low pro-inflammatory response.

Another group of receptors, the pattern recognition receptors (PPR), are likely to be responsible for the immune recognition of pathogens and thus for the pro-inflammatory cell signalling rather than bacterial uptake. This group includes Fc receptors and Toll like receptors (TLR). Pathogenic mycobacteria avoid binding to this family of receptors being preferentially uptake by mannose receptors preventing a strong pro-inflammatory response at early stages of infection. If the host immune system secretes high levels of γ-IFN at this stage the mannose receptors are downregulated as stated before forcing *M. tuberculis* uptake mediated by PRRs and TLR.

Mamalian TLR proteins derive their name from the *Drosophila* Toll protein, to which they have sequence similarity. TLRs were first identifies in *Drosophila*, where they are important for resistance to microbial antigens. Subsequently a large number of TLRs were identified in mammals and two of them, TLR2 and TLR4, have been implicated in the activation macrophages by mycobacteria involving MAP kinases (ERK 1 /2, p38 and JNK), Janus kinase/ signal transducer and activator of transcription (JAK/STAT) and NF-κB pathways.

The activation of host-cell signalling cascades, such as MAP kinases or JAK/STAT pathways results in the production of pro-inflammatory cytokines (such as IL-1, TNF-α and interferons) and chemokines. Pathogenic but not non-pathogenic mycobacteria have evolved mechanisms to suppress these signal transduction cascades and thereby attenuate the cytokine-induced immune response.

Extracellular signal-regulated kinases (ERK 1 /2) and p38 are members of MAP kinase family that became activated through the phosphorylation of tyrosine and threonine residues. Pathogenic mycobacteria such as *M. avium* and *M. tuberculosis* modulate MAP kinase activity. This leads to a decrease in pro-inflammatory response exemplified by a decrease in cytokine secretion such as TNF-α and their downstream effector nitric oxide (NO). Since TNF-α receptors are true death receptors the decrease production of this cytokine induced by blockade of NF-κB and MAP kinase activation results in apoptosis inhibition. The classical programmed cell death pathway is believed to constitute a effective mechanism of intracellular mycobacteria killing [25]. However, many bacterial pathogens alter host apoptotic pathways [26]. For example, infection of macrophages with virulent strains of *M. tuberculosis* induces much lower levels of apoptosis than does infection with attenuated strains [27].

MYCOBACTERIA PERSISTENCE AND HOST DEFENCE MECHANISMS

Macrophages play a unique role in host response to mycobacteria infections. These cells represent both the primary effector cell for killing the pathogen and the habitat in whish mycobacteria reside. In order to survive pathogenic mycobacteria developed strategies to avoid important anti-mycobacteria mechanisms such as NO production and phagosome lysosome fusion.

NO and reactive nitrogen radicals (RNI) synthesis

The tolerance of mycobacteria *in vitro* to RNI is strain-, dose- and time-dependent, with pathogens being inherently more resistant than non-pathogens [28-31]. This suggests that pathogenic mycobacteria express genes that counteract the bactericidal or bacteriostatic effects of RNI. Different experimental approaches lead to the identification of *nox*R1 and *nox*R3 which are able to confer RNI, and also reactive oxygen intermediates (ROI), resistance by a still unknown mechanism [32,33]. Another gene involved in protection from oxidative stress is *ahp*C [34]. The product of *ahp*C, the alkyl hydroperoxide reductase subunit C (AhpC), can metabolise peroxynitrite anion into nitrite, thereby contributing to detoxifying this highly reactive species [35]. Peroxynitrite is a powerful oxidant produced by activated macrophages that can exert its toxic effects through protein modification [36]. *In vitro* studies have shown that *M. tuberculosis* is resistant to this oxidant specie but *M. smegmatis* and BCG are susceptible [37].

NO produced by the inducible nitric oxide synthase (iNOS) and its derivatives are produced by macrophages in response to mycobacteria infection. Pro-inflammatory cytokines (e.g. γ-IFN and TNF-α) and bacterial lipopolisaccharides (LPS) enhance NO synthesis [38-40]. The anti-mycobacterial effects of these intermediates were shown experimentally in macrophage cultures infected with *Mycobacterium* [41,42]. Other studies in the murine model of infection involving iNOS inhibitors or mice with disruption in *nos*2 gene highlighted the crucial role played by RNI in host defence against *Mycobacterium* infection [43-46]. In contrast the importance of NO and RNI in human defence against *M. tuberculosis* is a matter of controversy [47,48].

Although there is experimental evidence that NO made by iNOS or NOS2 (in humans) is required for mycobacteria killing it is unlikely that an effective killing would be achieved without delivery of bacteria to acidic compartments (late endosome / lysosomes) [45,49]. Recent analysis of γ-IFN activated macrophages provided evidence

that NO and RNI derived from NOS2 mediated killing is insufficient to clear mycobacteria in the absence of a GTPase: LRG47. Experiments with infected macrophages have shown that LGR47 favour maturation of *M. tuberculosis* containing phagosomes through acquisition of vacuolar ATPase (V-ATPase) and ultimately enhance NO killing effects [49]. More recently it was shown that LRG47 mediated lysosomal fusion is involved in autophagy rather than in phagosome maturation [50].

Phagolysosome biogenesis

Phagocytosis of pathogenic microorganisms by macrophages is the first step towards their eventual degradation. The phagosome eventually matures into a phagolysosome an organelle with acid pH, high content of hydrolases, defensins and the ability to generate toxic oxidative compounds, responsible for routine elimination of microorganisms [51,52]. In order to avoid their degradation intracellular pathogens developed several strategies including escaping from the maturing phagosome to the cytoplasm (e.g. *Listeria, Shigella*, *Ricketsia* and *Trypanossoma cruzi*)[53,54], escaping from the endosomal pathway to a endoplasmic reticulum derived vacuole (e.g. *Chlamydia*, *Legionella*, *Brucella*)[55-58], modification of the phagosome or adaptation to the environment of the phagolysosome (e.g. *Coxiella, Leishmania*)[59,60] and arrest phagosome maturation at late phase (e.g. *Salmonella*, *Histoplasma*) [61,62] or at an early phage (e.g. *Mycobacterium*, *Nocardia*, *Rhodococcus*) [63-65]. The notorious success of *M. tuberculosis*, a facultative intracellular pathogen, rests upon the ability to arrest the biogenesis of the phagolysome. The ability of this pathogen to enter host macrophages and persist in friendly phagosomes, which do not mature into phagolysosomes [63,66-70], is crucial to tuberculosis infection, latency, disease activation, spread and suppression of immunological detection by the host [52,71-73]. The maturation of a phagosome is a complex and ordered process involving interaction of the nascent phagosome with vesicles from the endocytic pathway (Figure 1).

When an inert particle as a latex bead (LB) is uptaked by macrophages the formed phagosome triggers a sequential series of fission and fusion events described by the kiss and run model of phagosome maturation [74]. Shortly after their formation phagosomes bind to microtubules and start to fuse with early endosomes in a rab 5 dependent fashion. The early endosome is characterized by the presence of rab 5, transferin receptor (TfRs) or early endosome antigen 1 (EEA1), a relatively poor content of

proteases and a mildly acid pH around 6. As a consequence early endosomes contain, not only components characteristic of the plasma membrane but also of the early endosome.

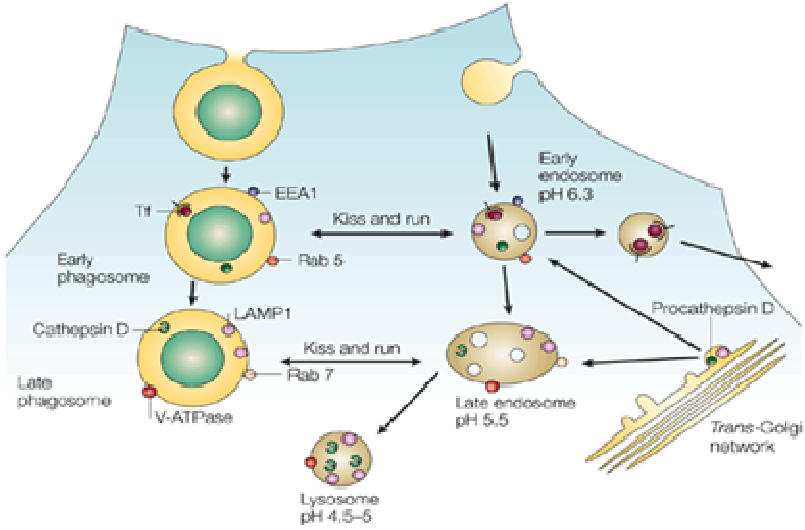

Figure 1. Phagolysosome biogenesis

Diagram showing the parallels between endosome progression to lysosome and maturation of a latex bead containing phagosome. The fusion of phagosomes with compartments of the endosomal pathway follows the kiss and run model proposed by M. Desjardins[75]. After internalization, the phagosome shows transient access to the rapid recycling pathway illustrated by the presence of transferin (Tf) its classical marker. During this early stage the phagosome has many of the markers found on early endosomes, such as EEA1 and rab5. However phagosomes rapidly acquire proteins associated with late endosomes, such as LAMP 1, rab7 and V-ATPase. Proforms of lysosomal hydrolases such as procathepsin D also appears in early phagosomes. Nevertheless, the processing of cathepsin D to its mature form seems to coincide with V-ATPase acquisition and pH drop. Figure from [76]

These early markers are then recycled from the phagosomal membrane as maturation proceeds [77,78]. Through fission and fusion events (kiss and run) phagosomes acquire new molecules and recycle others. Therefore the acquisition of rab 7 and the lost of rab 5 enable subsequent fusion of the phagossome with older organelles as late endosomes and lysosomes [74,75]. Although the kinetics of maturation differ greatly depending both on the particle phagocytised and the cell, phagosomes begin to fuse with late endosomes and becoming refractory to early endosomes about 15-30 minutes after formation [78-80]. As a consequence of phagosome aging they become enriched in late endosome

molecules best exemplified by rab 7, lysobisphosphatidic acid (LBPA) and the mannose-6-phosphate receptor cation independent [79,81]. Nevertheless its presence is also transitory since the late phagosome evolved to a phagolysosome characterized by the presence of mature forms of lysosomal enzymes such as cathepsin D, lysosome associated membrane protein 1 (LAMP 1) and a luminal acidic pH [80].

Following phagocytosis, the bacteria continue to reside within a membrane-bound vacuole of host origin. The seminal studies of D'Arcy Hart in the early 1970s described how the absence of fusion correlated with viability of the infecting bacteria [66,82,83]. The capacity of *M. tuberculosis* to regulate the fusogenicity of their phagosomes is shared with other pathogenic mycobacteria such as *M. avium* and *M. bovis*.

In 1986, Frehel and colleagues observed transient delivery of lysosomal tracers to phagosomes containing *M. avium* and suggest that these phagosomes had access to early endosomal compartment [84]. Then in 1991 Crowle *et al.* [85] reported that phagosomes containing *M. avium* and *M. tuberculosis* were less acidic than neighbouring lysosomes. Sturgill-Kozycki [86] reported that pH of mycobacteria containing phagosomes is around 6.2-6.3 and the deficient recruitment of V-ATPases responsible for the acidification of phagosomes.

Later was shown that mycobacteria containing phagosomes are highly dynamic compartments. They had a paucity of V-ATPase complexes and a profile of endosomal constituents consistent with the arrest of phagosome maturation at a point that retained fusion with early endosomes [87]. Consequently, markers of the recycling endosomal system, namely transferin receptor could be shown to traffic through the mycobacteria containing phagosome [87,88]. Although certain "lysosomal" markers, such as cathepsin D, could be detected in this compartment, careful analysis revealed that it is an immature form of the enzyme [87,89]. Most researchers in this field now work under the assumption that the phagosome containing pathogenic *Mycobacterium spp* are blocked at an early stage of their maturation process [52,70,76,90-92].

The exact point where mycobacteria stop the phagosome maturation process is not yet identified. Nevertheless the retention of rab5 in mycobacteria containing phagosomes indicates that the process is arrested at an early phase between the steps controlled by rab5 and rab7 (Figure 1) [81,93].

The regulation of membrane fusion in endosome biogenesis at this stage of the differentiation process is still debated although the major players have been identified [94,95]. In essence, rab5 binds Vps34, a class III phosphatidylinositol 3-kinase that

generates phosphatidylinosithol 3-phosphate (PI 3-P) on the cytosolic face of the phagosome. PI 3-P acts has an acceptor for the EEA1 which also complexes with rab5. EEA1 binds calmodulin in a Ca^{2+}/calmodulin dependent process [96,97]. Acquisition and accumulation of EEA1 are necessary for accumulation of rab7, the small GTPase that is enriched in lysosomes.

Malik *et al.* reported that *M. tuberculosis* blocked the normal calmodulin dependent signal transduction observed in maturation of phagosomes containing latex beads (LB) or dead bacteria [98,99]. These authors also shown that blockage in Ca^{2+} mediated signalling by live bacteria was due to an inhibition in sphingosine kinase activity [100]. In another study by *Anes et al.* it was demonstrated that sphingosine 1-phosphate content of the phagosome membrane influenced actin polymerization on isolated phagosomes and that *M. tuberculosis* containing phagosomes were deficient in actin nucleation [101].

Fratti *et al.* showed that while *M. bovis* BCG containing phagosomes acquired rab5 and accumulated Vps34, they failed to bind the PI 3-P-binding protein EEA1 [79]. According to Vergne *et al* this would be due to the absence of PIP-3-P on the cytosolic face of the bacterium containing phagosome resulting of the interference with the kinase activity of Vps34 through a Ca^{2+}/ calmodulin mediated process [102]. For Corvera and collegues calmodulin did not affect Vps34 kinase activity but instead blocked EEA1 binding to PI 3-P [96].

Despite the apparent controversy between the data generated by different groups it is clear that the point of arrest in phagosome maturation is the accumulation of EEA1. This process is modulated by molecules that affect Ca^{2+}/ calmodulin and class III PI 3-kinase activity.

ROLE OF ACTIN CYTOSKELETON IN HOST-PATHOGEN INTERACTION

The actin cytoskeleton is involved in several stages of host-pathogen interaction. For a long time was accepted that actin was involved in the first step of phagocytosis [103,104]. More recently was suggested that organelle trafficking and spatial distribution was not only dependent on microtubules, but also involve actin cytoskeleton [105,106].

The first step of phagocytosis, the bacterial uptake, is known to be an actin dependent process. Pathogens recognition by phagocytic receptors induces a rapid and massive actin assembly locally at the plasma membrane. The phagocytic cup is formed allowing

phagosome formation but most of F-actin was lost soon after this step. Many pathogens developed mechanisms to subvert the cellular actin cytoskeleton to trigger their internalization into normally non phagocytic host cells in order to escape the humoral immune defence. The invasive strategies used by pathogens to enter non-phagocytic cells are known as induced phagocytosis via the zipper and trigger mechanisms. In both cases actin assembly is stimulated by activation of the Rho-family GTPases Rac1 and Cdc42, both capable of eliciting Arp2/3 complex activation via proteins of the Wiskott-Aldrich syndrome protein (WASP) and WASP family verpolin homologus (WAVE) proteins families [107]. In the trigger mechanism, adopted by *Salmonella* and *Shigella*, the pathogen delivers to the host cell virulence factors that induce actin polymerization via type III secretion systems. The first evidence for a role of actin in intracellular trafficking events came from studies on the interaction of *Listeria* and vaccinia virus [53,108]. Both pathogens once within the cytosol are able to recruit G-actin and form actin tail comets thus providing the driving force within the infected cell and also to spread infection to the neighbouring cells. Since vaccinia virus and small endocytic vacuoles are similar in size, researchers wonder when formation of actin tail comets would be an ordinary event during small vesicles trafficking.

Pathogens that show actin based motility can be separated into two groups depending on whether they mimic a cellular nucleation-promoting factor (NFP) or they require the recruitment of a cellular NPF to the bacteria surface to promote Arp 2/3 mediated motility. The members of the Wiskott- Aldrich syndrome protein (WASP) family are an example of NFP recruited by pathogens as *Shigella*. Other pathogens such as *Listeria* and *Ricketsia* produce proteins that mimic WASP [109,110]. Although the mechanism of tail formation induced by *Mycobacterium marinum* is largely unknown probably it is NFP (WASP) and actin related proteins complex 2/3 (Arp 2/3) dependent [111,112].

In recent years Griffiths provide evidence for the involvement of the actin cytoskeleton at late phases of phagocytosis/ endocytosis of latex beads by a mechanism independent of ARP 2/3 and alternative to actin tail comets[113]. In the actin track model the actin nucleation machinery is dependent of the ezrin, radixin and moesin (ERM) family of proteins and postulates that if a membrane phagosome is able to filament actin this will provide tracks for other organelles to bind and move towards the actin nucleation source. In the context of phagolysosome biogenesis this will aid phagosome maturation increasing the number of fission and fusion events. Moreover the actin cytoskeleton must also be involved in phagosome maturation since poisons of actin such as

cytochalasin D and latrunculin A can inhibit this process in 50 % [114,115]. In addition actin was found associated with endosomes and lysosomes [116,117] as well as several actin binding proteins as myosins [114] and moesin [118]. Indeed *in vitro* studies showed that actin filaments are able to mediate fusion between late but not early endocytic organelles and phagosomes [119]. In the context of mycobacterial infections the role of the actin cytoskeleton was still in the infancy when our group started to work in this field in the beginning of the 3rd millennium. By that time Chantal de Chastellier group reported that pathogenic mycobacteria were able to disrupt the actin cytoskeleton within infected cells [120].

Using an *in vitro* assay that monitors membrane-dependent assembly of actin was possible to show that this process is regulated by lipids. The effect of different lipids at physiologic (1-5 mM: High ATP) and ischaemic (0.2 mM: Low ATP) concentrations of ATP are summarized in figure 2. In physiological conditions this class of lipids integrates the phagosome membrane in different amounts depending on the degree of vesicle maturation. While early phagosomes are enriched in phosphatidylcholine (a negative efector), late phagosomes are enriched in sphingomyelin the precursor of ceramide (both positive efectors). Thus by changing lipid composition we were able to switch on or block actin assembly/ fusion ability *in vitro*.

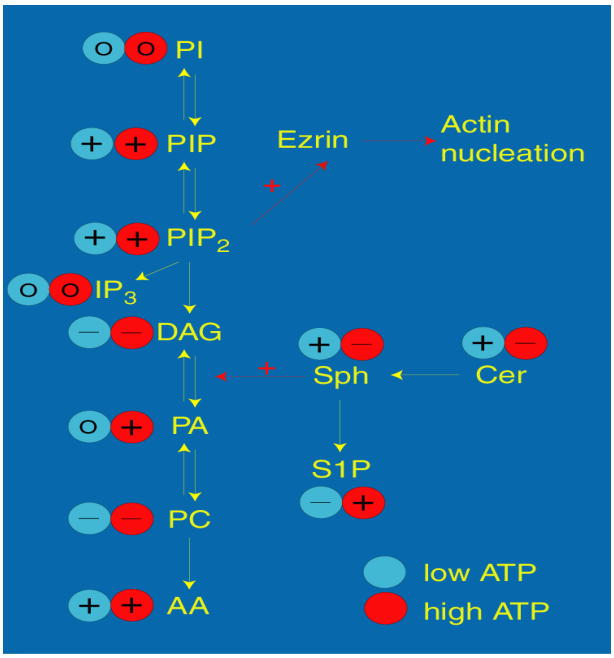

Figure 2. Effect of lipids in actin nucleation by LBP

The effects of lipids on LBP actin nucleation at high and low ATP concentrations. Stimulation (+), inhibition (-) or no effect (0) relative to the standard conditions at low and high ATP

concentrations are indicated. Abbreviations: AA, arachidonic acid; Cer, ceramide; PC, phosphatidylcholine; PA, phosphatidate; Sph, sphingosine; S1P, sphingosine-1-phosphate. Figure from [101].

When instead of LBPs were used phagosomes enclosing the non pathogenic mycobacteria *M. smegmatis* we observed that these phagosomes were able to nucleate actin *in vitro* similarly to LBPs. However when phagosomes containing pathogenic mycobacteria, such as *M. avium* or *M. tuberculosis*, were used the actin nucleation was effectively blocked. This enable us to established a link between the ability of mycobacteria to assemble actin, phagosome maturation and intracellular pathogen killing [101]. The most striking result arose from the fact that actin assembly by mycobacteria containing phagosomes could be controlled using signalling lipids such as arachidonic acid (AA), phosphatidylinositol biphosphate (PIP_2) and ceramide (Cer). These lipids are potent inducers of actin assembly even in *M. tuberculosis* containing phagosomes allowing the overcome of phagosome maturation block and thus inducing an increase in mycobacterial killing within macrophages.

This study highlighted the opposite role played by two classes of dietary lipids in host defence to mycobacteria infections. The polyunsaturated fatty acids (PUFA) omega n-3 inhibited *in vitro* and *in vivo* actin nucleation stimulating mycobacteria survival within macrophages whereas the omega n-6 (AA) had the opposite effects. The positive effect on actin nucleation by phagosomes was observed not only by adding AA but also by addition of its metabolites such as prostaglandin F2 (PGF2) (Gordon Shore, University Sterling, Scotland, personal communication). The finding that another metabolite of AA, PGE2, when added to the system blocked actin assembly make hard to draw straigth prediction for the effect of AA in animal models of infection.

DIETARY FATTY ACIDS AND IMMUNE RESPONSE

In western diets omega-6-fatty acids (PUFA n-6) account for the majority of PUFA in the food supply. When diets are supplemented with omega-3-fatty acids, the latter partially replace the omega-6 fatty acid in the membrane of practically all cells [121,122]. This change has profound effects on both inflammatory and immune response mediated by different mechanisms.

PUFA n-3 competes with AA as substrates for different enzymes (Fig 3). Competition at the level of ciclooxygenase (COX) and 5-lipoxygenase (5-LOX) [123,124] is of particular important since they are involved in the synthesis of key inflammatory mediators as prostaglandin, leukotriene (LT) and lipoxins. Thus higher levels of PUFA n-3 in cell membranes reduce the production, in the COX mediated pathway, of pro-inflammatory eicosanoids (PGE2, LTB4) from n-6 PUFA and increase production of eicosanoids from n-3 PUFA (PG3, LTB5) which have weaker or opposite activity. However, the situation is complicated, because eicosanoids derived from one precursor did not share all the effects. While LT4 tends to enhance NKcells activity and Th-1 cytokine production (IL-1, IL-6, TNF-α, IFN-γ) PGE2 tends to suppress this functions.
The role played by products of 5-LOX pathway in host resistance to *M. tuberculosis* is less documented. Nevertheless, there is experimental evidence in mice of the importance of lipoxin A_4 in infection control [125,126].

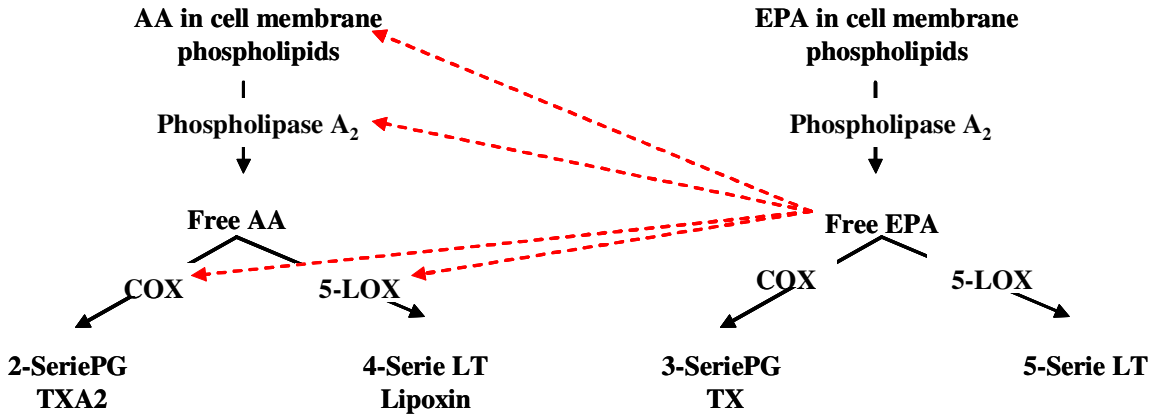

Figure 3: Synthesis of eicosanoids from AA and EPA
AA and EPA compete for prostaglandin (PG) and leukotriene (LT) synthesis at cyclooxigenase (COX) and lipoxygenase (LOX) level. The PG and LT derived from AA have an overall pro-inflammatory effect while the ones derived from EPA have anti-inflammatory effect or a weaker potent pro-inflammatory effect. In this figure TXA2 means Tromboxane A2

Changes in membrane lipid composition can also interfere with signal transduction. The most obvious way would be synthesis of different signalling molecules or the same signalling molecule with different biological activity due to changes in fatty acid composition [127,128]. A reduction in membrane AA decrease ceramide availability and

conducts to the synthesis of a less potent DAG [129] leading to a less potent anti-inflammatory response. Another mechanism that can account for a different inflammatory response is difference in binding of this and other molecules, as cytokines [130,131], to their receptors in cell membrane.

Omega-3 fatty acids can also modulate gene expression of important immune genes. Among these are cytokines (TNF-α, IL-1β and IL-6) [132-134], i-NOS[135] and transcription factors as NF-κB [136]. Changes in gene expression can result from direct or indirect effects of omega-3 fatty acids. The mechanisms are not fully understood may differ from cell types to cell type. For cytokine production, bind of EPA to a class of transcription factors known as peroxisome proliferator activactor receptor (PPAR) can account for inhibition of macrophage activation and production of TNF-α, IL-1β and IL-6 [128]. And at least, for TNF-α, another indirect mechanism mediated by inhibition of NF-κB activation can account for inhibition of TNF-α production. Collectively, we can conclude that omega-3 fatty acids can affect the balance between Th-1 and Th-2 cytokines that are of capital importance in mycobacteria infections [137].

INTERPLAY BETWEEN NUTRITION AND TUBERCULOSIS

Under or over nutrition and diet related chronic diseases are unbalanced nutrition status that constitutes a critical risk factor to infections. As stated before nutrients in the diet play a crucial role in maintaining an optimal immune response, such that deficient or excessive intakes can have negative consequences on susceptibility to a variety of pathogens. Under nutrition states and metabolic diseases as diabetes favour the establishment of infectious diseases including malaria, AIDS and TB while over nutrition states favours opportunistic and fungal infections [138,139].

The link between malnutrition and active TB has been recognized for many years. This notion is largely based on historical reports of the first and second world wars and also on more recent studies in animals [140,141]. In fact food intake increases the levels of γ-IFN but not IL-4 secretion whereas starvation enhances IL-4 response but not γ-IFN levels. The severe malnutrition observed in tuberculosis patients is the major argument for the provision of nutritional supplementation of such individuals.

In the classical era the Greeks designated TB as “phthisis” meaning waste a way and later during the 18th and 19th centuries it was called “consumption”. Nowadays this

connection gained importance due to several reasons (i) TB is the most frequent and serious opportunistic infection in human immunodeficiency virus (HIV) infected individuals, (ii) general use of nutritional supplements and (iii) the increase of TB incidence among populations with nutritional deficiencies both in undeveloped and developed countries.

A link between a particular diets and higher TB incidence has been established on the basis of epidemiologic studies. Populations following a strictly vegetarian diet consume minimal amounts of cobalamin (also known as vitamine B_{12}) and register a significant higher incidence of TB comparing with omnivores [142]. This can be explained by the important role played by cobalamin in intracellular pathogens killing [143,144].

Eskimos and Inuits following a diet rich in oily fish and fish oil, the best characterized sources of omega-3 (PUFA n-3), and register an higher incidence of TB and diarrhea but a low incidence of cardiovascular diseases (CDV), chronic inflammatory or autoimmune diseases [145-147]. In developing countries CDV are an important cause of mortality and morbidity. The WHO estimates that in 2010 CDV will be the major cause of death in these countries [148]. The preventive treatment of these diseases include a diet enrich in omega-3 lipid because they reduce serum cholesterol, low density lipoproteins (LDL) and triacyglycerol concentrations [149]. However in the context of tuberculosis the reduction in cholesterol levels can account for an increase in the active disease. Indeed cholesterol rich diets were shown to accelerate clearance of bacilli during the treatment of tuberculosis [150,151].

THESIS GOALS

Environmental and non-intracellular microorganisms such as *E. coli* are efficiently and quickly cleared by macrophages (within 4 h). Nevertheless, *Mycobacterium smegmatis* universally classified as a saprophyte and non-intracellular species possess the ability to persist for 48 h within macrophages [101,152]. Since macrophages play a major role as primary effectors cells for pathogen killing this fact provides evidence that even a saprophyte microorganism can behave, at least partially, as a pathogen and thus have transiently intracellular survival ability. Taking advantage of this fact we started to study the mechanisms involved in mycobacteria clearance by macrophages and how *M. smegmatis* is able to circumvent the bacterial killing factors of the infected macrophage.

After following in great detail how macrophages kill the fast growing species *M. smegmatis* we studied how these mechanisms can be modulated or blocked during the infection with pathogenic, intracellular species. The mycobacteria used were the vaccine strain BCG and a virulent strain of *M. bovis*. Since there are no extensive studies on the host cell type species interaction with mycobacteria we extend our studies from the mouse model to natural hosts of the mycobacteria used. In the present study since we use different strains of *M. bovis* we used human and bovine macrophages. Our work was important in deciphering new macrophage compartments where bacteria can be killed and outlined the real importance of the nitric oxide and the phagosome lysosome biogenesis during the course of the mycobacterial infection.

Finally, previous work from the group showed that the actin cytoskeleton on the phagosomal membranes is important to provide tracks to other organelles to move towards the actin nucleating source and thus help phagosome maturation and fusion with lysosomes [101,119,153]. We have also, previously found that this ability can be modulated by signalling lipids [101] and, in the context of TB, some lipids such as arachidonic acid and ceramide could overcome the actin nucleation blockade by *M. tuberculosis* containing phagosomes, while the omega 3 lipid EPA had the opposite effect. In conclusion, lipids can have a pro or anti-inflammatory role mediated by its ability to control actin assembly in the membrane of mycobacteria containing phagosomes, which ultimately induces more intracellular mycobacteria killing or survival. In the present work we proposed to understand how we could use this signalling to modulate the intracellular survival of *M. tuberculosis*, and thus try to find potential therapeutic alternatives for TB treatment or prevention. From the literature there are a lot of conflicting results on the effects of essential lipids such as AA or EPA during the course of mice infection with intracellular pathogens. Here we studied the system in depth, using not only simple models (cells in culture) but also complex models, namely animal models of infection.

Since in the present work we defined a kind of biological clock for killing or survival of *M. smegmatis* during the course of the infection we asked how could these lipids affect the signalling states of the macrophage if they were added to the system at different metabolic states of the infected macrophage. The same was applied during *M. tb* infection.

Our results were surprising since they showed that there is a complexity of signalling states during the time course of the infection and that no dietary lipids are recommended during mycobacterial infections.

REFERENCE LIST

1. Shah,N.S. *et al.* Worldwide emergence of extensively drug-resistant tuberculosis. *Emerg. Infect. Dis.* **13**, 380-387 (2007).

2. Van Rie,A. & Enarson,D. XDR tuberculosis: an indicator of public-health negligence. *Lancet* **368**, 1554-1556 (2006).

3. WHO. 2007 Tuberculosis facts. 2007.
Ref Type: Internet Communication

4. Smith,N.H., Gordon,S.V., Rua-Domenech,R., Clifton-Hadley,R.S. & Hewinson,R.G. Bottlenecks and broomsticks: the molecular evolution of *Mycobacterium bovis*. *Nat. Rev. Microbiol.* **4**, 670-681 (2006).

5. Huard,R.C. *et al.* Novel genetic polymorphisms that further delineate the phylogeny of the *Mycobacterium tuberculosis* complex. *J Bacteriol.* **188**, 4271-4287 (2006).

6. Boddinghaus,B., Rogall,T., Flohr,T., Blocker,H. & Bottger,E.C. Detection and identification of mycobacteria by amplification of rRNA. *J Clin. Microbiol.* **28**, 1751-1759 (1990).

7. Sreevatsan,S. *et al.* Restricted structural gene polymorphism in the *Mycobacterium tuberculosis* complex indicates evolutionarily recent global dissemination. *Proc. Natl. Acad. Sci U. S. A* **94**, 9869-9874 (1997).

8. Mostowy,S. *et al.* Revisiting the evolution of *Mycobacterium bovis*. *J Bacteriol.* **187**, 6386-6395 (2005).

9. Brosch,R. *et al.* A new evolutionary scenario for the *Mycobacterium tuberculosis* complex. *Proc. Natl. Acad. Sci U. S. A* **99**, 3684-3689 (2002).

10. Garnier,T. *et al.* The complete genome sequence of *Mycobacterium bovis*. *Proc. Natl. Acad. Sci U. S. A* **100**, 7877-7882 (2003).

11. Thoen,C., Lobue,P. & de,K., I. The importance of *Mycobacterium bovis* as a zoonosis. *Vet. Microbiol.* **112**, 339-345 (2006).

12. Rua-Domenech,R. Human *Mycobacterium bovis* infection in the United Kingdom: Incidence, risks, control measures and review of the zoonotic aspects of bovine tuberculosis. *Tuberculosis (Edinb.)* **86**, 77-109 (2006).

13. Buddle,B.M., Pollock,J.M. & Hewinson,R.G. Tuberculosis and the tubercle bacillus. Stewart T.Cole (ed.), pp. 537-560 (ASM Press, Washington,2005).

14. Russell,D.G. Highlighting the parallels between human and bovine tuberculosis. *J Vet. Med. Educ.* **30**, 140-142 (2003).

15. Means,T.K. *et al.* Human toll-like receptors mediate cellular activation by Mycobacterium tuberculosis. *J Immunol* **163**, 3920-3927 (1999).

16. Bodnar,K.A., Serbina,N.V. & Flynn,J.L. Fate of Mycobacterium tuberculosis within murine dendritic cells. *Infect. Immun.* **69**, 800-809 (2001).

17. Henderson,R.A., Watkins,S.C. & Flynn,J.L. Activation of human dendritic cells following infection with Mycobacterium tuberculosis. *J Immunol* **159**, 635-643 (1997).

18. Hertz,C.J. *et al.* Microbial lipopeptides stimulate dendritic cell maturation via Toll-like receptor 2. *J Immunol* **166**, 2444-2450 (2001).

19. Ernst,J.D. Macrophage receptors for Mycobacterium tuberculosis. *Infect. Immun.* **66**, 1277-1281 (1998).

20. Zimmerli,S., Edwards,S. & Ernst,J.D. Selective receptor blockade during phagocytosis does not alter the survival and growth of Mycobacterium tuberculosis in human macrophages. *Am. J Respir. Cell Mol. Biol.* **15**, 760-770 (1996).

21. Schlesinger,L.S., Hull,S.R. & Kaufman,T.M. Binding of the terminal mannosyl units of lipoarabinomannan from a virulent strain of *Mycobacterium tuberculosis* to human macrophages. *J Immunol* **152**, 4070-4079 (1994).

22. Schlesinger,L.S., Kaufman,T.M., Iyer,S., Hull,S.R. & Marchiando,L.K. Differences in mannose receptor-mediated uptake of lipoarabinomannan from virulent and attenuated strains of *Mycobacterium tuberculosis* by human macrophages. *J Immunol* **157**, 4568-4575 (1996).

23. Schreiber,S. *et al.* Regulation of mouse bone marrow macrophage mannose receptor expression and activation by prostaglandin E and IFN-gamma. *J Immunol* **151**, 4973-4981 (1993).

24. Gaynor,C.D., McCormack,F.X., Voelker,D.R., McGowan,S.E. & Schlesinger,L.S. Pulmonary surfactant protein A mediates enhanced phagocytosis of *Mycobacterium tuberculosis* by a direct interaction with human macrophages. *J Immunol* **155**, 5343-5351 (1995).

25. Winau,F., Hegasy,G., Kaufmann,S.H. & Schaible,U.E. No life without death-apoptosis as prerequisite for T cell activation. *Apoptosis.* **10**, 707-715 (2005).

26. Spira,A. *et al.* Apoptosis genes in human alveolar macrophages infected with virulent or attenuated Mycobacterium tuberculosis: a pivotal role for tumor necrosis factor. *Am. J Respir. Cell Mol. Biol.* **29**, 545-551 (2003).

27. Keane,J., Remold,H.G. & Kornfeld,H. Virulent *Mycobacterium tuberculosis* strains evade apoptosis of infected alveolar macrophages. *J Immunol* **164**, 2016-2020 (2000).

28. Long,R., Light,B. & Talbot,J.A. Mycobacteriocidal action of exogenous nitric oxide. *Antimicrob. Agents Chemother.* **43**, 403-405 (1999).

29. Long,R. *et al.* Inhaled nitric oxide treatment of patients with pulmonary tuberculosis evidenced by positive sputum smears. *Antimicrob. Agents Chemother.* **49**, 1209-1212 (2005).

30. O'Brien,L., Carmichael,J., Lowrie,D.B. & Andrew,P.W. Strains of *Mycobacterium tuberculosis* differ in susceptibility to reactive nitrogen intermediates *in vitro*. *Infect. Immun.* **62**, 5187-5190 (1994).

31. Rhoades,E.R. & Orme,I.M. Susceptibility of a panel of virulent strains of *Mycobacterium tuberculosis* to reactive nitrogen intermediates. *Infect. Immun.* **65**, 1189-1195 (1997).

32. Ehrt,S. *et al.* A novel antioxidant gene from *Mycobacterium tuberculosis*. *J Exp Med.* **186**, 1885-1896 (1997).

33. Ruan,J., St John,G., Ehrt,S., Riley,L. & Nathan,C. noxR3, a novel gene from *Mycobacterium tuberculosis*, protects *Salmonella typhimurium* from nitrosative and oxidative stress. *Infect. Immun.* **67**, 3276-3283 (1999).

34. Chen,L., Xie,Q.W. & Nathan,C. Alkyl hydroperoxide reductase subunit C (AhpC) protects bacterial and human cells against reactive nitrogen intermediates. *Mol. Cell* **1**, 795-805 (1998).

35. Bryk,R., Griffin,P. & Nathan,C. Peroxynitrite reductase activity of bacterial peroxiredoxins. *Nature* **407**, 211-215 (2000).

36. Beckman,J.S. & Koppenol,W.H. Nitric oxide, superoxide, and peroxynitrite: the good, the bad, and ugly. *Am. J Physiol* **271**, C1424-C1437 (1996).

37. Yu,K. *et al.* Toxicity of nitrogen oxides and related oxidants on mycobacteria: *M. tuberculosis* is resistant to peroxynitrite anion. *Tuber. Lung Dis.* **79**, 191-198 (1999).

38. Chan,E.D. *et al.* Induction of inducible nitric oxide synthase-NO* by lipoarabinomannan of *Mycobacterium tuberculosis* is mediated by MEK1-ERK, MKK7-JNK, and NF-kappaB signaling pathways. *Infect. Immun.* **69**, 2001-2010 (2001).

39. Morris,K.R. *et al.* Role of the NF-kappaB signaling pathway and kappaB cis-regulatory elements on the IRF-1 and iNOS promoter regions in mycobacterial lipoarabinomannan induction of nitric oxide. *Infect. Immun.* **71**, 1442-1452 (2003).

40. Webb,J.L., Harvey,M.W., Holden,D.W. & Evans,T.J. Macrophage nitric oxide synthase associates with cortical actin but is not recruited to phagosomes. *Infect. Immun.* **69**, 6391-6400 (2001).

41. Chan,J., Xing,Y., Magliozzo,R.S. & Bloom,B.R. Killing of virulent *Mycobacterium tuberculosis* by reactive nitrogen intermediates produced by activated murine macrophages. *J. Exp. Med.* **175**, 1111-1122 (1992).

42. Denis,M. Interferon-gamma-treated murine macrophages inhibit growth of tubercle bacilli via the generation of reactive nitrogen intermediates. *Cell Immunol* **132**, 150-157 (1991).

43. Chan,J., Tanaka,K., Carroll,D., Flynn,J. & Bloom,B.R. Effects of nitric oxide synthase inhibitors on murine infection with *Mycobacterium tuberculosis*. *Infect. Immun.* **63**, 736-740 (1995).

44. Flynn,J.L., Scanga,C.A., Tanaka,K.E. & Chan,J. Effects of aminoguanidine on latent murine tuberculosis. *J Immunol* **160**, 1796-1803 (1998).

45. Macmicking,J.D. *et al.* Identification of nitric oxide synthase as a protective locus against tuberculosis. *Proc. Natl. Acad. Sci. U. S. A* **94**, 5243-5248 (1997).

46. Scanga,C.A. *et al.* The inducible nitric oxide synthase locus confers protection against aerogenic challenge of both clinical and laboratory strains of *Mycobacterium tuberculosis* in mice. *Infect. Immun.* **69**, 7711-7717 (2001).

47. Nathan,C. Inducible nitric oxide synthase in the tuberculous human lung. *Am. J Respir. Crit Care Med.* **166**, 130-131 (2002).

48. Chan,E.D., Chan,J. & Schluger,N.W. What is the role of nitric oxide in murine and human host defense against tuberculosis?Current knowledge. *Am. J Respir. Cell Mol. Biol.* **25**, 606-612 (2001).

49. Macmicking,J.D., Taylor,G.A. & McKinney,J.D. Immune control of tuberculosis by IFN-gamma-inducible LRG-47. *Science* **302**, 654-659 (2003).

50. Gutierrez,M.G. *et al.* Autophagy is a defense mechanism inhibiting BCG and *Mycobacterium tuberculosis* survival in infected macrophages. *Cell* **119**, 753-766 (2004).

51. Haas,A. The phagosome: compartment with a license to kill. *Traffic.* **8**, 311-330 (2007).

52. Russell,D.G., Mwandumba,H.C. & Rhoades,E.E. *Mycobacterium* and the coat of many lipids. *J Cell Biol.* **158**, 421-426 (2002).

53. Cossart,P. & Sansonetti,P.J. Bacterial invasion: the paradigms of enteroinvasive pathogens. *Science* **304**, 242-248 (2004).

54. Fernandes,M.C., L'Abbate,C., Kindro,A.W. & Mortara,R.A. *Trypanosoma cruzi* cell invasion and traffic: influence of *Coxiella burnetii* and pH in a comparative study between distinct infective forms. *Microb. Pathog.* **43**, 22-36 (2007).

55. Hackstadt,T., Rockey,D.D., Heinzen,R.A. & Scidmore,M.A. *Chlamydia trachomatis* interrupts an exocytic pathway to acquire endogenously synthesized sphingomyelin in transit from the Golgi apparatus to the plasma membrane. *EMBO J* **15**, 964-977 (1996).

56. Celli,J. *et al. Brucella* evades macrophage killing via VirB-dependent sustained interactions with the endoplasmic reticulum. *J Exp Med.* **198**, 545-556 (2003).

57. Roy,C.R. & Tilney,L.G. The road less traveled: transport of *Legionella* to the endoplasmic reticulum. *J Cell Biol.* **158**, 415-419 (2002).

58. Fernandez-Moreira,E., Helbig,J.H. & Swanson,M.S. Membrane vesicles shed by *Legionella pneumophila* inhibit fusion of phagosomes with lysosomes. *Infect. Immun.* **74**, 3285-3295 (2006).

59. Howe,D., Melnicakova,J., Barak,I. & Heinzen,R.A. Maturation of the *Coxiella burnetii* parasitophorous vacuole requires bacterial protein synthesis but not replication. *Cell Microbiol.* **5**, 469-480 (2003).

60. Lerm,M. *et al. Leishmania donovani* requires functional Cdc42 and Rac1 to prevent phagosomal maturation. *Infect. Immun.* **74**, 2613-2618 (2006).

61. Holden,D.W. Trafficking of the *Salmonella* vacuole in macrophages. *Traffic.* **3**, 161-169 (2002).

62. Strasser,J.E. *et al.* Regulation of the macrophage vacuolar ATPase and phagosome-lysosome fusion by *Histoplasma capsulatum*. *J Immunol* **162**, 6148-6154 (1999).

63. Vergne,I., Chua,J., Singh,S.B. & Deretic,V. Cell biology of mycobacterium tuberculosis phagosome. *Annu. Rev. Cell Dev. Biol.* **20**, 367-394 (2004).

64. Fernandez-Mora,E., Polidori,M., Luhrmann,A., Schaible,U.E. & Haas,A. Maturation of *Rhodococcus equi*-containing vacuoles is arrested after completion of the early endosome stage. *Traffic.* **6**, 635-653 (2005).

65. Black,C.M., Palieschekey,M., Beaman,B.L., Donovan,R.M. & Goldstein,E. Acidification of phagosomes in murine macrophages: blockage by *Nocardia asteroides*. *J Infect. Dis.* **154**, 952-958 (1986).

66. Armstrong,J.A. & Hart,P.D. Response of cultured macrophages to *Mycobacterium tuberculosis*, with observations on fusion of lysosomes with phagosomes. *J Exp. Med.* **134**, 713-740 (1971).

67. Clemens,D.L. & Horwitz,M.A. Characterization of the *Mycobacterium tuberculosis* phagosome and evidence that phagosomal maturation is inhibited. *J Exp. Med.* **181**, 257-270 (1995).

68. Russell,D.G. *Mycobacterium tuberculosis* and the four minute phagosome. *ASM News* **71**, 459-463 (2005).

69. Clemens,D.L. Characterization of the Mycobacterium tuberculosis phagosome 1. *Trends Microbiol.* **4**, 113-118 (1996).

70. Clemens,D.L. Characterization of the *Mycobacterium tuberculosis* phagosome. *Trends Microbiol.* **4**, 113-118 (1996).

71. Flynn,J.L. & Chan,J. Immune evasion by Mycobacterium tuberculosis: living with the enemy. *Curr. Opin. Immunol* **15**, 450-455 (2003).

72. Russell,D.G. Mycobacterium tuberculosis: here today, and here tomorrow 1. *Nat. Rev. Mol. Cell Biol.* **2**, 569-577 (2001).

73. Tufariello,J.M., Chan,J. & Flynn,J.L. Latent tuberculosis: mechanisms of host and bacillus that contribute to persistent infection. *Lancet Infect. Dis.* **3**, 578-590 (2003).

74. Desjardins,M. Biogenesis of phagolysosomes: the 'kiss and run' hypothesis. *Trends Cell Biol.* **5**, 183-186 (1995).

75. Desjardins,M., Huber,L.A., Parton,R.G. & Griffiths,G. Biogenesis of phagolysosomes proceeds through a sequential series of interactions with the endocytic apparatus. *J Cell Biol.* **124**, 677-688 (1994).

76. Russell,D.G. *Mycobacterium tuberculosis*: here today, and here tomorrow. *Nat. Rev. Mol. Cell Biol.* **2**, 569-577 (2001).

77. Duclos,S. *et al.* Rab5 regulates the kiss and run fusion between phagosomes and endosomes and the acquisition of phagosome leishmanicidal properties in RAW 264.7 macrophages. *J Cell Sci* **113 Pt 19**, 3531-3541 (2000).

78. Pitt,A., Mayorga,L.S., Stahl,P.D. & Schwartz,A.L. Alterations in the protein composition of maturing phagosomes. *J Clin. Invest* **90**, 1978-1983 (1992).

79. Fratti,R.A., Backer,J.M., Gruenberg,J., Corvera,S. & Deretic,V. Role of phosphatidylinositol 3-kinase and Rab5 effectors in phagosomal biogenesis and mycobacterial phagosome maturation arrest. *J Cell Biol.* **154**, 631-644 (2001).

80. Vieira,O.V., Botelho,R.J. & Grinstein,S. Phagosome maturation: aging gracefully. *Biochem. J* **366**, 689-704 (2002).

81. Via,L.E. *et al.* Arrest of mycobacterial phagosome maturation is caused by a block in vesicle fusion between stages controlled by rab5 and rab7. *J Biol. Chem.* **272**, 13326-13331 (1997).

82. Armstrong,J.A. & Hart,P.D. Phagosome-lysosome interactions in cultured macrophages infected with virulent tubercle bacilli. Reversal of the usual nonfusion pattern and observations on bacterial survival. *J Exp Med.* **142**, 1-16 (1975).

83. Brown,C.A., Draper,P. & Hart,P.D. Mycobacteria and lysosomes: a paradox. *Nature* **221**, 658-660 (1969).

84. Frehel,C., de Chastellier,C., Lang,T. & Rastogi,N. Evidence for inhibition of fusion of lysosomal and prelysosomal compartments with phagosomes in macrophages infected with pathogenic *Mycobacterium avium*. *Infect. Immun.* **52**, 252-262 (1986).

85. Crowle,A.J., Dahl,R., Ross,E. & May,M.H. Evidence that vesicles containing living, virulent *Mycobacterium tuberculosis* or *Mycobacterium avium* in cultured human macrophages are not acidic. *Infect. Immun.* **59**, 1823-1831 (1991).

86. Sturgill-Koszycki,S. *et al.* Lack of acidification in *Mycobacterium* phagosomes produced by exclusion of the vesicular proton-ATPase. *Science* **263**, 678-681 (1994).

87. Sturgill-Koszycki,S., Schaible,U.E. & Russell,D.G. *Mycobacterium*-containing phagosomes are accessible to early endosomes and reflect a transitional state in normal phagosome biogenesis. *EMBO J* **15**, 6960-6968 (1996).

88. Clemens DL & Horwitz MA. The *Mycobacterium tuberculosis* phagosome interacts with early endosomes and is accessible to exogenously administered transferrin. *J Exp Med.* **1**, 1349-1355 (1996).

89. Ullrich,H.J., Beatty,W.L. & Russell,D.G. Direct delivery of procathepsin D to phagosomes: implications for phagosome biogenesis and parasitism by *Mycobacterium*. *Eur. J Cell Biol.* **78**, 739-748 (1999).

90. de Chastellier,C. & Thilo,L. Modulation of phagosome processing as a key strategy for *Mycobacterium avium* survival within macrophages. *Res. Immunol* **149**, 699-702 (1998).

91. Deretic,V. & Fratti,R.A. *Mycobacterium* tuberculosis phagosome. *Mol. Microbiol.* **31**, 1603-1609 (1999).

92. Vergne,I., Chua,J. & Deretic,V. *Mycobacterium tuberculosis* phagosome maturation arrest: selective targeting of PI3P-dependent membrane trafficking. *Traffic.* **4**, 600-606 (2003).

93. Clemens,D.L., Lee,B.Y. & Horwitz,M.A. Deviant expression of Rab5 on phagosomes containing the intracellular pathogens *Mycobacterium tuberculosis* and *Legionella pneumophila* is associated with altered phagosomal fate. *Infect. Immun.* **68**, 2671-2684 (2000).

94. Stenmark,H. & Gillooly,D.J. Intracellular trafficking and turnover of phosphatidylinositol 3-phosphate. *Semin. Cell Dev. Biol.* **12**, 193-199 (2001).

95. Christoforidis,S., McBride,H.M., Burgoyne,R.D. & Zerial,M. The Rab5 effector EEA1 is a core component of endosome docking. *Nature* **397**, 621-625 (1999).

96. Lawe,D.C. *et al.* Essential role of Ca2+/calmodulin in Early Endosome Antigen-1 localization. *Mol. Biol. Cell* **14**, 2935-2945 (2003).

97. Mills,I.G., Urbe,S. & Clague,M.J. Relationships between EEA1 binding partners and their role in endosome fusion. *J Cell Sci* **114**, 1959-1965 (2001).

98. Malik,Z.A., Denning,G.M. & Kusner,D.J. Inhibition of Ca(2+) signaling by *Mycobacterium tuberculosis* is associated with reduced phagosome-lysosome fusion and increased survival within human macrophages. *J Exp Med.* **191**, 287-302 (2000).

99. Malik,Z.A., Iyer,S.S. & Kusner,D.J. *Mycobacterium tuberculosis* phagosomes exhibit altered calmodulin-dependent signal transduction: contribution to

inhibition of phagosome-lysosome fusion and intracellular survival in human macrophages. *J Immunol* **166**, 3392-3401 (2001).

100. Malik,Z.A. *et al.* Cutting edge: *Mycobacterium tuberculosis* blocks Ca2+ signaling and phagosome maturation in human macrophages via specific inhibition of sphingosine kinase. *J Immunol* **170**, 2811-2815 (2003).

101. Anes,E. *et al.* Selected lipids activate phagosome actin assembly and maturation resulting in killing of pathogenic mycobacteria. *Nat. Cell Biol.* **5**, 793-802 (2003).

102. Vergne,I., Chua,J. & Deretic,V. Tuberculosis toxin blocking phagosome maturation inhibits a novel Ca2+/calmodulin-PI3K hVPS34 cascade. *J Exp Med.* **198**, 653-659 (2003).

103. Greenberg,S. & Silverstein,S.C. Fundamental Immunology. Paul,W.E. (ed.), pp. 941-964 (Raven Press, New York,1993).

104. Reaven,E.P. & Axline,S.G. Subplasmalemmal microfilaments and microtubules in resting and phagocytizing cultivated macrophages. *J Cell Biol.* **59**, 12-27 (1973).

105. Gavin,R.H. Microtubule-microfilament synergy in the cytoskeleton. *Int. Rev. Cytol.* **173**, 207-242 (1997).

106. Kelleher,J.F. & Titus,M.A. Intracellular motility: how can we all work together? *Curr. Biol.* **8**, R394-R397 (1998).

107. Stradal,T.E. *et al.* Regulation of actin dynamics by WASP and WAVE family proteins. *Trends Cell Biol.* **14**, 303-311 (2004).

108. Rottner,K., Stradal,T.E. & Wehland,J. Bacteria-host-cell interactions at the plasma membrane: stories on actin cytoskeleton subversion. *Dev. Cell* **9**, 3-17 (2005).

109. Gouin,E., Welch,M.D. & Cossart,P. Actin-based motility of intracellular pathogens. *Curr. Opin. Microbiol.* **8**, 35-45 (2005).

110. Stevens,J.M., Galyov,E.E. & Stevens,M.P. Actin-dependent movement of bacterial pathogens. *Nat. Rev. Microbiol.* **4**, 91-101 (2006).

111. Stamm,L.M. *et al. Mycobacterium marinum* escapes from phagosomes and is propelled by actin-based motility. *J Exp. Med.* **198**, 1361-1368 (2003).

112. Stamm,L.M. *et al.* Role of the WASP family proteins for *Mycobacterium marinum* actin tail formation. *Proc. Natl. Acad. Sci U. S. A* **102**, 14837-14842 (2005).

113. Defacque,H. *et al.* Involvement of ezrin/moesin in de novo actin assembly on phagosomal membranes. *EMBO J* **19**, 199-212 (2000).

114. Jahraus,A. *et al.* ATP-dependent membrane assembly of F-actin facilitates membrane fusion. *Mol. Biol. Cell* **12**, 155-170 (2001).

115. Toyohara,A. & Inaba,K. Transport of phagosomes in mouse peritoneal macrophages. *J Cell Sci* **94 (Pt 1)**, 143-153 (1989).

116. Taunton,J. *et al.* Actin-dependent propulsion of endosomes and lysosomes by recruitment of N-WASP. *J Cell Biol.* **148**, 519-530 (2000).

117. Taunton,J. Actin filament nucleation by endosomes, lysosomes and secretory vesicles. *Curr. Opin. Cell Biol.* **13**, 85-91 (2001).

118. Desjardins,M. *et al.* Molecular characterization of phagosomes. *J Biol. Chem.* **269**, 32194-32200 (1994).

119. Kjeken,R. *et al.* Fusion between phagosomes, early and late endosomes: a role for actin in fusion between late, but not early endocytic organelles. *Mol. Biol. Cell* **15**, 345-358 (2004).

120. Guerin,I. & de Chastellier,C. Pathogenic mycobacteria disrupt the macrophage actin filament network. *Infect. Immun.* **68**, 2655-2662 (2000).

121. Calder,P.C. Dietary modification of inflammation with lipids. *Proc. Nutr. Soc.* **61**, 345-358 (2002).

122. Gibney,M.J. & Hunter,B. The effects of short- and long-term supplementation with fish oil on the incorporation of n-3 polyunsaturated fatty acids into cells of the immune system in healthy volunteers. *Eur. J Clin. Nutr.* **47**, 255-259 (1993).

123. Calder,P.C. Use of fish oil in parenteral nutrition: Rationale and reality. *Proc. Nutr. Soc.* **65**, 264-277 (2006).

124. Simopoulos,A.P. Omega-3 fatty acids in inflammation and autoimmune diseases. *J Am. Coll. Nutr.* **21**, 495-505 (2002).

125. Bafica,A. *et al.* Host control of *Mycobacterium tuberculosis* is regulated by 5-lipoxygenase-dependent lipoxin production. *J Clin. Invest* **115**, 1601-1606 (2005).

126. Karp,C.L. & Cooper,A.M. An oily, sustained counter-regulatory response to TB. *J Clin. Invest* **115**, 1473-1476 (2005).

127. Yaqoob,P. Lipids and the immune response. *Curr. Opin. Clin. Nutr. Metab Care* **1**, 153-161 (1998).

128. Field,C.J., Johnson,I.R. & Schley,P.D. Nutrients and their role in host resistance to infection. *J Leukoc. Biol.* **71**, 16-32 (2002).

129. Bell,M.V. & Sargent,J.R. Effects of the fatty acid composition of phosphatidylserine and diacylglycerol on the in vitro activity of protein kinase C from rat spleen: influences of (n-3) and (n-6) polyunsaturated fatty acids. *Comp Biochem. Physiol B* **86**, 227-232 (1987).

130. Grimble,R.F. & Tappia,P.S. Modulatory influence of unsaturated fatty acids on the biology of tumour necrosis factor-alpha. *Biochem. Soc. Trans.* **23**, 282-287 (1995).

131. Stubbs,C.D. & Smith,A.D. The modification of mammalian membrane polyunsaturated fatty acid composition in relation to membrane fluidity and function. *Biochim. Biophys. Acta* **779**, 89-137 (1984).

132. Priante,G., Bordin,L., Musacchio,E., Clari,G. & Baggio,B. Fatty acids and cytokine mRNA expression in human osteoblastic cells: a specific effect of arachidonic acid. *Clin. Sci (Lond)* **102**, 403-409 (2002).

133. Blok,W.L., Katan,M.B. & van der Meer,J.W. Modulation of inflammation and cytokine production by dietary (n-3) fatty acids. *J. Nutr.* **126**, 1515-1533 (1996).

134. Lo,C.J., Chiu,K.C., Fu,M., Lo,R. & Helton,S. Fish oil decreases macrophage tumor necrosis factor gene transcription by altering the NF kappa B activity. *J Surg. Res.* **82**, 216-221 (1999).

135. Khair-El-Din,T. *et al.* Transcription of the murine iNOS gene is inhibited by docosahexaenoic acid, a major constituent of fetal and neonatal sera as well as fish oils. *J Exp. Med.* **183**, 1241-1246 (1996).

136. Camandola,S. *et al.* Nuclear factor kB is activated by arachidonic acid but not by eicosapentaenoic acid. *Biochem. Biophys. Res. Commun.* **229**, 643-647 (1996).

137. Zhang,M. *et al.* T-cell cytokine responses in human infection with *Mycobacterium tuberculosis*. *Infect. Immun.* **63**, 3231-3234 (1995).

138. Schaible,U.E. & Kaufmann,S.H. Malnutrition and Infection: Complex Mechanisms and Global Impacts. *PLoS. Med.* **4**, e115 (2007).

139. Joshi,N., Caputo,G.M., Weitekamp,M.R. & Karchmer,A.W. Infections in patients with diabetes mellitus. *N. Engl. J. Med.* **341**, 1906-1912 (1999).

140. Cegielski,J.P. & McMurray,D.N. The relationship between malnutrition and tuberculosis: evidence from studies in humans and experimental animals. *Int. J. Tuberc. Lung Dis.* **8**, 286-298 (2004).

141. Faber,K. Tuberculosis and nutrition. *Acta Tuberc. Scand.* **12**, 287-335 (1938).

142. Chanarin,I. & Stephenson,E. Vegetarian diet and cobalamin deficiency: their association with tuberculosis. *J. Clin. Pathol.* **41**, 759-762 (1988).

143. Kaplan,S.S. & Basford,R.E. Effect of vitamin B12 and folic acid deficiencies on neutrophil function. *Blood* **47**, 801-805 (1976).

144. Skacel,P.O. & Chanarin,I. Impaired chemiluminescence and bactericidal killing by neutrophils from patients with severe cobalamin deficiency. *Br. J. Haematol.* **55**, 203-215 (1983).

145. Kaplan,G.J., Fraser,R.I. & Comstock,G.W. Tuberculosis in Alaska, 1970. The continued decline of the tuberculosis epidemic. *Am. Rev. Respir. Dis.* **105**, 920-926 (1972).

146. Kromann,N. & Green,A. Epidemiological studies in the Upernavik district, Greenland. Incidence of some chronic diseases 1950-1974. *Acta Med. Scand.* **208**, 401-406 (1980).

147. Dyerberg,J. & Bang,H.O. Haemostatic function and platelet polyunsaturated fatty acids in Eskimos. *Lancet* **2**, 433-435 (1979).

148. WHO-Cardiovascular disease. Strategic priorities of the WHO Cardiovascular Disease programme. 2007.
Ref Type: Internet Communication

149. Furst,P. & Kuhn,K.S. Fish oil emulsions: what benefits can they bring? *Clin. Nutr.* **19**, 7-14 (2000).

150. Perez-Guzman,C., Vargas,M.H., Quinonez,F., Bazavilvazo,N. & Aguilar,A. A cholesterol-rich diet accelerates bacteriologic sterilization in pulmonary tuberculosis. *Chest* **127**, 643-651 (2005).

151. Perez-Guzman,C. & Vargas,M.H. Hypocholesterolemia: a major risk factor for developing pulmonary tuberculosis? *Med. Hypotheses* **66**, 1227-1230 (2006).

152. Kuehnel,M.P. *et al.* Characterization of the intracellular survival of *Mycobacterium avium ssp*. paratuberculosis: phagosomal pH and fusogenicity in J774 macrophages compared with other mycobacteria. *Cell Microbiol.* **3**, 551-566 (2001).

153. Defacque,H. *et al.* Phosphoinositides regulate membrane-dependent actin assembly by latex bead phagosomes. *Mol. Biol. Cell* **13**, 1190-1202 (2002).

Chapter 2

Dynamic life and death interactions between *Mycobacterium smegmatis* and J774 macrophages

Dynamic life and death interactions between *Mycobacterium smegmatis* and J774 macrophages.

Elsa Anes[1,§], Pascale Peyron[2,3,§], Leila Staali[3,§], Luisa Jordao[1], Maximiliano G. Gutierrez[4], Holger Kress[3], Monica Hagedorn[3,*], Isabelle Maridonneau-Parini[2], Mhairi A. Skinner[5], Alan G. Wildeman[5], Stefanos A. Kalamidas[6], Mark Kuehnel[3] and Gareth Griffiths[3,¶].

[1] Molecular Pathogenesis Centre, Faculty of Pharmacy, University of Lisbon, Av. Forcas Armadas, 1600-083 Lisbon, Portugal.

[2] Institut de Pharmacologie et de Biologie Structurale, Centre National de la Recherche Scientifique, Toulouse, France.

[3] EMBL, Postfach 102209, 69117 Heidelberg, Germany.

[4] Laboratorio de Biología Celular y Molecular, IHEM-CONICET, Facultad de Ciencias Médicas, Universidad Nacional de Cuyo, Mendoza- Argentina

[5] Department of Molecular and Cellular Biology, University of Guelph, Guelph, Ontario N1G 2W1, Canada

[6] Department of Anatomy, Histology and Embryology, Medical School, University of Ioannina, Ioannina 45 110, Greece

[§] These authors contributed equally to the work.

[*] Present address: Department de Biochimie, Sciences II, CH-1211-Geneve-4, Switzerland
[¶] Correspondence should be addressed to Gareth Griffiths griffiths@embl.de

ABSTRACT

After internalization into macrophages non-pathogenic mycobacteria are killed within phagosomes. Pathogenic mycobacteria can block phagosome maturation and grow inside phagosomes but under some conditions can also be killed by macrophages. Killing mechanisms are poorly understood, although phago-lysosome fusion and nitric oxide production are implicated. We initiated a systematic analysis addressing how macrophages kill 'non-pathogenic' *M. smegmatis*. This system was dynamic, involving periods of initial killing, then bacterial multiplication, followed by two additional killing stages. Nitric oxide synthesis represented the earliest killing factor but its synthesis stopped during the first killing period. Phagosome actin assembly and fusion with late endocytic organelles coincided with the first and last killing phase, while recycling of phagosome content and membrane coincided with bacterial growth. Phagosome acidification and acquisition of the vacuolar V-ATPase followed a different pattern coincident with later killing phases. Moreover, V-ATPase localized to vesicles distinct from classical late endosomes and lysosomes. MAP kinase p38 is a crucial regulator of all processes investigated, except nitric oxide synthesis that facilitated the host for some functions while being usurped by live bacteria for others. A mathematical model argues that periodic high and low cellular killing activity is more effective than is a continuous process.

INTRODUCTION

The macrophage phago-lysosome (or 'late' or 'mature' phagosome) is potentially a hostile environment for microorganisms taken up by phagocytosis. Pathogenic mycobacteria such as *Mycobacterium tuberculosis* can block the fusion of phagosomes with late endosomes and lysosomes [1-3]. This inhibition facilitates pathogen growth, but when macrophages are 'activated' by effectors such as gamma interferon [4-7] or lipids [8] they can sometimes overcome the block and induce full phagosome maturation, an event that coincides with pathogen killing. Fusion with late endosomes and lysosomes, usually considered the most acidic compartments in cells [9-11] is thought to deliver both lysosomal enzymes and the vacuolar V-ATPase to phagosomes [12-15]. Lysosomal enzyme activity at low pH is widely considered to be the main killing mechanism against mycobacteria [16-19]. However, the production of nitric oxide (NO) by the iNOS enzyme provides an additional mechanism contributing to killing of pathogenic mycobacteria, *in vitro* [20], in cultured macrophages, in animals and in humans [21-23]. In contrast, reactive oxygen intermediates are generally considered far less important for mycobacterial killing [24-27].

The general view in the field is that pathogenic mycobacteria survive and grow in macrophages as a direct consequence of blocking phagosome maturation, while if maturation proceeds the bacteria are killed [1,28-34]. Most of this evidence is correlative: dying or dead bacteria are usually seen in lysosomes (pH 4.5-5.0) whereas living ones tend to remain in phago-endosomes (pH 6.2) [34]. However, pathogenic mycobacteria can also survive and, in the case of *M. avium* even grow in the low pH, hydrolase-rich environment of lysosomes under some conditions [35]. In most studies it is hard to rule out that a factor 'X' killed the bacteria, whose death then serves as a 'signal' for phagosome maturation. The question - how macrophages kill mycobacteria is crucial for understanding how 10 percent of humans carrying *M. tuberculosis* bacteria develop the disease whereas about 90 percent of the infected do not develop tuberculosis [36]. Perhaps we can develop therapies involving boosting the natural killing abilities of macrophages.

Here, we took advantage of the established ability of J774 macrophages to kill *M. smegmatis* within 48 h [8,37-39]. Focusing on this system, our goal was to understand the basic or innate cellular mechanisms which allow macrophages to kill intra-phagosomal mycobacteria in the absence of exogenous effectors.

In recent studies using both the model system latex bead phagosomes (LBP) and isolated mycobacterial phagosomes, we showed that the *de novo* nucleation/polymerization ('assembly') of F-actin by the membrane of phagosomes and late (but not early) endocytic organelles facilitates the fusion between them. Our data support an 'actin-track' model whereby these actin filaments emanating from the organelles provide tracks upon which lysosomes can move towards phagosomes to facilitate fusion [40,41]. A number of (mostly) pro-inflammatory lipids could activate actin assembly on both LBP and mycobacterial phagosomes *in vitro* and in cells. In agreement with the actin track model, these lipids stimulated phago-lysosome fusion and acidification and enhanced the killing of pathogenic mycobacteria (*M. avium* and *M. tuberculosis*) which normally survive in macrophages. In contrast, omega-3 polyunsaturated fatty acids inhibited phagosomal actin polymerization and facilitated pathogen growth [8]. In the present study we addressed phagosomal actin assembly in the context of *M. smegmatis* phagosome maturation in more detail.

In a routine screen of inhibitors that affect the LBP actin assembly *in vitro*, a specific inhibitor of the MAP kinase p38 (SB203580), but not of ERK1/2 was found to inhibit this process (Kuehnel et al, in preparation). In the present study we follow p38 in more detail.

MAP kinases are central players in cell signaling and much of their activities are localized on membranes [42]. There are three different classes of these kinases, namely ERK, JNK and p38. A number of studies have shown that these kinases are activated upon infection with mycobacteria [5]. Moreover, p38 and ERK are activated more during infection with non-pathogenic compared to pathogenic mycobacteria, implying that the pathogens inhibit these kinases [5,43]. The kinase p38 has been implicated in early endosome fusion; there, it can phosphorylate and activate Rab-GDI thereby locking Rab proteins in their inactive GDP-form and preventing fusion [44]. Fratti and colleagues[45] associated p38 activation with an inhibition of phagosome maturation in cells infected with *M. bovis* (BCG) [3].

Although *M. smegmatis* is widely considered to be a 'non-pathogenic bacterium', our data reveal it has a limited capacity to behave as a pathogen that actively manipulates the system. The initial infection appears to start a maturation 'clock', in which (after 2h) p38 plays a crucial role, involving cyclical patterns of signals to different functions. Surprisingly, both the macrophage and *M. smegmatis* take advantage of p38 in a molecular tug of war that, on this occasion the macrophage eventually wins.

RESULTS

Kinetics of survival of *M. smegmatis* in J774 macrophages

M. smegmatis infecting J774 cells are killed within 48 h [38,46]. Here, we used GFP-expressing *M. smegmatis* and followed the colony forming units (CFU) in bacterial culture medium over the course of the infection. In parallel, fluorescence microscopy was used to monitor the number of internalized bacteria per cell.

Using low infectivity (< 1 bacterium per cell) infection of almost confluent cells with exponentially growing *M. smegmatis* the bacteria were rapidly and reproducibly eliminated by 4 h post-infection (PI) (Fig. 1A.1; *killing phase-1*). However, at 5-10 or more bacteria per cell there was also effective killing of most bacteria within 4 h, followed by an unexpected and striking phase of intracellular growth of *M. smegmatis.* This started after 4 h and reached a peak at 9 h post-infection (Fig. 1A1). The rate of doubling was as efficient as that observed under optimal *in vitro* culture conditions (see Fig. 1A2). Examples of the intracellular localization of the bacteria at different infection times are shown in Supplementary Materials (Fig. S1C). However, between 9 and 12 h there was a striking second phase of rapid killing of the bacteria (Fig. 1A1; *Killing phase*-2). This was followed by a third, slower killing phase that lasted until 48 h, when essentially all bacteria had been killed (Fig. 1A1; Killing phase-3) [38]. The non-GFP parental strain of *M. smegmatis* gave similar results (Results not shown). In mouse bone marrow macrophages the dynamics of *M. smegmatis*-GFP showed a superimposable pattern to that seen in J774 cells (not shown; Jordao et al, in preparation).

Fig. 1A3 shows the fraction of intracellular *M. smegmatis* that can be stained with propidium iodide after isolating bacteria from cells, and are therefore presumably killed. As expected, the fraction of killed bacteria increases steadily over 24 h except during the period of bacterial growth (4-9 h). The quantitative analysis of extracellular *versus* intracellular bacteria (shown in Fig. S2) shows that after the first few hours the fraction of extra-cellular bacteria is negligible, arguing that we were essentially dealing only with intracellular bacteria throughout this study. The fact that after the phase of bacterial growth the macrophages subsequently recovered robustly, excluded trypan blue at all stages and grew normally after the resolution of infection argues against bacterial-induced necrosis or apoptosis.

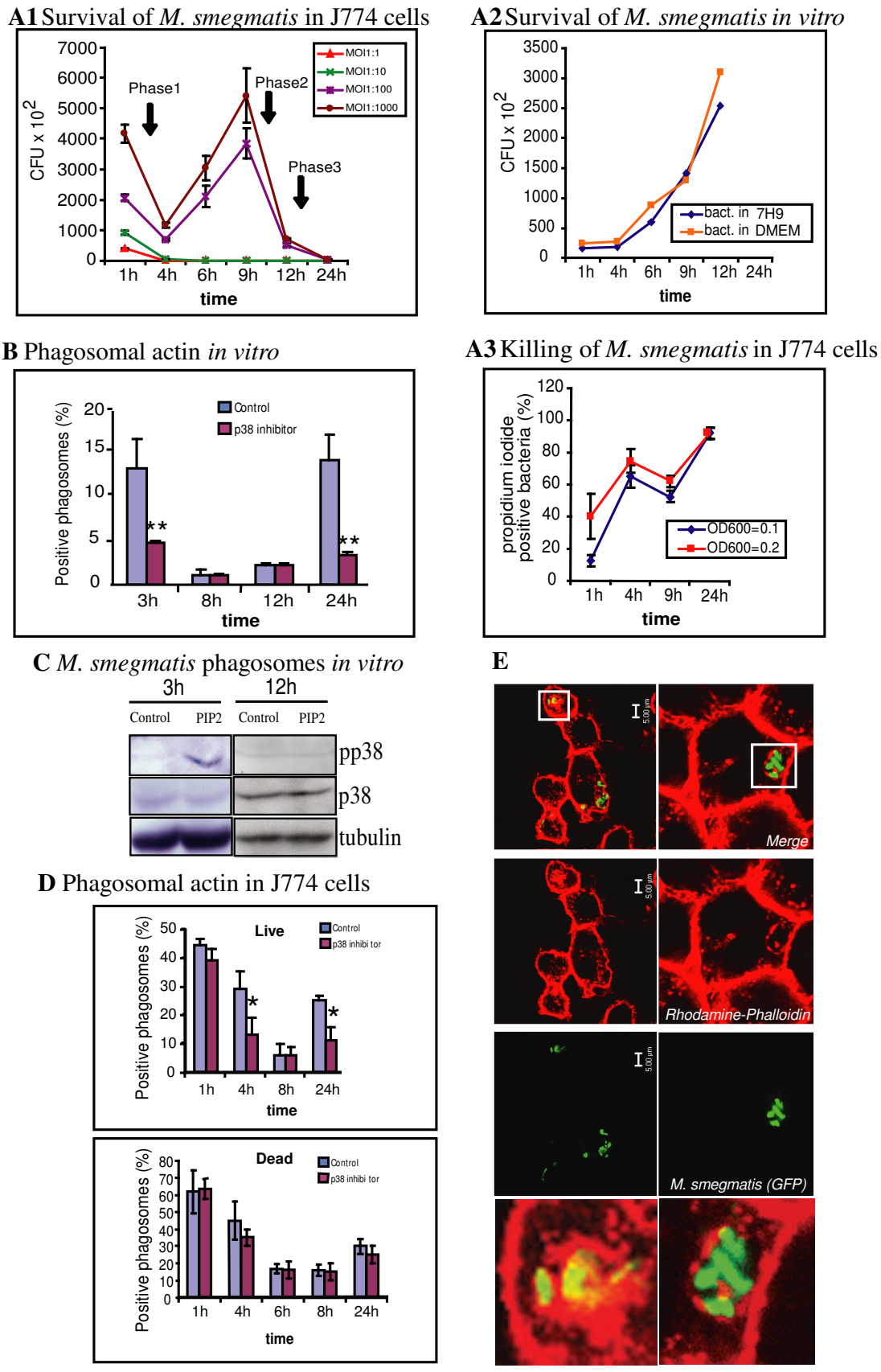

Figure 1. **Intracellular fate of *M. smegmatis* and phagosome assembly of actin.**

A1. Showing the CFU for *M. smegmatis* (GFP) in J774 cells over the time of infection. The three killing phases are indicated. MOI indicates multiplicity of infection, macrophages:

bacteria. A2. Showing *in vitro* growth of the bacteria in two different media. A3. Showing the percentage of dead bacteria inside macrophages over time. B. Quantification of *M. smegmatis* phagosome actin assembly *in vitro* with and without the p38 inhibitor. C. Western blots of p38 and phospho-p38 with *M. smegmatis* phagosomes isolated at 3h or 12 h post-infection with 0.2 mM ATP and without the co-incubation with 50 μM PIP_2. Anti tubulin was used as a loading control. D. Quantification of the percentage of phagosomes with associated actin, using rhodamine phalloidin, in cells infected with live and killed *M. smegmatis*, plus and minus the p38 inhibitor. E. Showing double label immunofluorescence microscopy of cells infected with live *M. smegmatis* (GFP-green) for 3 h labelled with rhodamine phalloidin (red). Asterisks indicate significant differences as determined by the Student's T test: *P<0.07; ** P<0.001.

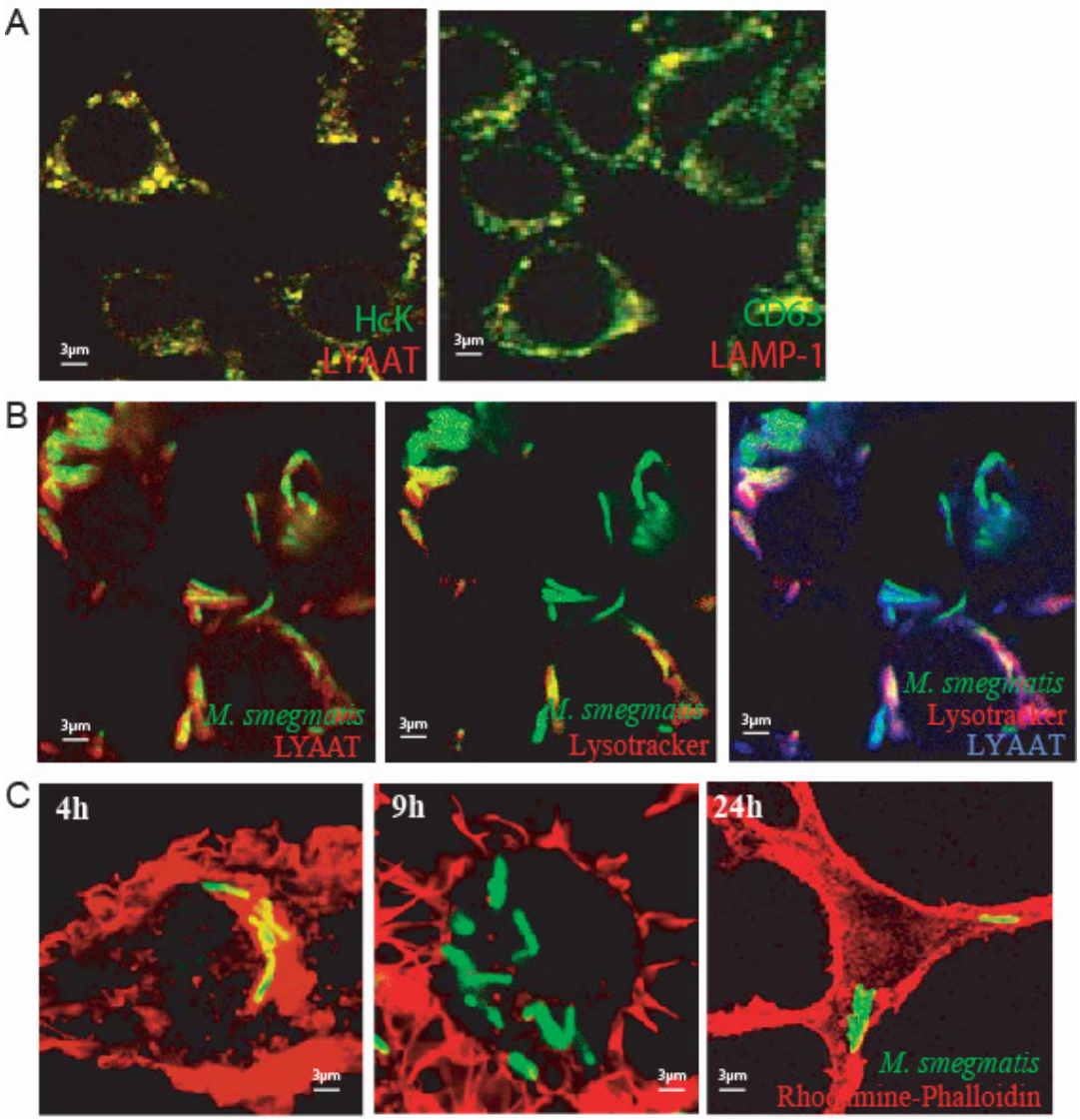

Figure S1. Co-localization of late endocytic markers in J774 cells

A. Uninfected J774 cells- left image, double labelled with LYAAT (red) and Hck (green) and right image, with CD 63 (green) and LAMP-1 (red). In both combinations there is extensive

overlap. B. Showing a triple label experiments with GFP-*M. smegmatis* infected J774 cells (2h infection) labelled with Lysotracker red and LYAAT, in red in the original (left panel) but converted to blue, false color in the right panel, which shown three-colors. C. Showing intracellular *M. smegmatis* at the indicated times in J774 cells that were also labelled with rhodamine phalloidin.

This unexpected complexity of the interactions between the macrophages and *M. smegmatis* offered a kinetic, clockwise description of the process that provided the foundation for all subsequent experiments; in these, infection conditions giving approximately 5-10 bacteria per cell were used.

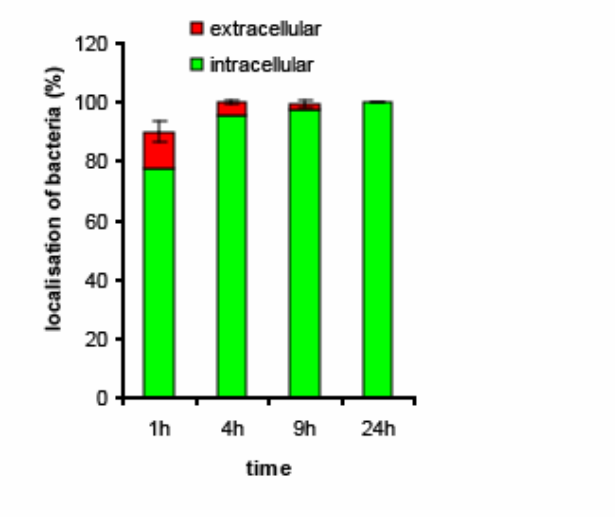

Figure S2. Quantitation of extracellular *versus* intracellular *M. smegmatis*.
Macrophages were infected with *M. smegmatis* and subsequently fixed at the indicated times with 2 % paraformaldehyde. Non internalized bacteria were detected using a rat anti *M. smegmatis* serum followed by an anti- rat antibody coupled to Cy3. Results are given as percentage of green (intracellular) and red (extracellular) bacteria.

In vitro assembly of actin by *M. smegmatis* phagosomes

The kinetics of survival of *M. smegmatis* in J774 cells resembled patterns of activities seen with LBPs. These showed a periodic pattern of activity in assembling actin *in vitro* and in macrophages, being active at 2-4 h and 24 h, but inactive at 12 h (maturation times before isolation)[47]; this also coincided with the LBP PIP_2-levels, and kinase-activities [48,49]. We therefore monitored *in vitro* actin assembly by live *M. smegmatis*-containing phagosomes isolated from macrophages at different infection times and phagosomes nucleating the polymerization of rhodamine actin were quantified [47]. As

shown in Fig. 1B, *M. smegmatis* phagosomes were active for actin assembly at 3 and 24 h, but not at 12 h, thus resembling the pattern seen with LBP. The periods of high activity coincide with the first and third, but not the second phase of *M. smegmatis* killing (Fig. 1A1).

As shown in Fig. 1B, the inhibitor of p38, SB203580 (which blocks macrophage p38 activation, see Fig. 2A3 and A4), inhibited the assembly of F-actin by live *M. smegmatis* phagosomes at both the 3 and 24 h 'active' stages, but did not influence the (already low activity) 8-12 h stages. Incubation of these phagosomes with a lipid effector known to activate actin assembly on LBP, phosphatidylinositol-4, 5 bis-phosphate (PIP_2), as well as 0.2mM ATP [8] led to a significant activation of the phosphorylated (active) form of p38 with active (3h) phagosomes, but not with inactive (12 h) phagosomes. When *M. smegmatis* (3h) phagosomes or 12 h phagosomes were treated with ATP in the absence of PIP_2 the level of activated p38 was below the level of detection (Fig. 1C). Collectively, these data argue that p38 activation is a positive regulator of actin assembly by *M. smegmatis* phagosomes.

Phagosomal actin in infected macrophages

We next investigated actin associated with the *M. smegmatis* phagosomes in J774 macrophages using rhodamine-phalloidin [8]. Labelled actin could be seen around many of the phagosomes (Fig.1E). As seen in Fig. 1D, F-actin accumulated around phagosomes enclosing live bacteria in a similar cyclical pattern to that seen *in vitro*, being high at 2-4 and 24 h and low at the 8 h time point. The results for phagosomes from cells having killed bacteria were very similar (Fig. 1D). A similar phenomenon was seen with LBPs in J774 cells [47].

The p38 inhibitor inhibited actin associated with phagosomes enclosing live bacteria at the 4 h and 24 h time points with no effect seen at other stages. In contrast, it had no effect on this parameter with the killed bacterial phagosomes (Fig. 1D). This provided the first hint that the presence of the live *M. smegmatis* could influence the interactions between the phagosomes and the macrophages via pathways involving p38.

Macrophage activation of p38 MAP kinase

Given the observed effects of p38 on actin assembly by *M. smegmatis* phagosomes we next followed the activity of p38 in macrophages over the time of infection. For this, we again took advantage of the antibody that specifically recognizes the active,

phosphorylated form of p38 as well as an antibody against the total protein. Uninfected (and unstimulated) cells showed a constant level of total p38 but no detectable phospho-p38 (Fig. 2A3 and A4). Following 'infection' with killed *M. smegmatis,* there was a significant activation of cellular p38 already after 20 min, with a small signal even after 5 min (Fig. 2A1). The bulk of an active p38 was then switched off by 1 h; a faint signal remained until 8 h. In contrast, infection with live bacteria reproducibly delayed total macrophage p38 phosphorylation until 2h (Fig. 2A2). By 4 h, (coincident with the end of killing 1), the levels of the active p38 were visibly reduced**,** but by 8 h (start of killing phase 2), there was again a robust re-activation of p38 with no activity detected at 24 h. These data argue that the presence of live *M. smegmatis* delays the ability of the cell to activate p38 until 2h, but thereafter a more complex pattern of activation, de-activation, re-activation was observed. Fig. 2A3 and A4 shows that the p38 inhibitor completely blocked phosphorylation of p38 in active stages of both live and killed *M. smegmatis*-infected macrophages.

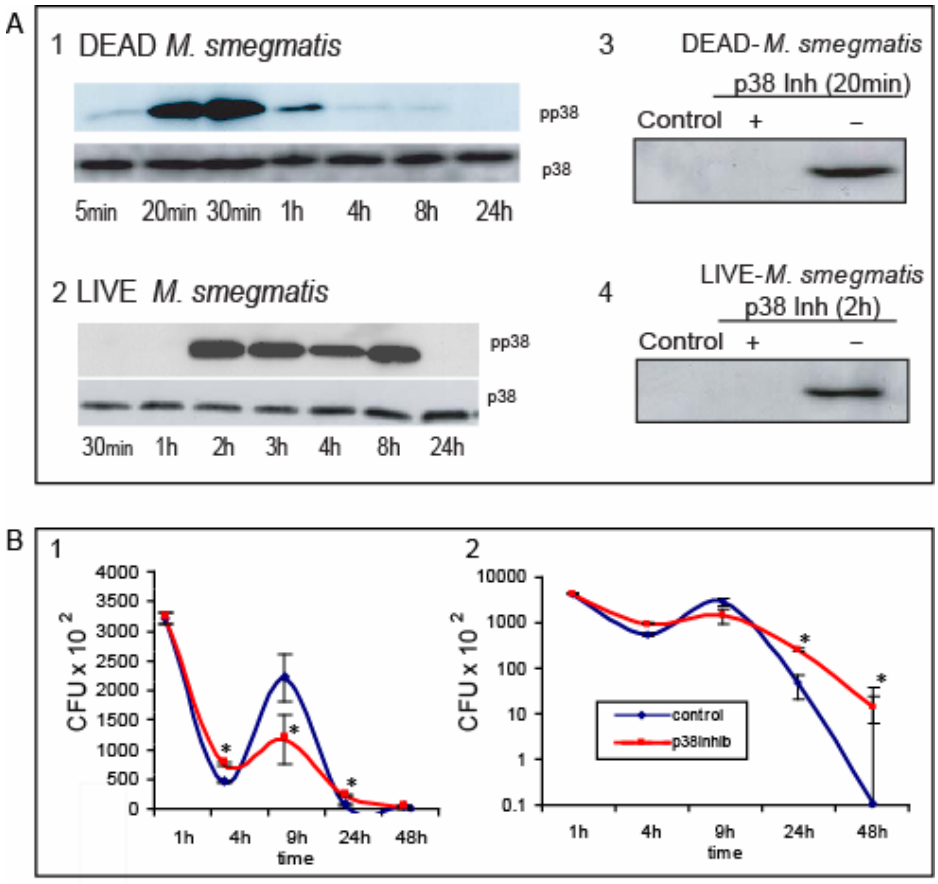

Figure 2. p38 activity in infected cells

A1 and A2. Western blots for total macrophage p38 and phospho-p38 (pp38) for live and killed *M. smegmatis*- infected cells over the time-course of infection. A3 and A4: The inhibitor

SB203580 completely blocks p38 activation in both live (2h) and killed *M. smegmatis*-infected cells (20 min). Control = uninfected J774 cells without treatment. B. Linear scale (left panel) and log scale (right panel) show the effects of the p38 inhibitor on *M. smegmatis* survival in J774 cells**.** The asterisks indicate significant differences as determined by Student's T-test * P< 0.001.

Role of p38 in intracellular survival of *M. smegmatis*

Because p38 appeared to regulate processes important for phagosome maturation but was also somehow subverted by the live *M. smegmatis* we tested the effects of its inhibitor on the survival of the bacteria in macrophages. As seen in Figs. 2B1 (linear scale) and B2 (log scale) treatment of infected cells with the p38 inhibitor led to a small but significant increase in bacterial numbers in the first and second/third killing phases relative to the untreated controls. By this score, p38 is mostly favouring the cell at early and late times of infection. However, during the central period this kinase seems to favor *M. smegmatis* growth because, when inhibited it significantly reduced bacterial multiplication. This provides evidence that the live bacterium takes advantage of p38 activity for some 'survival' functions.

Use of markers for late endocytic organelles

The notion that phago-'lysosome' fusion is implicated in killing is complicated by the fact that the term lysosome here actually refers to a still poorly defined assembly of late endocytic organelles. In many cells including J774 these compartments are conventionally separated into the more proximal late endosomes and the more distal lysosomes that are functionally distinct [50-53]. We therefore decided to undertake a detailed analysis of the acquisition of different late endocytic markers by live and killed *M. smegmatis* phagosomes, and the role of p38 in these events. As the phagosome is a more discrete structure than endosomes or lysosomes it is useful to identify different types of late endosomes by the extent by which they fuse with, and deliver their contents into phagosomes. When two membrane or content markers, from endocytic compartments are delivered into phagosomes with distinct rates it leads to the hypothesis that the compartments are distinct.

We analyzed up to seven different labels/markers known or expected to be in late endocytic organelles to follow their acquisition by GFP-*M. smegmatis* phagosomes by light microscopy. These were (i) Colloidal gold conjugated to rhodamine internalized

for 1 h plus 1 h chase [50,54,55]; (ii) LAMP-1 labelling, which labels both 'late endosomes' and 'lysosomes' [50]; (iii) Lyso-tracker labelling to identify organelles with a pH below 5.5-6.0; (iv) Immunofluorescence microscopy (IF) labelling for the V-0 subunit of the V-ATPase [56]; (v) IF for CD63, which, like LAMP is enriched in late endosomes' and 'lysosomes [57,58]; (vi) IF for LYAAT, a recently characterized membrane transporter for apolar amino acids out of ' lysosomes'[59,60]. This marker was found to significantly co-localize with Hck in human macrophages [61]; and (vii) finally IF for Hck [61].

Table 1. Colocalization of different late endocytic markers by immunofluorescence microscopy in uninfected J774 cells

Marker	LAMP-1	VATPase	LYAAT	CD63	Hck	Lyso	Gold
LAMP-1	---	1.8	3.1	75.2	13.6	39.4	43.3
VATPase	1.8	---	ND	ND	ND	67.9	17.2
LYAAT	3.1	ND	---	ND	67.8	39.5	13.2
CD63	75.2	ND	ND	---	ND	ND	ND
Hck	13.6	ND	67.8	ND	---	ND	ND
Lyso	39.4	67.9	39.5	ND	ND	---	63.6
Gold	43.3	17.2	13.2	ND	ND	63.6	---

ND, not determined

Table 1 shows a summary of an extensive series of double-labelling IF that we carried out on uninfected J774 cells. Examples of key experiments are shown in the Supplementrary Material (Fig. S3). Many surprises emerged from this analysis, which are relevant for the analysis of infected cells. Only 2 % of V-ATPase-positive vesicles were also labelled for LAMP-1, perhaps the most extensively used marker for both late endosomes and lysosomes. LAMP-1 itself significantly overlapped (though not completely) with CD63 (which was not used in subsequent experiments). Nevertheless the majority (67 %) of V-ATPase-positive structures were acidic enough to accumulate lyso-tracker; this value was actually higher than the fraction of gold-positive or LAMP-labelled structures that were acidic. The LYAAT labelled structures were also non-overlapping with LAMP-labelled structures although they strongly co-localised with Hck. While this analysis is certainly not definitive, and still restricted to the light

microscopy level, the results indicated that we could expect complex patterns when we followed the acquisition by phagosomes of five of these markers in detail.

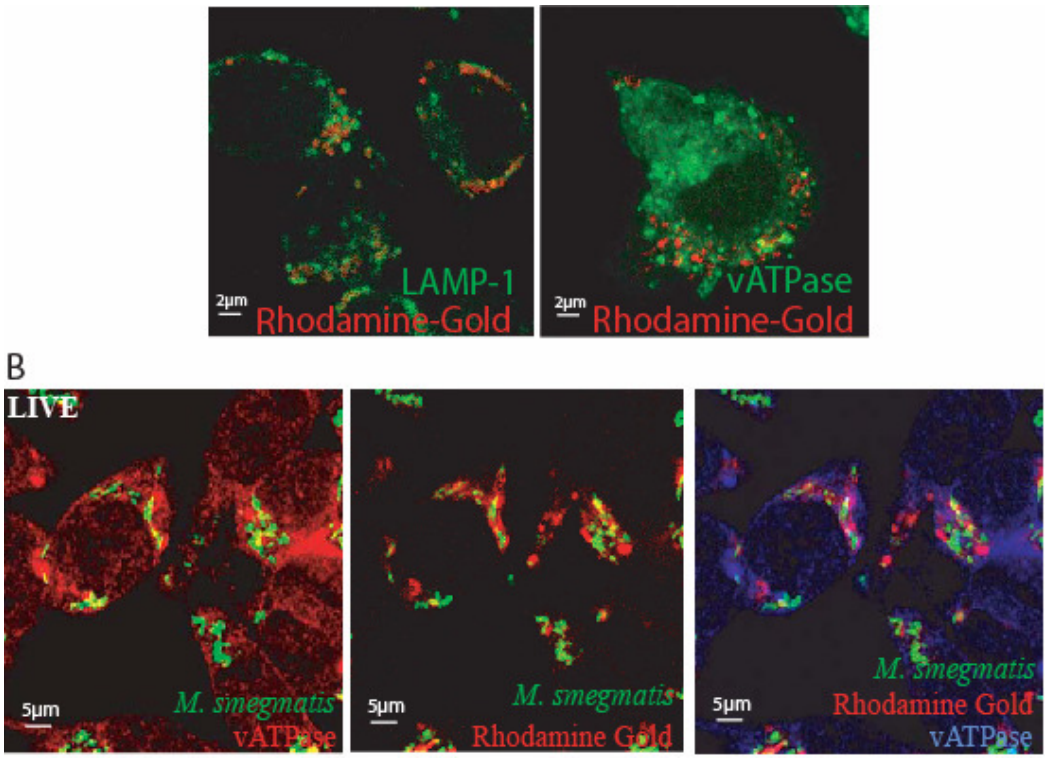

Figure S3. Co-localisation of markers with phagosomes

A. Showing colocalization of the indicated marker combinations in uninfected J774 cells. B. Showing a triple label experiments to show the distributions of live GFP-*M. smegmatis* relative to rhodamine gold (red) and V-ATPase (blue) at 4 h post-infection.

Phagosome-late endocytic organelle fusion

Content mixing: A new light microscopy-based fluorescence assay using colloidal gold conjugated to rhodamine was first applied to cells infected with *M. smegmatis* (see Experimental Procedures). We used conditions known from electron microscopy analysis to allow equilibrium filling with gold of (the accessible part of what we defined previously as) late endosomes and lysosomes [52,54,55]. This marker was preinternalised prior to infection with the GFP-*M. smegmatis*. Fusion is evident as bright fluorescent dots or a halo adjacent to the GFP-labelled bacteria (Fig. 3A and inset). Up to 90 % of live *M. smegmatis* phagosomes fused with gold compartments by 3h (Fig. 3B). There was a significant drop in the fraction of labelled phagosomes at the 4-12 h period, indicating recycling out of phagosomes, a process described by previously [14,62-65]. A second period in which gold was reaquired by phagosomes was seen between 12 and 24 h. As for the phagosomal actin assembly activity, the high fusion stages coincided with

killing phases 1 and 3, but not 2 (Fig. 1A1). For killed *M. smegmatis,* the initial rate of fusion was similar to that seen with live bacterial phagosomes. However, no detectable recycling of content out of these phagosomes was seen (Fig. 3C). Thus, the ability of the phagosome to recycle out content depends on the presence of the live bacterium.

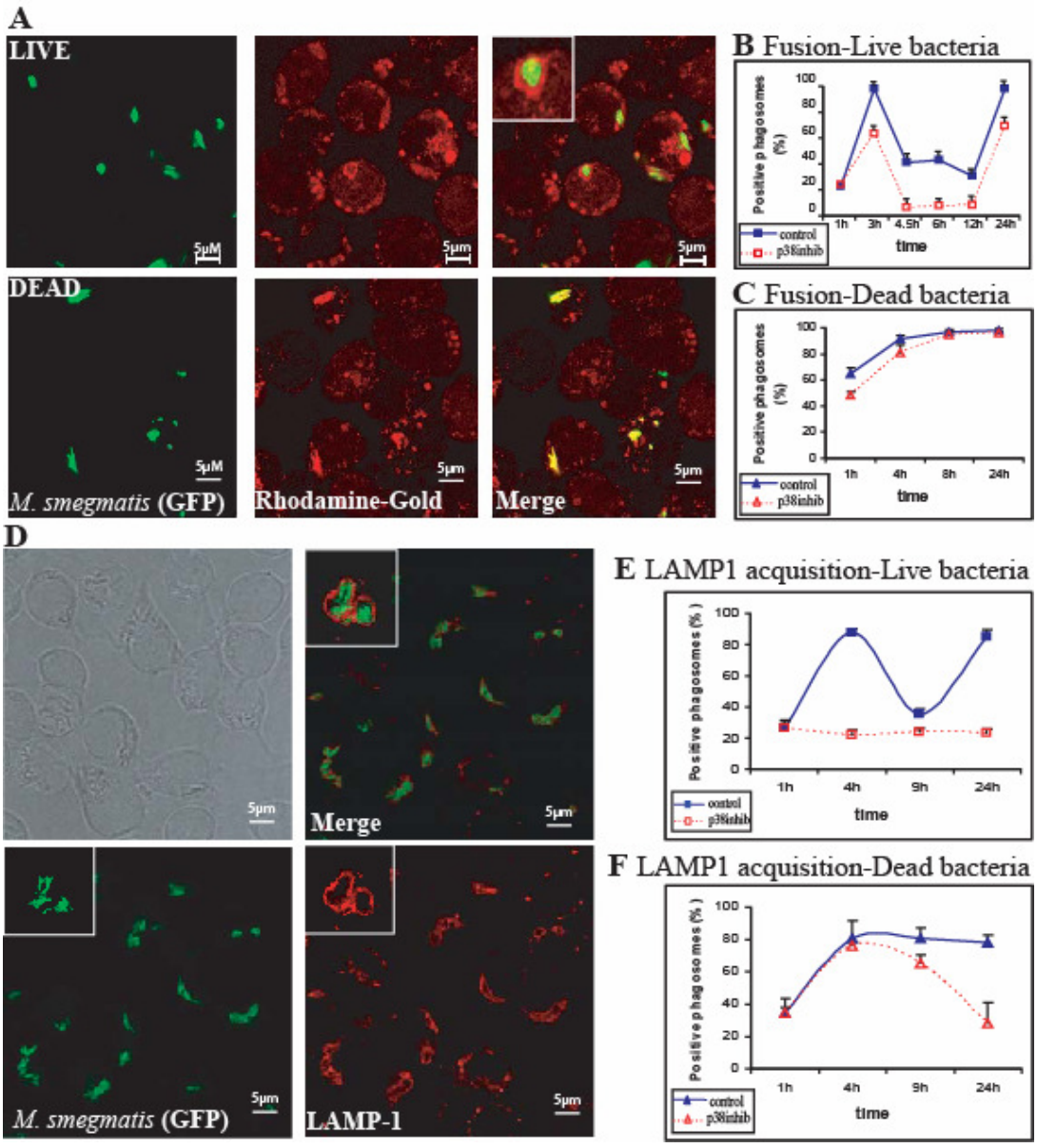

Figure 3. **Phagosome fusion with late endosomes and lysosomes**

A. Showing examples of the rhodamine-gold (7nm) (red) fusion assay with live and killed *M. smegmatis* (green) (3h) infected J774 cells. The inset shows a higher magnification of the colocalization of phagosomes having live bacteria with gold. B and C show the kinetic results for the acquisition of gold by live and killed *M. smegmatis* phagosomes, with and without p38 inhibitor. D-F. Showing the corresponding labelling and quantitation for LAMP-1.

Treatment with the p38 inhibitor over the course of the infection had a significant inhibitory effect on the fusion of live *M. smegmatis* phagosomes with gold-filled 'late endosomes' at all time points between 3 and 24 h, although less inhibition was observed at 24 h (Fig. 3B). This result could also be interpreted as an inhibition of p38 at the 3h time point with all subsequent processes behaving normally (because a downward shift of the curve is seen with the inhibitor). The inhibition at 3h fits well with the general macrophage activation of p38 at this time whereas the recycling out of phagosomes at 4.5h (Fig. 3B) coincides with a lowered amount of macrophage phospho-p38 at 4 h (Fig. 2A2).

The inhibitor had a less dramatic effect on the kinetics of fusion with dead bacterial phagosomes: a small but significant inhibition of fusion was seen at early, but not late times after phagocytosis (Fig. 3C). This fits with the restricted early activation of total p38 in response to dead bacteria (Fig. 2A1). These data argue that p38 activation favours the macrophage since its inhibition lowers the rate of acquisition of gold by phagosomes, at least at early stages.

LAMP-1: The unexpected recycling of content out of the phagosomes of live, but not killed *M. smegmatis* led us to test whether a membrane marker would behave similarly. We labelled live and killed bacteria-infected cells with anti-LAMP-1 (Figs. 3D and Fig. S3A). As shown in Fig. 3E and F, LAMP-1 was delivered efficiently to both live and killed bacterial phagosomes with kinetics similar to that of the gold content marker (Fig. 3B). LAMP-1 recycled out of phagosomes having live, but not killed bacteria (Fig. 3E and F). Thus, in what can be considered 'routine' or 'housekeeping ' phagocytosis LAMP is acquired by the majority of phagosomes by 4 h and remains there until 24 h, as it does with LBPs [66]. It was stricking that only with the live bacteria was the recycling of membrane (LAMP-1) marker and content (gold) seen after the initial fusion event. This recycling step was followed by a second wave of acquisition of both markers by phagosomes that coincide with killing stage 3. For LAMP-1 our data do not formally rule out the initial loss of signal is due to the molecule being locally degraded by live bacterial phagosomes followed by a subsequent wave of new synthesis.

The p38 inhibitor completely blocked the acquisition of LAMP-1 by live bacterial phagosomes, but it had no effect on LAMP-1 labelling of the killed bacterial phagosomes at early times, while strongly inhibiting its acquisition at late times of infection (Fig. 3E and F). These data argue that following 'housekeeping' phagocytosis,

the late fusion events that transfer LAMP (as for gold) to phagosomes are not dependent on p38. However, again, the presence of the live *M. smegmatis* dramatically alters the system such that the LAMP-fusion event is now totally dependent on p38. The different patterns of gold and LAMP-1 acquisition provided further evidence that the two compartments are not identical, although they significantly overlap (Table 1).

The amino acid transporter LYAAT: We next investigated LYAAT which is the least characterized marker of 'lysosomes' [59,60]. In uninfected cells, an anti-LYAAT antibody labelled vesicles that were widely distributed through the cell, but were quite distinct from structures enriched in LAMP-1 (Fig. S3A; Table 1). In cells infected with either live or killed *M. smegmatis* labelling for LYAAT could be seen around a fraction of phagosomes (Fig. S1). In both cases there was an early peak at 2h. However, no more than 40- 50 % of the live *M. smegmatis* phagosomes were positive for LYAAT at any time (Fig. 4A). Also for this marker some recycling out of phagosomes was seen between 4 and 10h. In contrast, the bulk (80 %) of the killed bacterial phagosomes acquired LYAAT within 1 h and maintained the marker thereafter, without a recycling event (Fig. 4A). These data are consistent with a 'constitutive' like process of the acquistion of LYAAT by the dead bacterial phagosomes with kinetics similar to the acquistion of LAMP-1. So, in 'routine' phagocytosis these different compartments (Table 1) fuse around the same time, and to similar extents with phagosomes. The presence of the live bacterium appears to actively modulate the system; unlike LAMP-1 which showed a dynamic recycling and re-acquisition after the first phase of fusion, the acquisition of LYAAT was apparently actively kept low at all infection times.

The inhibitor of p38 had no effect on LYAAT acquisition by either live or killed bacterial phagosomes in the first 4 h, with both showing a slight inhibition at 5h, and a continued inhibition was evident at some later times with live bacteria (Fig. 4A). Collectively, these data argue that LYAAT is delivered to phagosomes from a compartment distinct, and regulated differently, from gold- and LAMP-1-positive compartments. Again, these data show that live *M. smegmatis* actively modulates the system.

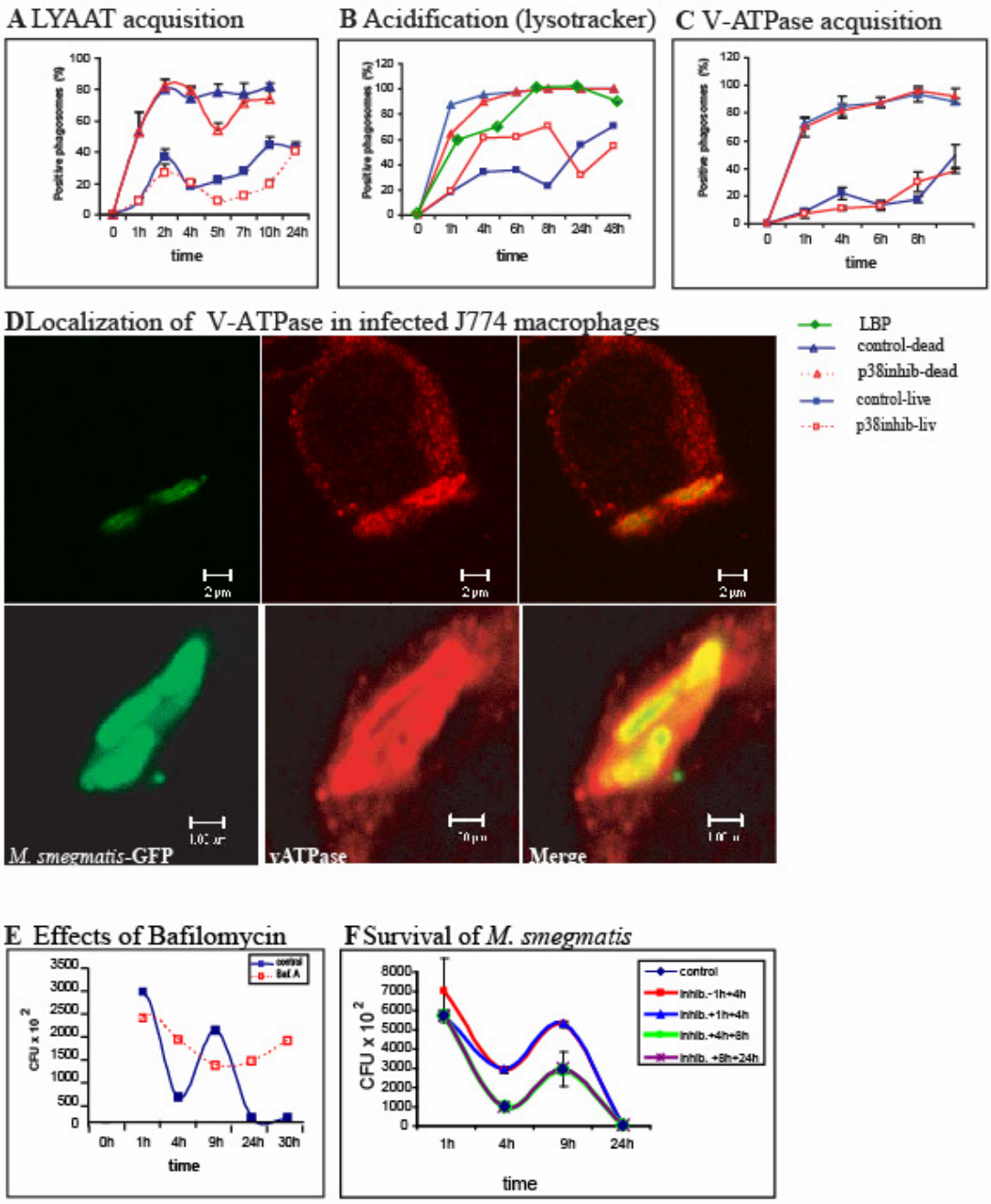

Figure 4. **Acquisition of late endocytic markers by *M. smegmatis* phagosomes**

A-C. Showing the quantification of the acquisition of the different indicated markers by live and killed *M. smegmatis* phagosomes, with and without p38 inhibitor. In B the acidfication profiles of latex bead phagosmes (LBP) are additionally shown in green. D. Showing double-labelling for V-ATPase (red) with live (green) *M. smegmatis* at 4 h post-infection. The lower panel shows a high magnification image. E. Indictating the effects of bafilomycin-A1 on intracellular survival of *M. smegmatis*. F. Showing the effect on *M. smegmatis* CFU of adding a cocktail of inhibitors of lysosomal proteases to the medium of cells either 1 h before infection or at the

indicated times. The lower curve is a superimposition of the blue, green and purple curves. The upper curve shows the two conditions in which the inhibitors were added coincident with the first killing period (blue triangles and red curves).

Phagosomal pH

Phagosomal pH is known to be important for optimal activities of most lysosomal enzymes and a pH below 5.5 is generally associated with a fully matured phagosome that is equipped to kill pathogens. We therefore analyzed the percentage of acidic phagosomes (pH < 5.5) in *M. smegmatis* infected cells for both live and killed bacteria using lyso-tracker-red [8]. With live bacteria only 20-25 % of the phagosomes accumulated lyso-tracker by 1 h PI, a level that rose only slightly over the next 7h (Fig. 4B). Only between 8 and 24 h did most phagosomes become acidic, coincident with killing phases 2 and 3 (Fig. 1A). In contrast, phagosomes containing the killed bacteria acidified rapidly, reaching levels above 80 % positive after 1 h and close to 100 % after 6h (Fig. 4B). This was similar to the kinetics of acidification seen with latex bead phagosomes (Fig. 4B). These results indicate that the live *M. smegmatis* actively delays the acidification process.

The p38 MAP kinase inhibitor had a surprising effect on the rate of acidification in live *M. smegmatis* phagosomes because it increased the fraction of phagosomes that acquired a low pH at early times (Fig. 4B). In contrast, it inhibited the acidification of dead bacterial phagosomes at 1 h, but not at later stages. This suggests that during 'housekeeping' phagocytosis the phagosomes are all acidified by about 4 h but only the early (1 h) stage of acidification is (positively) regulated by p38, a period in which the kinase is still active (Fig. 2A). In contrast, in the live *M. smegmatis*-infected cells p38-dependent signaling appears to be subverted by the bacteria to delay the full acidification of the phagosomes.

Vacuolar ATPase localisation

To acidify, the phagosomes must acquire the proton or vacuolar (V)-ATPase. We took advantage of a specific antibody against the Vo- (16KDa) subunit of the V-ATPase [56] to check for its presence on phagosomes. This labelled distinctly a fraction of the *M. smegmatis* phagosomes (Figs. 4D and Fig. S3). The kinetics and magnitude of the acquisition of the V-ATPase marker by live *M. smegmatis* phagosomes were similar to the corresponding pattern of acidification seen using lyso-tracker-Red (Fig. 4C; cf Fig.

4B). Thus, the 'housekeeping' dead bacterial phagosomes became almost all positive for V-ATPase by 6-8 h. In contrast, only 20 % of live bacterial phagosomes acquired the V-ATPase over the first 8 h, reaching around 50 % by 24 h. Thus the live bacteria actively modulate the system by inhibiting the acquisition by phagosomes of the V-ATPase.

In contrast to the effects seen with the acquisition of gold, LAMP-1 and LYAAT, there was little effect of the p38 inhibitor on the kinetics of acquisition of V-ATPase by either live or killed bacterial phagosomes. Here, we faced an apparent discrepancy between the lyso-tracker data (increase in acidification with p38 inhibitor) and the V-ATPase data (no increase). Possibly, V-ATPase from other compartments contributes to the increased acidification seen under some conditions. Related to this is the question of sensitivity. Lyso-tracker-positive organelles must, by definition have functional V-ATPase. However, many of these acidic vesicles do not label with the anti-V-ATPase, suggesting that they are below the detection levels for the enzyme by fluorescence microscopy. By this reasoning, the vesicles that do label must have relatively high concentrations of V-ATPase and are probably storage sites for the proton pump. Such an organelle might be analogous to V-ATPase-rich apical vesicles in gastric epithelial cells.

The comparison of the curves from Fig. 4A (LYAAT), Fig. 4B (acidification) and Fig. 4C (V-ATPase) for the live bacterial phagosomes shows very similar patterns and percentages of labelled phagosomes. This could suggest that LYAAT and the V-ATPase rich compartments are identical. However, whereas 68 % of the V-ATPase labelled phagosomes were lyso-tracker-positive only 40 % of the LYAAT-positive structures were acidic. Moreover, in parallel studies with *M. bovis* BCG we have found conditions where 80 % of phagosomes label for LYAAT whereas less that 15 % are positive for the V-ATPase in the same cells. We therefore feel justified in proposing a model whereby both these markers are enriched in functionally distinct compartments (Fig. 7B).

Effect of bafilomycin on *M. smegmatis* survival

The finding that the live *M. smegmatis* phagosome is able to delay the acidification of phagosomes suggests that a low pH is something the bacterium would prefer to avoid. If so, neutralising the pH of the phagosome should lead to an increase in survival. In agreement with this hypothesis the addition of bafilomycin A1, a potent inhibitor of the

V-ATPase to cells infected with live *M. smegmatis* prevented killing of the bacteria at all time points until 24 h PI (Fig. 4E). This indicates that a low pH is likely to be an important contributor to bacterial killing throughout the infection process. It is noteworthy that when the proton ATPase was blocked no growth of the bacteria was seen (Fig. 4E). Acidification of the phagosome may therefore serve to activate *M. smegmatis* for growth.

Role of lysosomal enzymes in bacterial survival.

The above data showed that many different late endocytic compartments fused with *M. smegmatis* phagosomes. Based on many studies by others we could expect that these fusion events delivered many 'lysosomal' hydrolases to the phagosomes [3]. We therefore asked whether some of these enzymes contributed to the ability of macrophages to kill *M. smegmatis*. Cells were therefore fed with a cocktail of lysosomal protease inhibitors (leupeptin, pepstatin, aprotinin) in order to load them by fluid-phase endocytosis into late endosomes and lysosomes. These were added either prior to the infection with live *M. smegmatis* or at the indicated times after infection (Fig. 4 F-upper curve). When added 1 h before infection and left on the cells until 3h, or added between 1 and 4 h PI, this cocktail significantly reduced the rate of the first bacterial killing stage (between 1 and 4 h), without affecting the subsequent growth of the bacteria until 9 h. As a consequence of the lowered killing when the inhibitors were added early in the infection the total growth seen subsequently was significantly higher than the untreated control (Fig. 4F). However, irrespective of when it was applied, it had no obvious effect on the subsequent stages of killing (Fig.4 F- lower curves). Thus, we conclude that the delivery of those lysosomal enzymes (susceptible to the inhibitors we used) into phagosomes during early times of fusion indeed contributes to the first-phase killing of the bacteria but, by these criteria we could not support the hypothesis that they were important in the two later killing phases.

Role of inducible NO-synthase and NO release

The best-characterised system for killing mycobacteria is that involving activation of iNOS to make NO and downstream metabolites that are known to facilitate killing of mycobacteria, including *M. smegmatis* [67,68]. We therefore investigated the role of this machinery in killing of *M. smegmatis.* For this, we first monitored NO using the Griess reagent. Cells infected with either live or killed bacteria produced detectable NO only at

early times (Fig. 5A). A more detailed analysis showed that between 15min and 2h similar levels of NO were made in cells infected with live or killed bacteria. The NO produced was the result of iNOS activation because a specific inhibitor of this enzyme (L-NAME; 500 µM) significantly inhibited NO release (Fig. 5A). Using an anti-iNOS antibody [69], by IF we could discern an increase in the level of iNOS expression in the cytoplasm after 1 h of infection with live or dead bacteria (Fig. 5G; not shown), in a pattern resembling that seen in γ-interferon treated-cells (Fig. S4). In infected cells, much of the labelling was detected in the vicinity of phagosomes (Fig. 5H; however, the association with phagosomes was difficult to quantify).

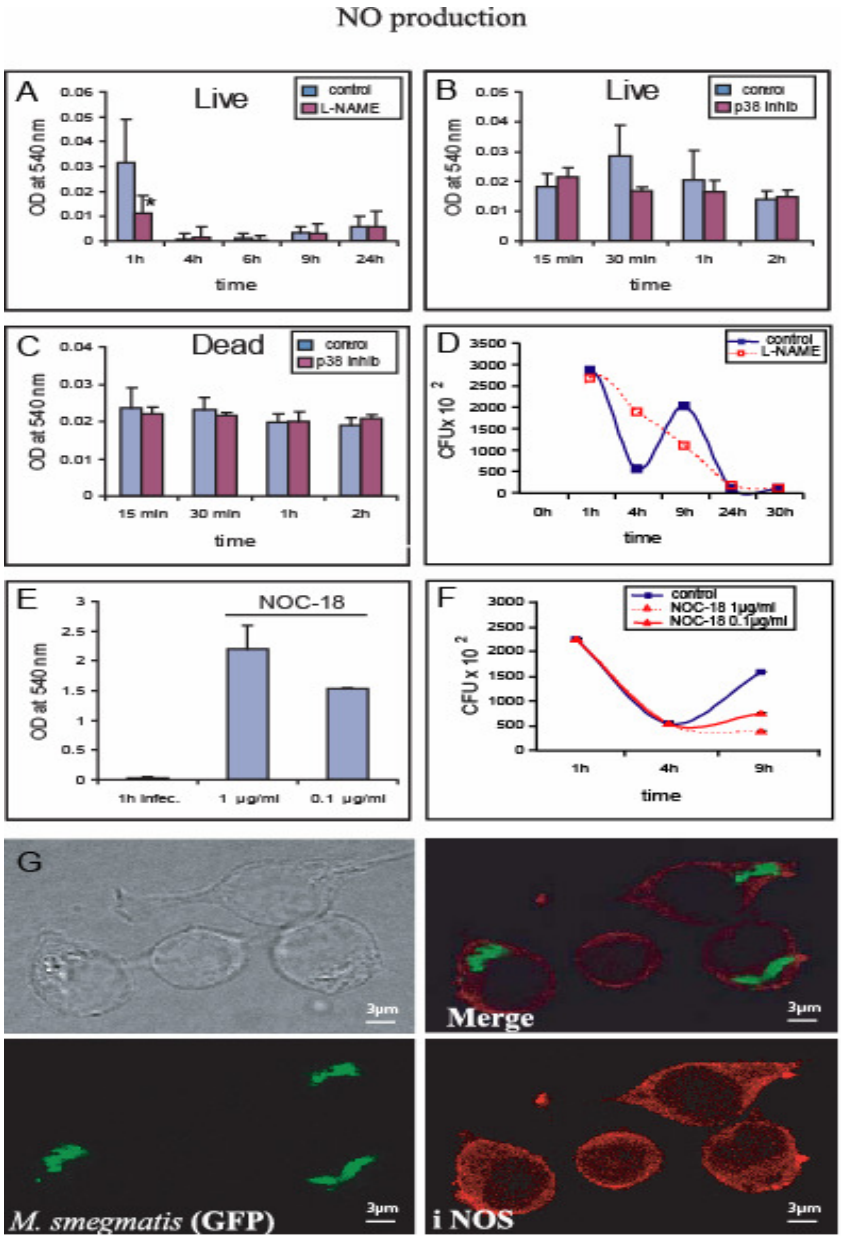

Figure 5. Nitric oxide release by infected J774 cells

A. Showing the synthesis of NO over the time course of *M. smegmatis* infection, with and without the iNOS inhibitor L-NAME; only the 1 h time point shows a significant difference between the untreated and the L-NAME treated cells by the Students t-test ($P<0.05$). B and C. Showing NO release from cells infected with live or killed *M. smegmatis*, with and without the p38 inhibitor, in the period when NO was produced. There were no significant differences in any of the values. D. Showing the effect of L-NAME on *M. smegmatis* intracellular survival. E. Showing the effect of the NO donor NOC-18 in elevating macrophage NO levels. F. Showing the effects of the NO donor NOC-18, added coincident with infection on CFU of *M. smegmatis*. G. Showing immunofluorescence labelling for iNOs in red in cells infected with GFP-*M. smegmatis*. The image in grey is the corresponding phase-contrast images.

The p38-inhibitor had no significant effect on the production of NO at any time in cells infected with either live or killed bacteria (Fig. 5B and C). The synthesis of NO by iNOS in this system is seen as an early, transient response to live or killed bacteria that is evidently independent of p38 signaling.

Effects of NO on survival of *M. smegmatis* in macrophages

The above data suggested that iNOS might contribute to killing *M. smegmatis,* but if so, this should be restricted to the first 2h when NO is detected. In agreement with this notion the inhibitor of iNOS (L- NAME) added coincident with infection was able to significantly block the first killing phase and thereafter a progressive killing was seen until 24 h. (Fig. 5D). As for bafilomycin treatment it was interesting to note that no bacterial growth was evident suggesting that RNI, like acidification, might provide positive cues for *M. smegmatis* growth. The addition of an artificial NO donor, NOC-18, that elevates NO levels in macrophages (Fig. 5E), when added between 4 and 9 h induced a dose-dependent inhibition of bacterial growth (Fig. 5F). Thus, even at this stage, *M. smegmatis* was still vulnerable to the effects of NO (or related metabolites). These data are consistent with the NO estimates and show that iNOS-dependent NO synthesis is an important first line of attack against *M. smegmatis.* However, under all conditions, this early phase was switched off before 4 h, the end of the first bacterial growth phase.

Mathematical modelling of intracellular bacterial growth

The cyclical behavior of the killing/growth of *M. smegmatis* opened up a paradox. At the end of 4 h the majority of bacteria are killed and at low multiplicities all of them are eliminated, in terms of their ability to grow in optimal media. Coinciding with this 4 h period, however is a period of recycling out of the phagosomes of a key membrane protein and its luminal contents. Why would the macrophage apparently work against its own killing needs, to the evident (transient) advantage of the bacteria?

We decided to investigate this using a mathematical model in which a defined number of live bacteria are added to a defined number of macrophages (Fig. 6A; for more details see Experimental Procedure). A doubling time of 3h was taken for *M. smegmatis* growing exponentially (Fig. 1A2). The model assumes that the macrophage has limited resources available that it can use in order to maintain an *average* killing rate k. We then assume that the cell can either maintain this killing rate constant or that it can modulate it with time. The experimental data (Fig. 1A1) suggest that cellular killing is less efficient for high numbers of bacteria per cell relative to low numbers. To satisfy this experimental observation we introduce an 'efficiency factor' e for the killing rate that is maximal (e = 1) for low numbers of bacteria and minimal (e = 0) for high numbers.

If the killing rate k is set constant at $k = k_0$ and if the effective killing rate *e* x k is lower than the bacterial growth rate exponential growth of bacteria is observed (Fig. 6E, high infectivity). However, when the killing activity was allowed to oscillate in time such that the average activity was still at the level k_0, two different scenarios were seen depending on the initial infection load. At low numbers (one bacterium per cell) a one-step killing was seen between 1 and 4 h (Fig. 6G - low infectivity). At high infection rates (seven bacteria per cell) cyclic phases of killing interspersed by bacterial growth was seen. Remarkably, the kinetics of both high and low number infections were in agreement with our experimental data (Fig. 1A1). In addition, the percentage of killed bacteria as a function of time (Fig. 6H) is in good agreement with the experimental data shown in Fig.1A3. A comparison of the constant versus oscillating killing activity (Fig. 6E and G; high infectivity) shows that in both cases that the activity was on average maintained at the same level (k_0), with the bacteria growing exponentially in one case (constant $k=k_0$ effective growth rate 0.16 h^{-1}) but were finally killed in the other case (oscillating k). These simulations provide a rationale for why the J774 and primary

macrophages may have evolved an oscillating type of killing activity toward *M. smegmatis*.

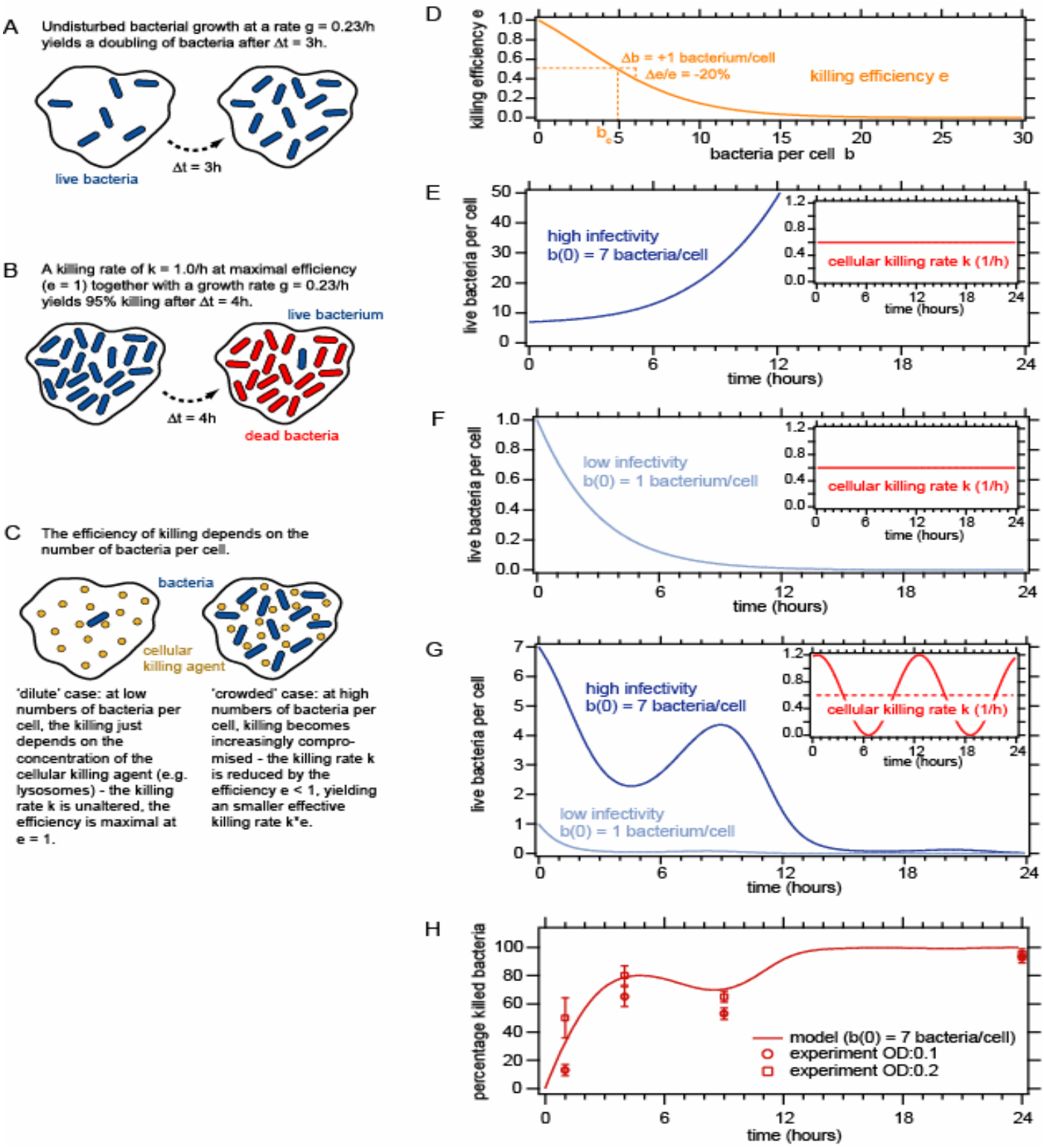

Figure 6. Mathematical modeling of infection

A. Undisturbed bacterial growth. B. Bacterial killing together with bacterial growth. C. The killing efficiency depends on the number of bacteria per cell. D. The killing efficiency is

maximal (e = 1) for low numbers of bacteria per cell and minimal (e = 0) for high numbers. E and F. Dynamics of live bacteria per cell in the case of a constant cellular killing activity for high (E) and low infectivity (F). G. Live bacteria per cell with an oscillating cellular killing activity for high and low infectivity. The insets (red curves) show the corresponding dynamics of the stable and oscillating conditions. H. Showing agreement between the predicted percentage of killed bacteria over time and the corresponding experimental results (cf Fig. 1A-3).

DISCUSSION

Here, we focused on *M. smegmatis* in J774 cells because we knew from previous work that this macrophage cell line invariably kills *M. smegmatis* within 48 h [8,38]. We initiated a broad cell biological analysis towards revealing the mechanisms by which this macrophage kills a so-called non-pathogenic mycobacterium. A role for NO and lysosomal proteases in killing *M. smegmatis* was identified. We expect that many of these mechanisms will also be relevant to understanding how pathogenic mycobacteria, the focus of our ongoing studies, are killed by macrophages.

J774 cells efficiently internalize both live and killed *M. smegmatis* and, in both cases, by 1-2 hr the vast majority of bacteria are in a potentially degradative (late) phagosomal compartment. Indeed, at low infection loads all live bacteria can be eliminated by 4 h. However, as the macrophage was challenged with increasing numbers of live bacteria a surprising complexity is seen in the dynamics of cell-bacterial interactions. This reflects the molecular tug of war for survival between the two protagonists. A summary of our data is shown in Fig. 7A which emphasizes the three major phases of killing and one of bacterial growth. Figure 7B is our working model whereby four different late endocytic compartments fuse with phagosomes.

Killing phase 1

The first detectable response of the cells is to release NO, starting already after 15 min but was over by the end of killing phase 1 (4 h) irrespective of whether the bacteria were alive or killed. NO contributed to killing as blocking its synthesis prevented the first killing phase (Fig. 5D). The macrophage evidently becomes programmed for releasing NO for a rather limited period in response to live or dead *M. smegmatis*. Live bacteria did not, however, become resistant to NO at later stages since an artificial increase in NO after 4 h could still efficiently kill them (Fig. 5F). Why the macrophage switches off iNOS activity remains an open question. It cannot be to protect the cell since J774 macrophages can secrete detectable NO for many days when they are infected with *M. bovis*-BCG (unpublished data). A fact to consider in future studies is if NO can directly activate the transcription of a large number of genes in cells infected with *M. tuberculosis* [70].

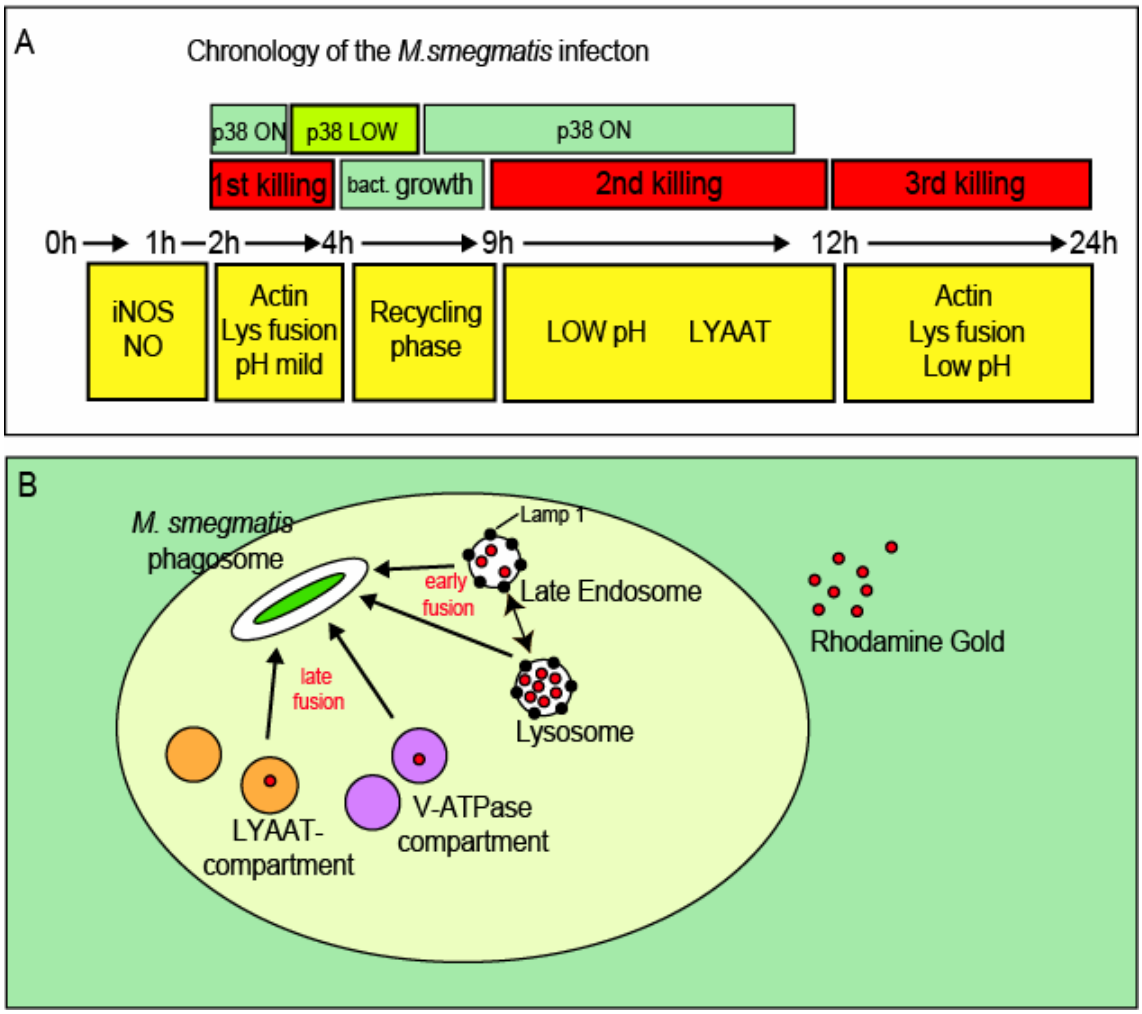

Figure 7. Summary models

A. Schematic description of the data with respect to the *M. smegmatis* life cycle. B. A summary of the up to four different vesicular compartments that appear to fuse with late stages of *M. smegmatis* phagosomes. The reversible arrow between LE and the lysosome indicates interactions seen earlier in J774 cells [52,53].

In the first killing phase (1-4 h) the macrophage evidently 'attacks' with its second weapon: late endosomes and lysosomes (defined by their accumulation of gold, and LAMP-1). These fuse with more than 90 % of phagosomes. As for NO release, the kinetics of this early event was similar for both live and killed bacteria. The lysosomal enzymes transferred to phagosomes must have contributed to killing because pre-loading macrophages with a (limited) cocktail of lysosomal enzyme inhibitors significantly reduced the early (but not later) killing effects (Fig. 2C). The overall pattern of the fusion events between phagosomes and late endosomes and lysosomes

coincided with phagosome actin assembly, providing still more evidence for links between these processes [8,40,41].

Although most phagosomes were lysotracker-negative (pH < 5.5-6) during the first 4 h, bafilomycin treatment of cells still prevented killing period 1 (Fig. 4C). Possibly this treatment neutralizes phagosomes having a pH above 6 but below 7. Intriguingly, under this conditions no bacterial growth was seen suggesting that low pH (like NO) may even favour bacterial growth. It should also be noted that bafilomycin treatment is known to stimulate some phagosome fusion events and inhibit others (or stimulate selective recycling out of phagosomes) [62]. Interpretation is also complicated by the observation that V-ATPase has recently been directly implicated in the mechanics of membrane fusion events [71,72].

Intracellular growth of *M. smegmatis*

By 4 h the macrophage could clear a 'light' infection with live *M. smegmatis*, but at numbers above about 1-5 per cell, these bacteria multiplied rapidly. Growth of *M. smegmatis* in monocytes was seen by others, but only after 1-4 days infection [37,39]. Thus, even a non-pathogenic strain of mycobacterium that normally grows in soil can express some 'pathogenic' characteristics. However, *M. smegmatis* growth was stringently limited (or loss) to the 4-9 h period; in J774 cells and in mouse primary macrophages it was followed by an efficient killing phase (which by itself argues against the notion that the growth of *M. smegmatis* at higher infection loads was detrimental to the macrophages). This growth-permissive period coincided with a striking recycling of a membrane protein, LAMP-1 and gold content marker out of most phagosomes with live, but not killed *M. smegmatis*. Whether this unexpected recycling is a response of the host cell 'sensing' the live bacteria, and perhaps 'lowering its guard', perhaps to divert resources for antigen presentation, or whether it is actively induced by the live bacteria will require further studies.

Killing phase 2

There was a striking and reproducible second phase of killing between 9 h and 12 h after infection in J774cells. This suggests that fusion between phagosomes and additional compartments must be occurring just prior to this period. Clearly, these compartments had to be distinct from conventional late endosomes and lysosomes since the bulk of both internalized gold content and LAMP-1 had recycled out of the

phagosomes during this period; they were re-acquired only after 12 h, coinciding with the third killing period.

In searching for additional compartment(s) that could fuse with phagosomes to facilitate the second killing we were faced with surprising complexity. Most unexpected was that the bulk of the detectable V-ATPase resides in a compartment that is distinct from the late endosomes and lysosomes (see below) that fuses significantly with the phagosomes at a relatively late stage, just before and coincident with killing phase 2. The emergence of killing phase 2 also coincided with a significant increase in the fraction of acidified phagosomes. Live *M. smegmatis* was able to significantly delay the acquisition of a low pH by the majority of phagosomes until 8 h (relative to killed bacteria or latex bead phagosomes). This is likely due to the delay in the delivery of the V-ATPase, since the kinetics of lysotracker labelling and the acquisition of the V-ATPase were quite similar with live bacteria (Fig. 4B and D). The delivery of active V-ATPase and acidification of phagosomes are likely to be crucial for this second (and third) killing phase since bafilomycin prevented them.

There were interesting parallels between the delivery to phagosomes of the V-ATPase/ acidification, and the acquisition of the membrane transporter LYAAT. This recently discovered marker [60] was rapidly acquired by dead bacterial phagosomes but, as for the acidification process, the presence of the live *M. smegmatis* in phagosomes led to a delay in LYAAT acquisition. Like the V-ATPase, the LYAAT compartments were mostly distinct from those that labelled for gold or LAMP-1 (see below). The tyrosine kinase HcK, which co-localizes with LYAAT in human macrophages [61] behaved similarly to LYAAT also in our system (Table 1). Overall, our data lead us to conclude that the V-ATPase-enriched structures and the LYAAT-labelled ones were distinct from each other and from LAMP–labelled vesicles [(which can be sub-divided into two compartments[73]. However, all these compartments can be classified as late endocytic organelles since at least a fraction of all of them are accessible to rhodamine gold following a chase period (Table 1; Fig. 7B). We conclude that much remains to be done in characterizing late endocytic organelles but these different compartments will all have to be considered if we are to understand what in the lumen contributes to killing.

Killing phase 3

Between 12 h and 24 h the macrophages initiated the third killing phase that was able to eliminate almost all live *M. smegmatis*. This coincided with a second cycle of

phagosomal actin assembly (seen *in vitro* and in cells) and of late endosome/lysosome fusion, as seen by the further acquisition of LAMP-1 and gold. The feeding of cells with the inhibitors of lysosomal enzymes that we used did not affect this killing phase. Either proteases are not involved, or the protease and non-protease enzymes that are involved were not susceptible to the effectors we used. At this last stage, the vast majority of the phagosomes were strongly acidic and bafilomycin treatment also blocked this killing stage. We cannot rule out that additional, still to be identified compartments need to fuse with the phagosomes to initiate this third, as well as the second killing phases. Based on our data we tentatively conclude that four different late endocytic organelles need to fuse with the mycobacterial phagosomes for maximum killing activity (Fig. 7B).

Role of p38 MAP kinase

The MAP kinase p38 emerged as an important regulator of a number of the processes involved in killing *M. smegmatis*, in agreement with other studies on mycobacteria [3,5,43,74-76]. Earlier studies linked p38 to endocytic fusion events [44] and to phagosome-endosome fusion [7] while here we additionally provide evidence for its importance in regulating phagosomal actin assembly, a process linked to some membrane fusion events [41]. Inhibiting this kinase blocked (the active periods of) phagosome actin assembly [8] *in vitro* while the addition of PIP_2 to *M. smegmatis*, that activates phagosome actin assembly, stimulated p38 activation (Figs. 1B and C). The inhibitor also blocked phagosomal actin in macrophages and, in agreement with our recent studies [8,41] this coincided with a corresponding inhibition of the fusion of phagosomes with late endosomes/lysosomes, most prominently seen with *M. smegmatis*. The MAP kinase p38 also regulates some stages in the delivery of LYAAT, as well as the delivery of the functional V-ATPase to acidify the phagosomes. While the complexity of this system defies a simple model, it is clear that p38 is a key regulator of both phagosome actin assembly and of most of the late fusion events involving phagosomes.

An unexpected finding was that p38 signaling could favour the macrophage for some functions but some cascades regulated by this kinase appear to have been subverted by *M. smegmatis* for its benefit. As evident in Fig. 2A1 and A2 the pattern of activation of macrophage p38 by live and killed *M. smegmatis* was totally different, with the cell responding quickly but transiently to the dead bacteria but showing a complex pattern of p38 activity with live ones. It is noteworthy that there was high p38 activity during at

least two of the killing periods. The macrophage and the live *M. smegmatis* thus appear to be in a 'tug of war' situation with respect to p38 signaling. Collectively, our data argue that these signaling events are part of the macrophage pro-inflammatory response. The activity of this MAP kinase normally facilitates many macrophage processes, but the live bacterium seems to have diverted part of its signaling response towards (i) delaying initial activation of p38 (Fig. 2A1 and A2); (ii) Delaying the delivery of V-ATPase and LYAAT to phagosomes (Fig. 4A and D); and (iii) facilitating its own growth (Fig. 2B). The p38 signalling system may have evolved as a 'sensor' that informs the macrophage of the existence of live bacteria. If so, it is a sensor that the mycobacteria had learnt to co-opt, and disrupt for its own goal, survival.

Our mathematical model of the system complemented our data by providing a dynamic description of the infection process. Without invoking any mechanisms of killing this model is based only on the following experimental facts (i) J774 macrophages have the propensity to kill all *M. smegmatis*; (ii) the cell shows cycles of high and low activity with respect to bacterial killing factors; (iii) *M. smegmatis* divides every 3h (*in vitro*; Fig. 1A2) and (iv) the efficiency of bacterial killing is reduced at high numbers of bacteria per cell, above about 5 [77]. The model revealed that whereas a certain level of killing set at a critical value (k_0) led to exponential bacterial growth, a time-modulated level of killing with an average value at k_0 not only prevented growth but led to effective killing. The dynamics of the *M. smegmatis* growth/killing seen experimentally in Fig. 1A1 at both low and high bacterial infection levels could be effectively simulated by this model (Fig. 6G). In addition, the time course of the percentage of killed bacteria was calculated (Fig. 6H) and shown to be in good agreement with the experimental data shown in Fig. 1A3. These simulations suggest that the macrophage can be more effective against the bacteria when it concentrates its killing activity to transient periods than when it 'spreads it out' evenly in a continuous manner. Another consideration is that the macrophage may be using up limited resources in every 'attack' that need to be thereafter replenished.

Evidently, the interactions between a macrophage cell line and a live mycobacterium destined for death is far more complex than one might expect. The macrophage does not (and to some extent is not allowed to) kill *M. smegmatis* by firing all its 'guns' in one 'shot' but rather the whole process is a dynamic interplay between the normal killing processes, that have a finite limit and capacity, and the presence in phagosomes of the live bacterium, that is fighting to survive. The activation of iNOS and of the fusion of

up to four (perhaps more) different compartments with phagosomes, all of which are likely contribute to the killing process, shows striking temporal regulation (Fig. 7A). Besides NO and some lysosomal proteases implicated in this study all the other factors that presumably operate to kill mycobacteria within the phagosome lumen remain to be identified.

MATERIALS AND METHODS

Cell Line and Bacterial Culture Conditions: The mouse macrophage cell line J774A.1 was cultured as described previously [8]. *M. smegmatis* mc2 155 harbouring a p19-(long-lived) EGFP plasmid was grown in medium containing Middlebrook's 7H9 broth Medium (Difco), Nutrient broth (Difco) (4.7 g; 5g per liter, respectively), supplemented with 0.5 % glucose and 0.05 % Tween 80 at 37°C on a shaker at 220 rpm. In order to stabilize GFP expression medium was supplemented with Hygromycin (50 µg per ml) and bacteria were subcultured every day in fresh medium for 7-10 days before use in infection studies.

Macrophage infection: Bacterial cultures in exponential growth phase were pelleted, washed twice in PBS pH 7.4 and re-suspended in DMEM medium to a final OD_{600}:0.1. Clumps of bacteria were removed by ultrasonic treatment of bacteria suspensions in a ultrasonic waterbath for 15 min followed by a low speed centrifugation (120 *g*) for 2 min. Single cell suspension was verified by light microscopy.

J774 cells were seeded onto 24 well tissue culture plates at a density of $0.5x10^5$ cells per well and were incubated for two days until 90 % confluency and infected with bacteria at different multiplicity of infection (M.O.I). When we infected macrophages that were onl yaround 70 % confluent we observed significant macrophage cell death. To achieve more than five bacilli per macrophage after 1 h uptake, a M.O.I of 100:1 was used (OD_{600}~0.1). In each experiment, after 1 h infection gentamycin (10µgml^{-1}) was added. A number of control experiments were made to ensure that this concentration of antibiotic killed all extracellular bacteria without affecting the intracellular ones (Results not shown).

Treatment with Inhibitors: When required cells were treated with specific inhibitors, unless otherwise stated these were added from 0 to 1 h after uptake, and left throughout the experiment. The inhibitors were: p38 MAPK inhibitor SB203580 (2 µM) (Calbiochem), the V-ATPase inhibitor, bafilomycin A1, 100nM (Sigma), the iNOs inhibitor L-NAME [N(G)-nitro-L-arginine methyl ester hydrochloride (Sigma; 500µM)] and the NOC-18 (Sigma; 0.1 or 1µg ml^{-1}) For testing the protease inhibitors effect on the *M. smegmatis* survival, a cocktail of 100 µM of Leupeptin, Aprotinin and Pepstatin was added to the culture medium for the times shown in Fig. 2C. At the end of the

incubations, intracellular bacteria was recovered by lysis of infected macrophages using a 1 % Igepal CA-630 (Sigma) solution in water and plated in medium for CFU counting.

Epifluorescence and Confocal Fluorescence Microscopy: Macrophages grown on glass coverslips were allowed to take up latex beads or bacteria. Cells were fixed with 3 % paraformaldehyde in PBS at room temperature for 15 min. Cell permeabilization, when required, was achieved with 3 min treatment with 1 % Triton X100 in PBS. After blocking with 2 % fetal calf serum in 40mM glycine-PBS, cells were incubated for 30 min with primary antibody, followed for further 30 min by secondary antibody. For actin labelling *in vivo* rhodamine phalloidin was used as described before [8]. Lysotracker Red DND-99 (Molecular Probes) staining of acidic organelles was carried out by adding a 1:20,000 dilution in DMEM that was added for the last 30 min of the experiments. For propidium iodide staining infected macrophages were washed with PBS and lysed with 1 % Igepal in water. Bacteria were recovered by 10 min centrifugation at 10000 rpm in a table-top centrifuge and washed twice in water. Subsequently, dead bacteria were stained by 5 $\mu g ml^{-1}$ propidium iodide. Confocal microscopy images were collected using the Zeiss LSM510 and the percentage of colocalisation was calculated using either the Image J software system or manually. Fluorescence labelling and viability of mycobacteria was performed as described [8].
The following antibodies were used for immunofluorescence microscopy: Anti CD63 and anti Hck were from Santa-Cruz. The rabbit antibody against LYAAT-1 [60] was kindly provided by Dr B. Giros (Créteil, France). Anti-mouse LAMP-1 was purchased from the Iowa Hybridoma bank. The rabbit V-ATPase antibody against the 16 KDa subunit was described by Skinner *et al* [78].The rabbit iNOS antibody was kindly provided by Dr Michael Marletta (University of Berkeley) [69]. For co-localization experiments of LAMP-1 and V-ATPase or LAMP-1 and LYAAT1 the secondary antibodies were linked with Cy3 and Alexa 488, respectively.

Fusion assay: Analysis of phagosome lysosome fusion was done using 7 or 15nm gold particles prepared according to Slot and Geuze. Gold particles were saturated with 20 % of BSA and centrifuged once for 45 min, 10 000*g*. The pellet was suspended in PBS-Rhodamine-NHS (1mg ml^{-1}) and rotated on a wheel for 1 h, washed three times with PBS Glycine 50 mM and resuspended in a small volume of PBS - Glycine 50mM -

azide 0.02 % (for storage; this was dialyzed away before use). The OD was estimated at 520 nm and the rhodamine gold particles are used with an OD_{520} of 1 in culture medium in all fusion experiments. Cells were pulsed for 1 h with these gold particles, washed 3 times with PBS and chased for 1 h or longer in complete culture medium. Infection with mycobacteria was then allowed for 1 h (OD_{600} of 0.1 for mycobacteria) in complete medium without antibiotics. Cells were washed extensively with PBS and chased for the different, indicated time points of fusion, fixed in PBS-paraformaldehyde (4 %) and analyzed by confocal microscopy.

Isolation of phagosomes: Latex bead or mycobacterial containing phagosomes were isolated as described before [8].

Actin nucleation: This assay was described in detail by Defacque *et al.* [48]. In all experiments described the errors reported are the standard deviations from at least three separate experiments.

Nitric oxide: was measured using Griess reagent following the supplier's (Sigma) instructions.

Preparation of whole cell extracts and immunoblot analysis: Cells where washed twice with PBS and lysed in IP buffer (50 mM Tris pH 7.5, 150 mM sodium chloride, 1 mM EDTA, 1 mM EGTA, 1 % NP-40 and protease inhibitors) at 4ºC for 30 minutes. The extracts were sonicated in 5 s bursts until complete homogenization and centrifuged at 13000*g* for 10 min to remove cell debris. When SB203508 was used, cells were treated for 1 h before infection with 2 μM SB203508. After 1 h uptake the medium was removed, cells were washed three times and new drug was added to the medium. Equal amounts of protein were loaded on a 12 % SDS-PAGE, transferred to nitrocellulose membrane and probed with a rabbit anti-phospho p38 and anti total p38 (Cell Signaling Technology). Enhanced chemi-luminescence (Pierce biotechnology) was used to visualize antibody binding.

M. smegmatis (live or heat killed) phagosomes were isolated as previously described [8]. For the incubations with PIP_2 phagosomes were incubated under actin nucleation conditions (without actin and thymosin beta 4) with 0.2mM ATP, with or without the lipid. For membrane purification prior to running SDS gels phagosomes were

centrifuged at 24000g for 30 min. Pellets were treated as described above for preparation of whole cell extracts and immunoblot analysis. Anti-tubulin (Sigma) was used to assess the amount of total protein in the different membrane isolates.

Mathematical modeling.

Principle of the simulation: A defined number of intracellular bacteria B were contained within a defined number of macrophage cells C. If they were not disturbed by cellular defense mechanisms, the intracellular bacteria grew exponentially with a growth rate g (see also Fig. 6A)

$$dB/dt = g \times B \qquad (1)$$

$$\Rightarrow \quad B(t) = B(0) \times \exp(g \times t)$$

The growth rate g is related to the doubling time t_2 by

$$g = \ln(2) / t_2 \qquad (2)$$

The cellular response to invading bacteria was described by a cellular killing rate k (see also Fig. 6B)

$$dB/dt = -k \times B \qquad (3)$$

$$\Rightarrow \quad B(t) = B(0) \times \exp(-kxt)$$

We assumed that an individual cell has only limited resources available in order to maintain a certain *average* killing rate k_0 (Rook, 1981). The rate can either be constant over time $k = k_0$ (inset Fig. 6E and F) or it can be a function of time $k = k(t)$ (inset Fig. 6G) with an *average* rate k_0 (dashed line) determined by the limited resources available.

As the experimental data shows cycles of high and low cellular activity, we assumed a sinusoidal modulation of the killing rate as a first approximation (inset Fig. 6G)

$$k(t) = k_0 + k_1 \times \sin(2\pi \times \nu \times t) \qquad (4)$$

where k_0 is the time-averaged killing rate and k_1 the amplitude of the modulation with a frequency ν.

The experimental data (Fig. 1A1) suggests that cellular killing is less efficient for high numbers of bacteria per cell b = B/C compared to low numbers of b. Therefore we introduced a killing efficiency factor e(b) that was multiplied to the killing rate :

$$dB/dt = - e(b) \times k(t) \times B \qquad (3')$$

The killing efficiency has to be maximal (e = 1) for low numbers of bacteria per cell ($b \rightarrow 0$) and minimal (e = 0) for high numbers of b. Such a behavior is described by a sigmoidal curve (Fig. 6D)

$$e(b) = [1 + \exp(-b_0 \times s)] / \{1 + \exp[(b-b_0) \times s] \} \qquad (5)$$

At a critical bacterial density

$$b_c = \ln[2 + \exp(b_0 \times s)] / s \qquad (6)$$

the killing efficiency drops to its half value $e(b_c) = 0.5$ The parameter s describes how sensitive the efficiency e(b) depends on the bacterial density at $b = b_c$. A high value for s (unit cells per bacterium) means that the killing efficiency e(b) depends strongly on the bacterial density b, a low value that it depends weakly on b.

In our model, the total number of cells C was assumed to be fixed, therefore the efficiency e(b) depends directly on the number of bacteria B and can be written as e(B). Taking together the equations (1) and (3') yields the following differential equation for the number of bacteria B

$$dB/dt = [g - e(B) \times k(t)] \times B \qquad (7)$$

This equation was solved in order to derive the graphs shown in Fig. 6 (E - H).

Parameters: For the graphs shown in Fig. 6 (D - H), the following parameters were chosen: The doubling time t_2 = 3 h of *M. smegmatis* was derived from Fig. 1A2 yielding a growth rate of g = 0.23 h^{-1} according to equation (2).

The killing rates can be estimated from intracellular bacterial survival curves (Fig. 1A1). For the case of an oscillating killing rate (Fig. 6G and H), the oscillation frequency was ν = 2/day to ensure a transition between high and low killing rates every 6 h as observed experimentally. The average of the killing rate was chosen k_0 = 0.6 h^{-1} and the amplitude was k_1 = 0.6 h^{-1} ensuring almost complete killing within the first 4 h in case of low infectivity (Fig. 6G, low infectivity). In order to compare the case of a constant killing rate with the case of an oscillating one, the constant killing rate k = k_0 = 0.6 h^{-1} was used for Fig. 6E and F.

To model the observed reduced killing efficiency for high numbers of bacteria per cell a critical bacterial density of b_c = 4.9 bacteria per cell (b_0 = 2.8 bacteria per cell) and a sensitivity of s = 0.3 cells per bacterium was used for the graphs in Fig. 6.D - H. With these parameters, the killing efficiency drops by $\delta e/e$ = -20 % if the bacterial density is increased by δb = +1 bacterium per cell around the critical density b_c (Fig. 6D).

The kinetics of live bacteria for high and low infectivity shown in Fig. 6G are in agreement with our experimental data (Fig. 1A1). In addition, the percentage of killed bacteria (number of killed bacteria divided by total number of bacteria) as a function of time was calculated (Fig. 6H) and shown to be in good agreement with the experimental data from Fig. 1A3. A comparison of the constant (Fig. 6E) versus the oscillating killing activity (Fig. 6G, high infectivity) at high infectivity shows the following: Although the killing rate was on average at the same level (k_0 = 0.6 h^{-1}), the bacteria grow exponentially (with an effective growth rate of 0.16 h^{-1}) in case of a constant rate (Fig. 6E) but are finally killed in the case of an oscillating rate (Fig. 6G).

Acknowledgments

We thank Sergei Kuznetsov, Sabrina Marion, Edith Elliott, Albert Haas and Maria Isabel Colombo for their constructive comments and support. Drs Bernard Giros and

Michael Marletta generously supplied us with antibodies against LYAAT and iNOS, respectively. We also acknowledge generous funding from the Deutsche Forshungs Gemeinshaft to Gareth Griffiths. This investigation also received financial support from the UNICEF/UNDP/World Bank/WHO Special Program for research and Training in tropical diseases (TDR) (to GG). Elsa Anes's work was supported by Fundação para a Ciência e a Tecnologia (FCT) grant POCTI/38983/BCI/2001 with co-participation of the European Community Fund FEDER.

REFERENCE LIST

1. Armstrong,J.A. & Hart,P.D. Phagosome-lysosome interactions in cultured macrophages infected with virulent tubercle bacilli. Reversal of the usual nonfusion pattern and observations on bacterial survival. *J Exp Med.* **142**, 1-16 (1975).

2. Cosma,C.L., Sherman,D.R. & Ramakrishnan,L. The secret lives of the pathogenic mycobacteria. *Annu. Rev. Microbiol.* **57**, 641-676 (2003).

3. Vergne,I., Chua,J., Singh,S.B. & Deretic,V. Cell biology of mycobacterium tuberculosis phagosome. *Annu. Rev. Cell Dev. Biol.* **20**, 367-394 (2004).

4. Denis,M. Involvement of cytokines in determining resistance and acquired immunity in murine tuberculosis. *J Leukoc. Biol.* **50**, 495-501 (1991).

5. Roach,S.K. & Schorey,J.S. Differential regulation of the mitogen-activated protein kinases by pathogenic and nonpathogenic mycobacteria. *Infect. Immun.* **70**, 3040-3052 (2002).

6. Schaible,U.E., Collins,H.L. & Kaufmann,S.H. Confrontation between intracellular bacteria and the immune system. *Adv. Immunol* **71**, 267-377 (1999).

7. Via,L.E. *et al.* Effects of cytokines on mycobacterial phagosome maturation. *J Cell Sci* **111 (Pt 7)**, 897-905 (1998).

8. Anes,E. *et al.* Selected lipids activate phagosome actin assembly and maturation resulting in killing of pathogenic mycobacteria. *Nat. Cell Biol.* **5**, 793-802 (2003).

9. Nolta,K.V., Rodriguez-Paris,J.M. & Steck,T.L. Analysis of successive endocytic compartments isolated from *Dictyostelium discoideum* by magnetic fractionation. *Biochim. Biophys. Acta* **1224**, 237-246 (1994).

10. Paroutis,P., Touret,N. & Grinstein,S. The pH of the secretory pathway: measurement, determinants, and regulation. *Physiology. (Bethesda.)* **19**, 207-215 (2004).

11. Rodman,J.S., Stahl,P.D. & Gluck,S. Distribution and structure of the vacuolar H+ ATPase in endosomes and lysosomes from LLC-PK1 cells. *Exp Cell Res.* **192**, 445-452 (1991).

12. Desjardins,M. & Griffiths,G. Phagocytosis: latex leads the way. *Curr. Opin. Cell Biol.* **15**, 498-503 (2003).

13. Lukacs,G.L., Rotstein,O.D. & Grinstein,S. Phagosomal acidification is mediated by a vacuolar-type H(+)-ATPase in murine macrophages. *J Biol. Chem.* **265**, 21099-21107 (1990).

14. Pitt,A., Mayorga,L.S., Stahl,P.D. & Schwartz,A.L. Alterations in the protein composition of maturing phagosomes. *J Clin. Invest* **90**, 1978-1983 (1992).

15. Sun-Wada,G.H., Wada,Y. & Futai,M. Lysosome and lysosome-related organelles responsible for specialized functions in higher organisms, with special emphasis on vacuolar-type proton ATPase. *Cell Struct. Funct.* **28**, 455-463 (2003).

16. de Chastellier,C., Lang,T. & Thilo,L. Phagocytic processing of the macrophage endoparasite, *Mycobacterium avium*, in comparison to phagosomes which contain *Bacillus subtilis* or latex beads. *Eur. J Cell Biol.* **68**, 167-182 (1995).

17. Lowrie,D.B., Andrew,P.W. & Peters,T.J. Analytical subcellular fractionation of alveolar macrophages from normal and BCG-vaccinated rabbits with particular reference to heterogeneity of hydrolase-containing granules. *Biochem. J* **178**, 761-767 (1979).

18. Silva,M.T., Appelberg,R., Silva,M.N. & Macedo,P.M. *In vivo* killing and degradation of *Mycobacterium aurum* within mouse peritoneal macrophages. *Infect. Immun.* **55**, 20062016 (1987).

19. Sturgill-Koszycki,S. *et al.* Lack of acidification in *Mycobacterium* phagosomes produced by exclusion of the vesicular proton-ATPase. *Science* **263**, 678-681 (1994).

20. Long,R., Light,B. & Talbot,J.A. Mycobacteriocidal action of exogenous nitric oxide. *Antimicrob. Agents Chemother.* **43**, 403-405 (1999).

21. Jagannath,C., Actor,J.K. & Hunter,R.L., Jr. Induction of nitric oxide in human monocytes and monocyte cell lines by *Mycobacterium tuberculosis*. *Nitric. Oxide.* **2**, 174-186 (1998).

22. Macmicking,J.D. *et al.* Identification of nitric oxide synthase as a protective locus against tuberculosis. *Proc. Natl. Acad. Sci. U. S. A* **94**, 5243-5248 (1997).

23. Rich,E.A. *et al. Mycobacterium tuberculosis* (*MTB*)-stimulated production of nitric oxide by human alveolar macrophages and relationship of nitric oxide production to growth inhibition of *MTB*. *Tuber. Lung Dis.* **78**, 247-255 (1997).

24. Chan,E.D., Chan,J. & Schluger,N.W. What is the role of nitric oxide in murine and human host defense against tuberculosis?Current knowledge. *Am. J Respir. Cell Mol. Biol.* **25**, 606612 (2001).

25. Flynn,J.L. & Chan,J. Immune evasion by Mycobacterium tuberculosis: living with the enemy. *Curr. Opin. Immunol* **15**, 450-455 (2003).

26. Nathan,C. & Shiloh,M.U. Reactive oxygen and nitrogen intermediates in the relationship between mammalian hosts and microbial pathogens. *Proc. Natl. Acad. Sci U. S. A* **97**, 8841-8848 (2000).

27. Zahrt,T.C. & Deretic,V. Reactive nitrogen and oxygen intermediates and bacterial defenses: unusual adaptations in *Mycobacterium tuberculosis*. *Antioxid. Redox. Signal.* **4**, 141-159 (2002).

28. Armstrong,J.A. & Hart,P.D. Response of cultured macrophages to *Mycobacterium tuberculosis*, with observations on fusion of lysosomes with phagosomes. *J Exp. Med.* **134**, 713-740 (1971).

29. Clemens,D.L. & Horwitz,M.A. Characterization of the *Mycobacterium tuberculosis* phagosome and evidence that phagosomal maturation is inhibited. *J Exp. Med.* **181**, 257-270 (1995).

30. Clemens,D.L., Lee,B.Y. & Horwitz,M.A. Purification, characterization, and genetic analysis of *Mycobacterium tuberculosis* urease, a potentially critical determinant of host-pathogen interaction. *J Bacteriol.* **177**, 5644-5652 (1995).

31. Crowle,A.J., Dahl,R., Ross,E. & May,M.H. Evidence that vesicles containing living, virulent *Mycobacterium tuberculosis* or *Mycobacterium avium* in cultured human macrophages are not acidic. *Infect. Immun.* **59**, 1823-1831 (1991).

32. Fenton,M.J. & Vermeulen,M.W. Immunopathology of tuberculosis: roles of macrophages and monocytes. *Infect. Immun.* **64**, 683-690 (1996).

33. Frehel,C., de Chastellier,C., Lang,T. & Rastogi,N. Evidence for inhibition of fusion of lysosomal and prelysosomal compartments with phagosomes in macrophages infected with pathogenic *Mycobacterium avium*. *Infect. Immun.* **52**, 252-262 (1986).

34. Sturgill-Koszycki,S., Schaible,U.E. & Russell,D.G. *Mycobacterium*-containing phagosomes are accessible to early endosomes and reflect a transitional state in normal phagosome biogenesis. *EMBO J* **15**, 6960-6968 (1996).

35. Gomes,M.S. *et al.* Survival of *Mycobacterium avium* and *Mycobacterium tuberculosis* in acidified vacuoles of murine macrophages. *Infect. Immun.* **67**, 3199-3206 (1999).

36. Flynn,J.L. & Chan,J. Immunology of tuberculosis. *Annu. Rev. Immunol* **19**, 93-129 (2001).

37. Barker,K. *et al.* Nonadherent cultures of human monocytes kill *Mycobacterium smegmatis*, but adherent cultures do not. *Infect. Immun.* **64**, 428-433 (1996).

38. Kuehnel,M.P. *et al.* Characterization of the intracellular survival of *Mycobacterium avium ssp*. paratuberculosis: phagosomal pH and fusogenicity in J774 macrophages compared with other mycobacteria. *Cell Microbiol.* **3**, 551-566 (2001).

39. Lagier,B. *et al.* Identification of genetic loci implicated in the survival of *Mycobacterium smegmatis* in human mononuclear phagocytes. *Mol. Microbiol.* **29**, 465-475 (1998).

40. Jahraus,A. *et al.* ATP-dependent membrane assembly of F-actin facilitates membrane fusion. *Mol. Biol. Cell* **12**, 155-170 (2001).

41. Kjeken,R. *et al.* Fusion between phagosomes, early and late endosomes: a role for actin in fusion between late, but not early endocytic organelles. *Mol. Biol. Cell* **15**, 345-358 (2004).

42. Morrison,D.K. & Davis,R.J. Regulation of MAP kinase signaling modules by scaffold proteins in mammals. *Annu. Rev. Cell Dev. Biol.* **19**, 91-118 (2003).

43. Schorey,J.S. & Cooper,A.M. Macrophage signalling upon mycobacterial infection: the MAP kinases lead the way. *Cell Microbiol.* **5**, 133-142 (2003).

44. Cavalli,V. *et al.* The stress-induced MAP kinase p38 regulates endocytic trafficking via the GDI:Rab5 complex. *Mol. Cell* **7**, 421-432 (2001).

45. Fratti,R.A., Chua,J. & Deretic,V. Induction of p38 mitogen-activated protein kinase reduces early endosome autoantigen 1 (EEA1) recruitment to phagosomal membranes. *J Biol. Chem.* **278**, 46961-46967 (2003).

46. Anes,E. *et al.* Dynamic life and death interactions between *Mycobacterium smegmatis* and J774 macrophages. *Cell Microbiol.* **8**, 939-960 (2006).

47. Defacque,H. *et al.* Involvement of ezrin/moesin in de novo actin assembly on phagosomal membranes. *EMBO J* **19**, 199-212 (2000).

48. Defacque,H. *et al.* Phosphoinositides regulate membrane-dependent actin assembly by latex bead phagosomes. *Mol. Biol. Cell* **13**, 1190-1202 (2002).

49. Emans,N., Nzala,N.N. & Desjardins,M. Protein phosphorylation during phagosome maturation. *FEBS Lett.* **398**, 37-42 (1996).

50. Griffiths G. On vesicles and membrane compartments. *Protoplasma* **195**, 37-58 (1996).

51. Jahraus,A., Storrie,B., Griffiths,G. & Desjardins,M. Evidence for retrograde traffic between terminal lysosomes and the prelysosomal/late endosome compartment. *J Cell Sci* **107 (Pt 1)**, 145-157 (1994).

52. Tjelle,T.E., Brech,A., Juvet,L.K., Griffiths,G. & Berg,T. Isolation and characterization of early endosomes, late endosomes and terminal lysosomes: their role in protein degradation. *J Cell Sci* **109 (Pt 12)**, 2905-2914 (1996).

53. Luzio,J.P. *et al.* Membrane traffic to and from lysosomes. *Biochem. Soc. Symp.* 77-86 (2005).

54. Jahraus,A. *et al. In vitro* fusion of phagosomes with different endocytic organelles from J774 macrophages. *J Biol. Chem.* **273**, 30379-30390 (1998).

55. Rabinowitz,S., Horstmann,H., Gordon,S. & Griffiths,G. Immunocytochemical characterization of the endocytic and phagolysosomal compartments in peritoneal macrophages. *J Cell Biol.* **116**, 95-112 (1992).

56. Skinner,M.A., MacLaren,L.A. & Wildeman,A.G. Stage-dependent redistribution of the V-ATPase during bovine implantation. *J Histochem. Cytochem.* **47**, 1247-1254 (1999).

57. Escola,J.M. *et al.* Selective enrichment of tetraspan proteins on the internal vesicles of multivesicular endosomes and on exosomes secreted by human B-lymphocytes. *J Biol. Chem.* **273**, 20121-20127 (1998).

58. Kobayashi,T. *et al.* The tetraspanin CD63/lamp3 cycles between endocytic and secretory compartments in human endothelial cells. *Mol. Biol. Cell* **11**, 1829-1843 (2000).

59. Boll,M., Foltz,M., Rubio-Aliaga,I., Kottra,G. & Daniel,H. Functional characterization of two novel mammalian electrogenic proton-dependent amino acid cotransporters. *J Biol. Chem.* **277**, 2296622973 (2002).

60. Sagne,C. *et al.* Identification and characterization of a lysosomal transporter for small neutral amino acids. *Proc. Natl. Acad. Sci U. S. A* **98**, 72067211 (2001).

61. Astarie-Dequeker,C., Carreno,S., Cougoule,C. & Maridonneau-Parini,I. The protein tyrosine kinase Hck is located on lysosomal vesicles that are physically and functionally distinct from CD63-positive lysosomes in human macrophages. *J Cell Sci* **115**, 81-89 (2002).

62. Claus,V. *et al.* Lysosomal enzyme trafficking between phagosomes, endosomes, and lysosomes in J774 macrophages. Enrichment of cathepsin H in early endosomes. *J Biol. Chem.* **273**, 9842-9851 (1998).

63. Damiani,M.T. & Colombo,M.I. Microfilaments and microtubules regulate recycling from phagosomes. *Exp Cell Res.* **289**, 152-161 (2003).

64. Pitt,A., Mayorga,L.S., Schwartz,A.L. & Stahl,P.D. Transport of phagosomal components to an endosomal compartment. *J Biol. Chem.* **267**, 126132 (1992).

65. Pitt,A., Mayorga,L.S., Schwartz,A.L. & Stahl,P.D. Assays for phagosome-endosome fusion and phagosome protein recycling. *Methods Enzymol.* **219**, 21-31 (1992).

66. Desjardins,M., Huber,L.A., Parton,R.G. & Griffiths,G. Biogenesis of phagolysosomes proceeds through a sequential series of interactions with the endocytic apparatus. *J Cell Biol.* **124**, 677-688 (1994).

67. Ehrt,S. *et al.* A novel antioxidant gene from *Mycobacterium tuberculosis*. *J Exp Med.* **186**, 1885-1896 (1997).

68. Yu,K. *et al.* Toxicity of nitrogen oxides and related oxidants on mycobacteria: *M. tuberculosis* is resistant to peroxynitrite anion. *Tuber. Lung Dis.* **79**, 191-198 (1999).

69. Miller,B.H. *et al.* Mycobacteria inhibit nitric oxide synthase recruitment to phagosomes during macrophage infection. *Infect. Immun.* **72**, 2872-2878 (2004).

70. Ehrt,S. *et al.* Reprogramming of the macrophage transcriptome in response to interferon-gamma and Mycobacterium tuberculosis: signaling roles of nitric oxide synthase-2 and phagocyte oxidase. *J Exp Med.* **194**, 1123-1140 (2001).

71. Bayer,M.J., Reese,C., Buhler,S., Peters,C. & Mayer,A. Vacuole membrane fusion: V0 functions after trans-SNARE pairing and is coupled to the Ca2+-releasing channel. *J Cell Biol.* **162**, 211-222 (2003).

72. Muller,O., Neumann,H., Bayer,M.J. & Mayer,A. Role of the Vtc proteins in V-ATPase stability and membrane trafficking. *J Cell Sci* **116**, 1107-1115 (2003).

73. Tjelle,T.E., Lovdal,T. & Berg,T. Phagosome dynamics and function. *Bioessays* **22**, 255-263 (2000).

74. Bhattacharyya,A., Pathak,S., Kundu,M. & Basu,J. Mitogen-activated protein kinases regulate *Mycobacterium avium*-induced tumor necrosis factor-alpha release from macrophages. *FEMS Immunol Med. Microbiol.* **34**, 73-80 (2002).

75. Blumenthal,A., Ehlers,S., Ernst,M., Flad,H.D. & Reiling,N. Control of mycobacterial replication in human macrophages: roles of extracellular signal-regulated kinases 1 and 2 and p38 mitogen-activated protein kinase pathways. *Infect. Immun.* **70**, 4961-4967 (2002).

76. Tse,H.M., Josephy,S.I., Chan,E.D., Fouts,D. & Cooper,A.M. Activation of the mitogen-activated protein kinase signaling pathway is instrumental in determining the ability of *Mycobacterium avium* to grow in murine macrophages. *J Immunol* **168**, 825-833 (2002).

77. Rook,G.A. Chromosomes for the enzyme-linked immunosorbent assay (ELISA) using horse-radish peroxidase. *Lepr. Rev.* **52**, 281-283 (1981).

78. Skinner,M.A. & Wildeman,A.G. Suppression of tumor-related glycosylation of cell surface receptors by the 16kDa membrane subunit of vacuolar H+-ATPase. *J Biol. Chem.* **276**, 48451-48457 (2001).

Chapter 3

On the killing of mycobacteria by macrophages

On the killing of mycobacteria by macrophages

Luisa Jordao[1], Christopher K. E. Bleck[2], Luis Mayorga[2,3], Gareth Griffiths[2*] and Elsa Anes[1*]

[1] Molecular Pathogenesis Centre, Unit of Retrovirus and Associated Infections, Faculty of Pharmacy, University of Lisbon, Av. Forcas Armadas, 1600-083 Lisbon, Portugal.

[2] EMBL, Postfach 102209, 69117 Heidelberg, Germany.

[3] Laboratorio de Biología Celular y Molecular, IHEM-CONICET, Facultad de Ciencias Médicas, Universidad Nacional de Cuyo, Mendoza-Argentina

[*]Corresponding Authors

Accepted for publication.

ABSTRACT

Both pathogenic and non-pathogenic mycobacteria are internalized into macrophage phagosomes. Whereas the non-pathogenic types are invariably killed by all macrophages, the pathogens generally survive and grow. Here, we addressed the survival, production of reactive nitrogen intermediates (RNI) and intracellular trafficking of the non-pathogenic *M. smegmatis,* the pathogen-like, BCG and the pathogenic *M. bovis* in different mouse, human and bovine macrophages. The bacteriocidal effects of RNI were restricted for all bacterial species to the early stages of infection. EM analysis showed clearly that all the mycobacteria remained within phagosomes even at late times of infection. The fraction of BCG and *M. bovis* found in mature phagolysosomes rarely exceeded 10 % of total, irrespective of whether bacteria were growing, latent or being killed, with little correlation between the extent of phagosome maturation and the degree of killing. Theoretical modelling of our data identified two different potential sets of explanations that are consistent with our results. The model we favour is one in which a small but significant fraction of BCG is killed in an early phagosome, then maturation of a small fraction of phagosomes with both live and killed bacteria, followed by extremely rapid killing and digestion of the bacteria in phago-lysosomes.

INTRODUCTION

Infection with mycobacteria remains a major health problem. Although in the recent years infections by *M. avium* are gaining importance among imuno-suppressed individuals tuberculosis is still the major problem. Mycobacteria from *Mycobacterium tuberculosis* complex, *Mycobacterium africannum*, *Mycobacterium bovis* and *Mycobacterium tuberculosis*, are the etiological agents of this disease [1,2]. In a number of countries, *M. bovis* is responsible for important economic losses due to bovine tuberculosis [3,4]. This *Mycobacterium* can also infect humans, causing tuberculosis, with a patho-biology indistinguishable from that one caused by *M. tuberculosis* [2,5]. The success of these pathogens is to a large part dependent on their ability to inhibit host defence mechanisms and persist in a potentially hostile environment, the macrophage phagosome, and is also facilitated by the emergence of multi-drug resistant (MDR) strains and extensively drug-resistant (XDR) strains [6].

The crucial difference between non-pathogenic and pathogenic mycobacteria is that the latter arrest maturation of phagosomes at an early stage [7-10]. Although the mechanism responsible for this process is poorly understood the arrested phagosome provides a friendly environment for pathogen survival and even growth [11-13]. The mycobacterial phagosome has particular characteristics such as low content of vacuolar ATPase (V-ATPase) [14], and thereby incomplete luminal acidification, as well as a low content of mature lysosomal enzymes. Collectively these pathogen-altered conditions are assumed to facilitate survival of the mycobacteria [9,13].

The question of how and where mycobacteria are killed by macrophages is still open, both for the non-pathogenic and pathogenic forms [15]. From the literature two extreme models can be envisaged. In the first, the killing only occurs *after* phagolysosome fusion; in this model the macrophage killing potential depends on its abilty to fuse the phagosome with late endocytic organelles, here, often simplified as 'lysosomes'. Thereby, it is presumed that the combination of low pH and a battery of lysosomal hydrolases induce both killing and digestion/clearance of the bacteria. In agreement with this hypothesis are extensive data correlating a high incidence of phagosomal fusion with a high rate of killing, and a low extent of this fusion with high survival [13,15,16]. This model is widely favoured and is also supported by an early study by Cohn [17], who first showed that lysosomal extracts are potentially bacteriocidal; that study showed that extracts of macrophage or neutrophil lysosomes can induce killing of *E.*

coli within 1 min. In the case of *M. smegmatis* in J774 cells a rapid 1-4h killing period coincides with extensive phago-lysosome fusion and the internalisation of a cocktail of lysosomal enzyme inhibitors by endocytosis into infected macrophages strongly reduced the potency of this early killing period Anes *et al*. (2006) [18].

An alternative hypothesis emerged from the pioneering study by Armstrong and D'Arcy Hart (1971) [19]. Based on a thorough EM analysis in which endocytosed ferritin was used as a lysosomal marker these authors came to the conclusion that the live *M. tuberculosis* actively avoided phagolysosome fusion, a point that is widely appreciated. Less appreciated is their conclusion that only *after* being killed in a non-matured phagosome could the phagosome fuse with lysosomes. In contrast, when *M. tuberculosis* opsonised with a specific anti-*M. tuberculosis* antibody before internalisation the majority of the bacterial phagosomes now fused with lysosomes. However, *M. tuberculosis* nevertheless multiplied at the same rate as the non-opsonised bacteria, that were predominantly in non-mature phagosomes [11]. A similar conclusion was made later by Gomes *et al*. (1999) [20]. In these experiments the accumulation of pathogenic mycobacteria in a mature phagolysosome (that also contained *Coxiella burnetii*) did not induce killing of *M. tuberculosis* or *M. avium*. More recently elegant assays were used to select for *M. tuberculosis* mutants that can survive in mature phagosomes [12,21,22]. All these observations are clearly at odds with the model in which mycobacteria are killed in mature phagosomes.

NO produced from iNOS is a more well-defined component of host defence against intracellular pathogens including *M. tuberculosis* [23]. Phagocytes produce NO and a plethora of other potent mycobacteriocidal reactive nitrogen intermediates following stimulation with mycobacteria and this process is accentuated by inflammatory cytokines like γ-IFN and/ or bacterial lipopolysaccharides (LPS) [23-25]. The tolerance of mycobacteria *in vitro* to RNI is strain, dose and time-dependent, with the pathogens being inherently more resistant than the non-pathogens [26-29]. In our recent study of the non-pathogenic *M. smegmatis*, the macrophage needs at least 4 h, and up to 24-48 h after infection to completely kill the bacteria. Nevertheless, the expression of iNOS and the production of NO, that facilitated bacterial killing**,** was restricted to the first 2 hours [18].

Most published studies have compared up to two different cell types and two different mycobacteria, often with different virulence, such as *Mycobacterium tuberculosis* H37Ra and Rv. We decided to make a broader analysis of mycobacterial-macrophage

interactions. The main goal was to try to find a pattern of killing or survival that could be clearly correlated with macrophage killing mechanisms. Towards this goal, after preliminary studies with *M. smegmatis*, we tested different mycobacteria (*M. bovis* and *M. bovis* BCG) in up to six different cell types: mouse (bone marrow macrophages (BMM), J774 and RAW), human (monocyte derived macrophages from human peripheral blood (HMDM) and THP-1) and bovine macrophages (monocyte derived macrophages from bovine peripheral blood: BMDM). For *M. bovis spp* we first monitored intracellular survival following colony forming units (CFU) and then investigated the role of NO. Subsequently, different assays for phago-lysosome fusion and acidification were applied.

Our results suggest that a specific pathogen-induced macrophage 'program' is induced upon infection that correlates with the bacterial doubling time, in which phases of macrophage high killing potential often alternate with phases conducive to bacterial growth. RNI and low pH play key roles in killing during the first day(s) of infection of pathogenic mycobacteria. Subsequently, RNI and pH-independent mechanisms kill the bacteria within phagosomes. Our results, in conjunction with theoretical modelling for BCG infection argue that a significant killing of these mycobacteria must occur in non-matured, early phagosomes, in agreement with Armstrong and D'Arcy Hart (1971) [19]. However, the majority of BCG is more likely to be killed and digested after phago-lysosome formation.

RESULTS

Kinetics of *M. smegmatis* survival in different host macrophages

From previous studies *M. smegmatis* infecting J774 are killed completely within 48 h under all infection conditions [18,30,31]. *M. smegmatis* survival kinetics inside J774 is complex and was characterized in detail previously [18]. A striking observation was a dynamic interplay between bacteria and J774 cells (Fig. 1A). A first phase of killing (4 h) was followed by growth (4-8/9 h) and subsequent killing phases between 9 and 48 h. Here we used GFP-expressing *M. smegmatis* and followed the CFU in BMM derived from C57BL/6 mice and in HMDM. In BMM the dynamics of *M. smegmatis* showed a super-imposable pattern to that seen in J774 macrophages (Figs. 1A and C). In HMDM (Fig. 1D) and RAW (Fig. 1B) the initial killing phase was seen but thereafter different kinetics were observed, with the remaining *M. smegmatis* being killed slowly in a continuous fashion.

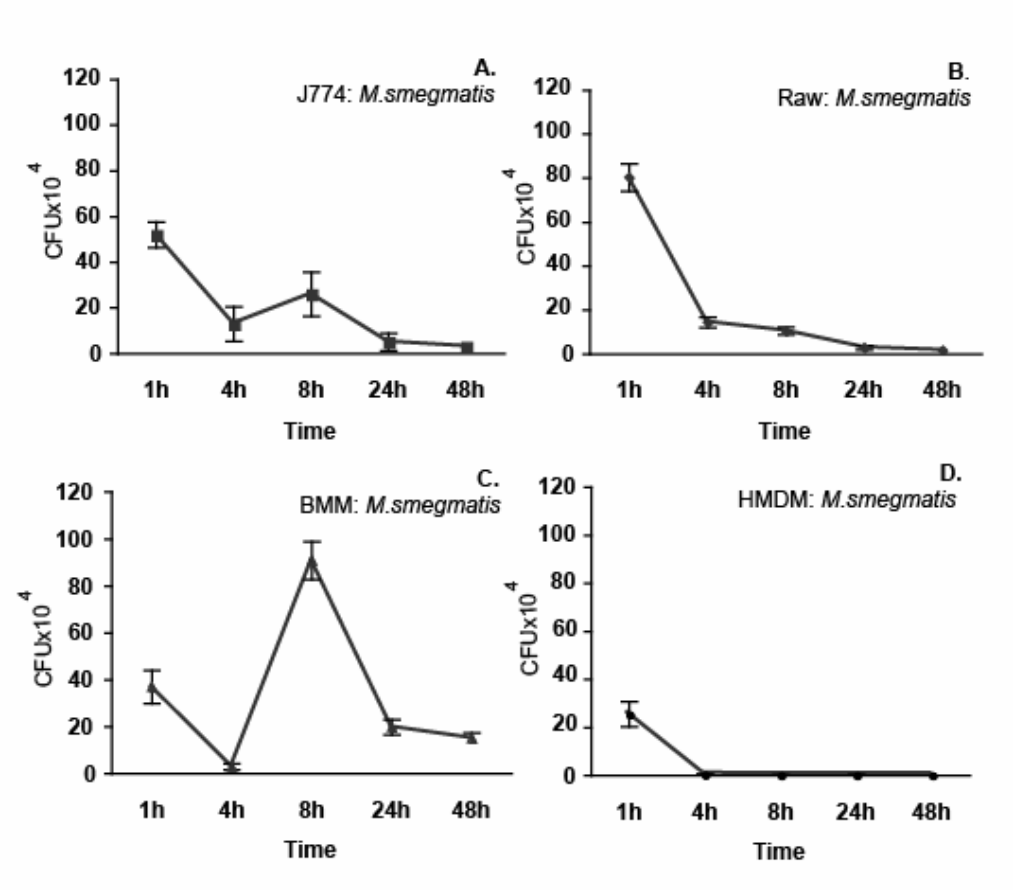

Figure 1. Intracellular fate of *M. smegmatis* in different macrophages

CFU estimates for *M. smegmatis* (GFP) are shown in J774 macrophages (A), RAW macrophages (B), BMM (C) and HMDM (E).

For HMDM the same pattern of killing by 4 h was also seen at higher levels of infection (Results not shown). It is striking, and surely no coincidence that in all four cell types the first killing period is found between 1 and 4 h, and, when growth is permitted, it peaks in both cells around 8 h. These data suggest that the timing of these cycles is likely to be induced by the bacteria- that divide every 3 hours.

Kinetics of *M. bovis spp* survival in different host macrophages

The above data suggested that the cycles of killing and growth might be induced by factors related to the cell cycle of the pathogen. This idea made it interesting to investigate pathogenic mycobacteria, which have a far longer division time (around 24 h) than *M. smegmatis*. We therefore tested BCG and *M. bovis* in six different cell lines: J774, BMM, the human monocytic like cell line THP-1, HMDM and BMDM (Figs. 2A to F).

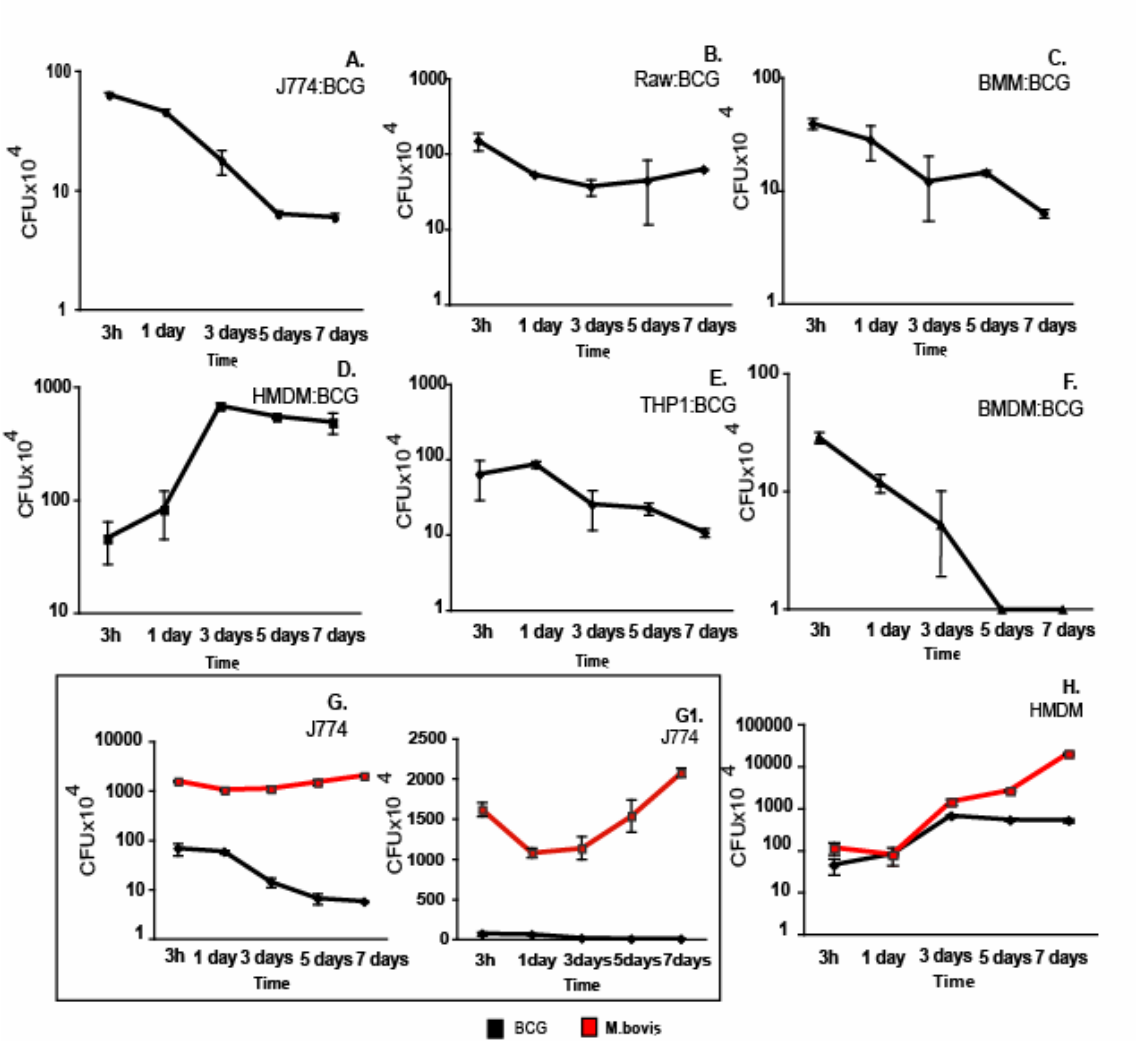

Figure 2. Intracellular fate of BCG (GFP) or *M. bovis* in different host macrophages

CFU estimates for BCG (GFP) in J774 macrophages (A), RAW macrophages (B), BMM (C), HMDM (D), THP-1 cells (E) and BMDM (F). A comparison between the CFU estimates for BCG (GFP) and *M. bovis* in J774 macrophages (G) and HMDM (H) is also shown. G and G1 show the same data plotted differently (see y axis).

We first established infection conditions for BCG-GFP in J774. This GFP strain grows at identical rates *in vitro* and in macrophages to the parental non-GFP strain (results not shown). Bacteria were added at OD_{600nm} 0.1 for 3 h; this gave on average 2 to 9 bacteria per cell. For the other cells the same conditions were used, except for HMDM and BMDM, in which case OD_{600nm} 0.1 appeared to be toxic for the cells. We therefore used an OD_{600nm} of 0.01 which allowed the cells to survive normally for at least 7 days. In all our reported experiments the total number of live macrophages remained almost constant over the period of infection, as accessed by cell counts.

Using the trypan blue exclusion method less than 1 % macrophage death was detected under all conditions. Thus, in this study macrophage cell death could be excluded as having any significant role in the killing of mycobacteria.

As shown in Figs. 2A to F we saw three different patterns of bacterial survival. In BMM, THP-1 and J774 an overall pattern of killing was observed over the 7 days period. With RAW neither significant growth nor killing was observed. In contrast, in HMDM BCG grew up to 3 days, and thereafter neither growth nor killing was seen. We initially used time-scales of hours for these experiments but it soon emerged that the switches from killing to growth, when they occurred, happened on a much slower time scale with the pathogenic mycobacteria, in agreement with the hypothesis that timing of the macrophage cycles of killing and growth is related to the bacterial growth/division time.

We next compared BCG with the virulent strain of *M. bovis* in J774 and HMDM. In J774 whereas BCG could be steadily killed over the course of 7 days infection (Fig. 2G) *M. bovis* could be killed only during the first 24h hours, that was following a growth phase; this is more easily observed using a linear scale (Fig. 2G1) rather than the semi-log scale used in Fig. 2G. With HMDM both BCG an *M. bovis* could steadily grow at a level easily seen on a semi log scale (Fig. 2H). Thus, both bacteria behave quite differently in the two macrophage cell types and are better adapted to survive and grow exponentially in the human primary macrophages.

It is difficult to visualize any meaningful trends in these data, although some cells (THP1 and BMM) tended towards a similar gradual killing of BCG. There was no obvious ranking of macrophage 'killer cells' when we compared their abilities to kill *M. smegmatis*, BCG or *M. bovis*. For example, J774 kills BCG better than RAW, but RAW is much more effective that J774 cells in clearing *M. smegmatis.*

Role of inducible NO synthase and nitric oxide release

We next related the pattern of intracellular growth/killing to the pattern of macrophage activation that is known to contribute to killing of mycobacteria. We first investigated NO production using the Griess reagent. In our recent study on *M. smegmatis*, in J774 cells we showed that NO is only produced up to 2 h after infection, where it contributed to the first killing phase [18]. Here we focussed on BCG and *M. bovis*.

First we tested the susceptibilities of different mycobacteria to NO *in vitro*. For these we used two NO sources NOC-18 (Figs. 3A and B) and acidic solutions of sodium nitrite (not shown). BCG could be killed by 0.1 μM NOC18 after 1 day but after 14 days in culture a 100-fold higher concentration of NOC-18 was needed for efficient killing (Fig. 3A). In contrast *M. bovis* was highly resistant; after 1 day in culture only partial killing was seen with 1 μM NOC-18 (a 10-fold higher concentration than that needed to kill BCG) and to achieve complete killing a 1000-fold higher concentration of NOC-18 was required (Fig. 3B).

We next investigated cell production of NO in response to BCG and *M. bovis*. NO was not detected in supernatants of HMDM under any conditions, in agreement with other studies on human macrophages [32]. γ-IFN is known to induce strong iNOS activity and often also an increase in mycobacterial killing [33-36]. As seen in Table 1, overnight treatment of J774 cells with γ-IFN before infection led to a highly significant increase in NO levels after 1 and 2 days infection with BCG or *M. bovis*.

We next tested the effects of NO on *M. bovis spp* survival in J774. For this we either increased NO artificially, using NOC-18 or γ-IFN, or decreased NO levels by blocking the enzyme (i-NOS) that synthesizes it, with a specific inhibitor: L-NAME. At 1 day post-infection 0.1 or 1 μM NOC-18 were able to significantly increase the killing of BCG and *M. bovis* (around 40 % increase in killing), respectively (Fig. 3C and D). The extent of killing by NOC-18 and γ-IFN were similar for *M. bovis* whereas γ-IFN had a small but insignificant effect on BCG survival at day 1 (Figs. 3C and D).

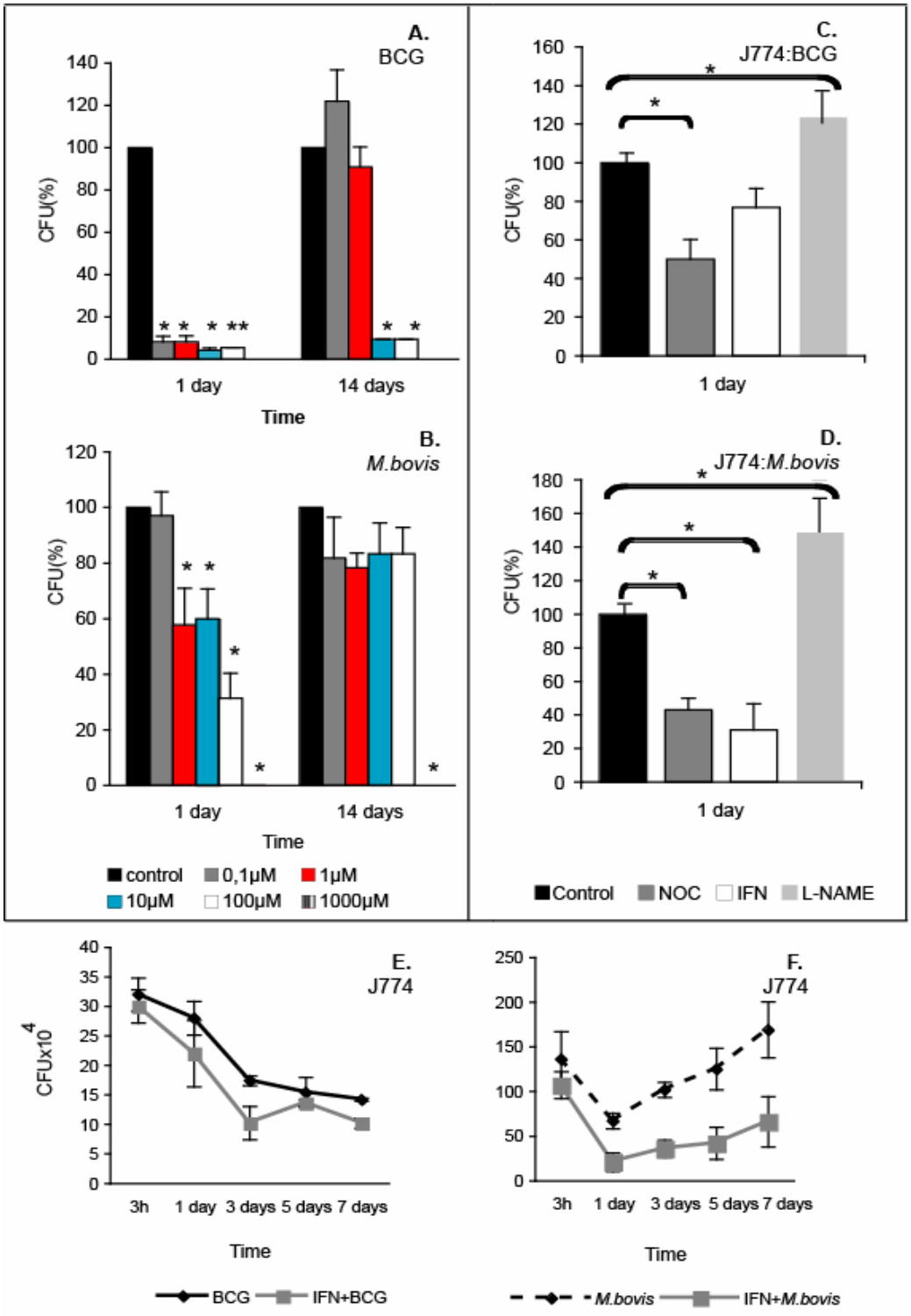

Figure 3. Role of nitric oxide (NO) in *M. bovis spp* survival

In vitro susceptibility of *M. bovis* BCG (GFP) (A) and *M. bovis* (B) to different concentrations of the NO donor NOC-18. Effect of L-NAME, NOC-18 and γ-IFN on intracellular survival of BCG (GFP) (C) or *M. bovis* (D) evaluated after 1 day infection. E and F show CFU estimates after 7 days of *M. bovis* BCG (GFP) (E) or *M. bovis* (F) in J774 macrophages treated with or without γ-IFN. (*p< 0.05; **p<0.001).

With L-NAME a reproducible and significant (30 and 40 %) increase in survival was observed after one-day infection of BCG and *M. bovis*-infected macrophages (Figs. 3C and D). After 1 day neither NOC-18 nor L-NAME affected mycobacteria survival (results not shown). Taking in account the limit of quantification of NO using the Griess method we observed low but detectable amounts of NO production during the early infection periods with both strains (Table 1: 3h and one day post-infection).

Table 1. Nitric oxide release by infected J774 macrophages

1.A. BCG

Time	[NO] μM			
	Control		γ-IFN	
	Average	SD	Average	SD
3h	< 1.0 *	0.40	< 1.0 *	0.40
1 day	1.0	0.5	18.7	0.12
2 days	2.8	0.40	20.5	0.09
3 days	3.2	0.20	4.4	0.03

1.B. *M. bovis*

Time	[NO] μM			
	Control		γ-IFN	
	Average	SD	Average	SD
3h	< 1.0 *	0.40	< 1.0 *	0.40
1 day	1.0	0.05	25.4	1.23
2 days	1.3	0.08	25.3	0.91
3 days	1.8	0.05	5.6	0.06

* extrapolated from the reference standard curve

Figures 3E and F show the effects of an extended treatment of infected cells with γ-IFN, until 7 days infection. These results show clearly that for BCG γ-IFN-treatment modestly but significantly increases bacterial killing until day 3 with little effect thereafter (Fig. 3E). With *M. bovis* (Fig. 3F) the effect of γ-IFN was predominantly seen between 3 h and 1 day. It is notable (and will become more evident in Fig. 7) that the main effect of γ-IFN in enhancing killing coincides with an innate early phase of bacterial killing. In another series of experiments we saw the same pattern with *M. tuberculosis* in response to γ-IFN (Fig. S1, Supplementary information). We presume that the main effect of γ-IFN in the killing process operates via the RNI system.

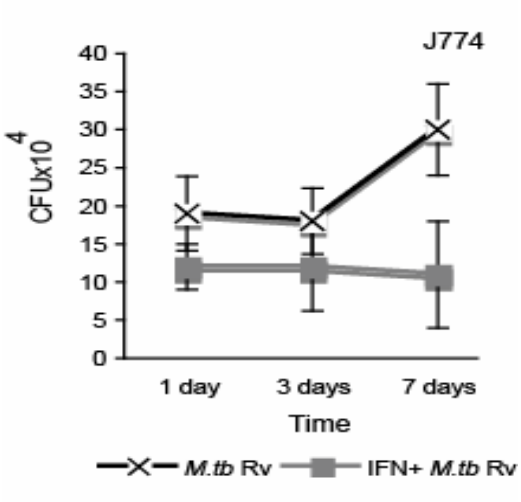

Figure S1. Comparison of CFU of *M. tuberculosis* in J774 macrophages up to 7 days infection with and without γ-IFN treatment.

Since the mouse macrophages made NO in response to the mycobacteria we next correlated the expression of iNOS the enzyme that makes it after infection of J774 cells with BCG and *M. bovis*. Using immunofluorescence microscopy we could not detect any signal for iNOS in uninfected cells (Fig. 4A) whereas a significant increase in cytoplasmic labelling for iNOS was already detected after 1h infection with *M. bovis* (Fig. 4C) or BCG (Fig. 4B). No specific association of iNOS with phagosomes of either BCG or *M. bovis* was seen, in agreement with the data of Anes *et al*. (2006) [18] and Miller *et al.* (2004) [37]. After treatment of uninfected (Fig. 4D) or infected macrophages (Fig. 4E) with γ-IFN a general increase in iNOS labelling was clearly observed. Immunofluorescence microscopy was a more sensitive estimator of iNOS that Western blotting. Although by Western blot iNOS could be detected after treatment with γ-IFN no band was detectable in untreated infected cells (Fig. 4F).

Thus, conditions where NO levels are high correlate with an increase in iNOS protein levels, as expected. Collectively, these data lead us to conclude that increased iNOs activity early, but not late in infection plays a role in killing mycobacteria in mouse cells. γ-IFN treatment enhances the early killing phase, predominantly by stimulating iNOS activity. However, the fact that human macrophages have a similar capacity to kill non-pathogenic and pathogenic mycobacteria but have no iNOS activity shows clearly that RNI is neither the only nor the main killing mechanism in macrophages.

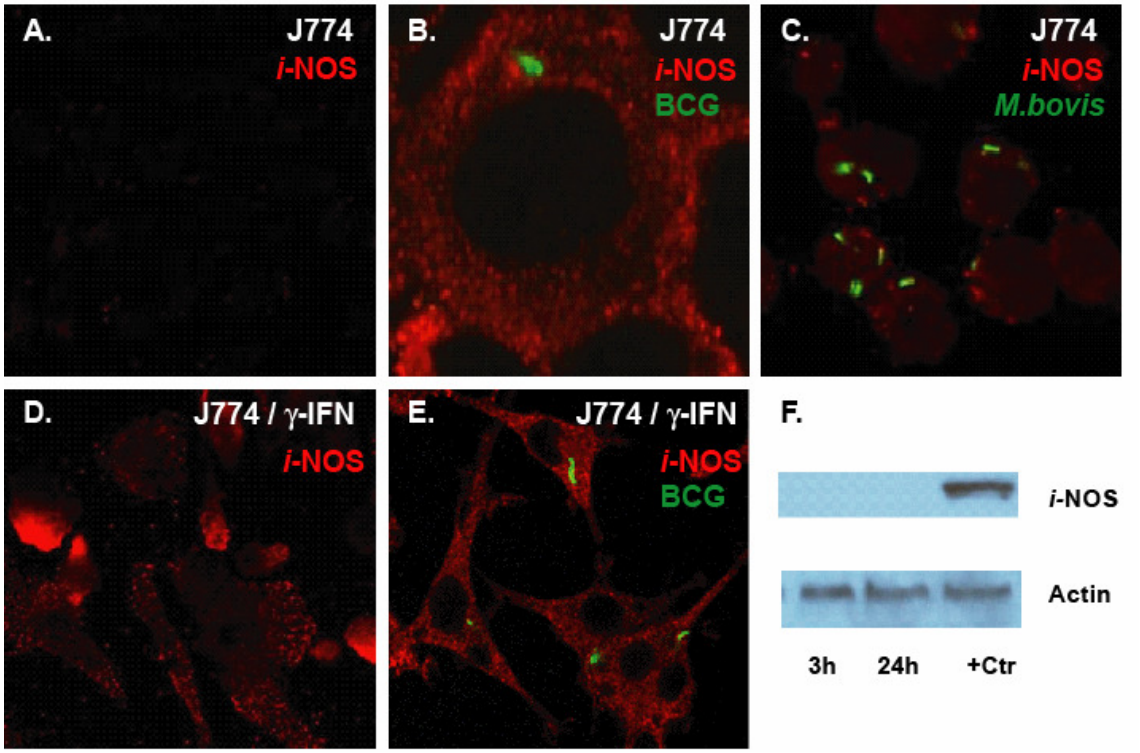

Figure 4. Localization of inducible NO synthase (iNOS) in J774 macrophages

Immunofluorescence labelling for iNOS in untreated and uninfected J774 cells (A), in macrophages infected with BCG (GFP) (B) or with *M. bovis* (C) for 3 h. D and E shows the effects of γ-IFN treatment on uninfected cells (D) or cells infected with BCG (GFP) (E). In all images iNOS was labelled with Cy3 (red channel) and *Mycobacterium spp* were labelled with GFP (BCG) or Oregon green *(M. bovis*) (green channel). Western blots for iNOS during J774 macrophages infection with BCG (GFP) during 3h and 1 day. Macrophages treated with γ-IFN were used as positive control**.** Actin was used as loading control (F).

Phagosome-lysosome fusion and pH

We next addressed the role of phagosome maturation in mycobacteria killing, focusing on phagosome-late-endosome/lysosome acidification and fusion. This is often assumed to be the major factor in the ability of the bacteria to survive (no fusion) and for the macrophage to kill them (fusion). If this is indeed the key factor, we would predict that by following phagosome maturation using a range of markers in different cell types infected with BCG and *M. bovis*, we would see significant correlations between the extent of fusion and the degree of killing.

Late endocytic organelles as well as late phagosomes are predominantly acidic and the acquisition of a low pH is an accepted marker for mature phagosomes [15,38-42]. Using the fluorescent dye lysotracker DND99, which accumulates in acidic compartments (pH<

6), the acidification of BCG and *M. bovis* was monitored by confocal microscopy, focusing on J774 and HMDM cells [10,18]. In J774 cells 3 h after infection only around 10 % of both types of mycobacterial phagosomes were acidic and this increased to 20 % at day 1. However, by day 3 these values decreased again to around 10 % (Fig. 5A). In contrast, in HMDM more BCG-containing phagosomes acidified at 3 h but thereafter the fraction of acidified phagosomes remained below 10 %. The fraction of acidic *M. bovis* containing phagosomes never exceeded 10 % and, after 3 days only 5 % were acidic enough to accumulate lysotracker (Fig. 5B).

We next followed phago-'lysosome' (late endosome and lysosome) fusion using an assay we recently introduced, in which nanogold particles labelled with rhodamine are internalised by late endocytic organelles (Figs. 5C and D) [18]. Under all conditions in J774 and HMDM cells less then 10 % of the phagosomes containing BCG or *M. bovis* fused with rhodamine-labeled 'lysosomes'. In HMDM cells at late time points less than 3 % *M. bovis* phagosomes had fused with this marker.

When J774 were fed with heat killed BCG the fraction of acidified phagosomes increased from 25 % at 3 h to around 80 % after 1 day (Fig. 5E). These argue that phagosome containing dead bacteria matured efficiently, as expected [7,32,43].

The fraction of phagosomes that fused with lysosomes also increased between 3 h and 1 day; however, whereas only 40 % of the heat killed BCG phagosomes had fused with lysosomes, the fraction that acidified was 80 %. This difference in the levels of acidification and fusion can be rationalised by our recent observation [18] showing that in J774 cells the bulk of V-ATPase is delivered to phagosomes from a late endocytic vesicle that is distinct from the "classical" late endosomes that label with LAMP-1 [32,44,45].

Using a different late endosome marker lysobisphosphatidic acid (LBPA) [46] with live BCG-infected J774 and HMDM cells a similar low fraction of phagosomes was found to co-localise with this marker (Fig. 5F). These data collectively show that overall, less than 10 % of BCG or *M. bovis* fused with late endosomes and lysosomes, or acidified in J774 or HMDM cells.

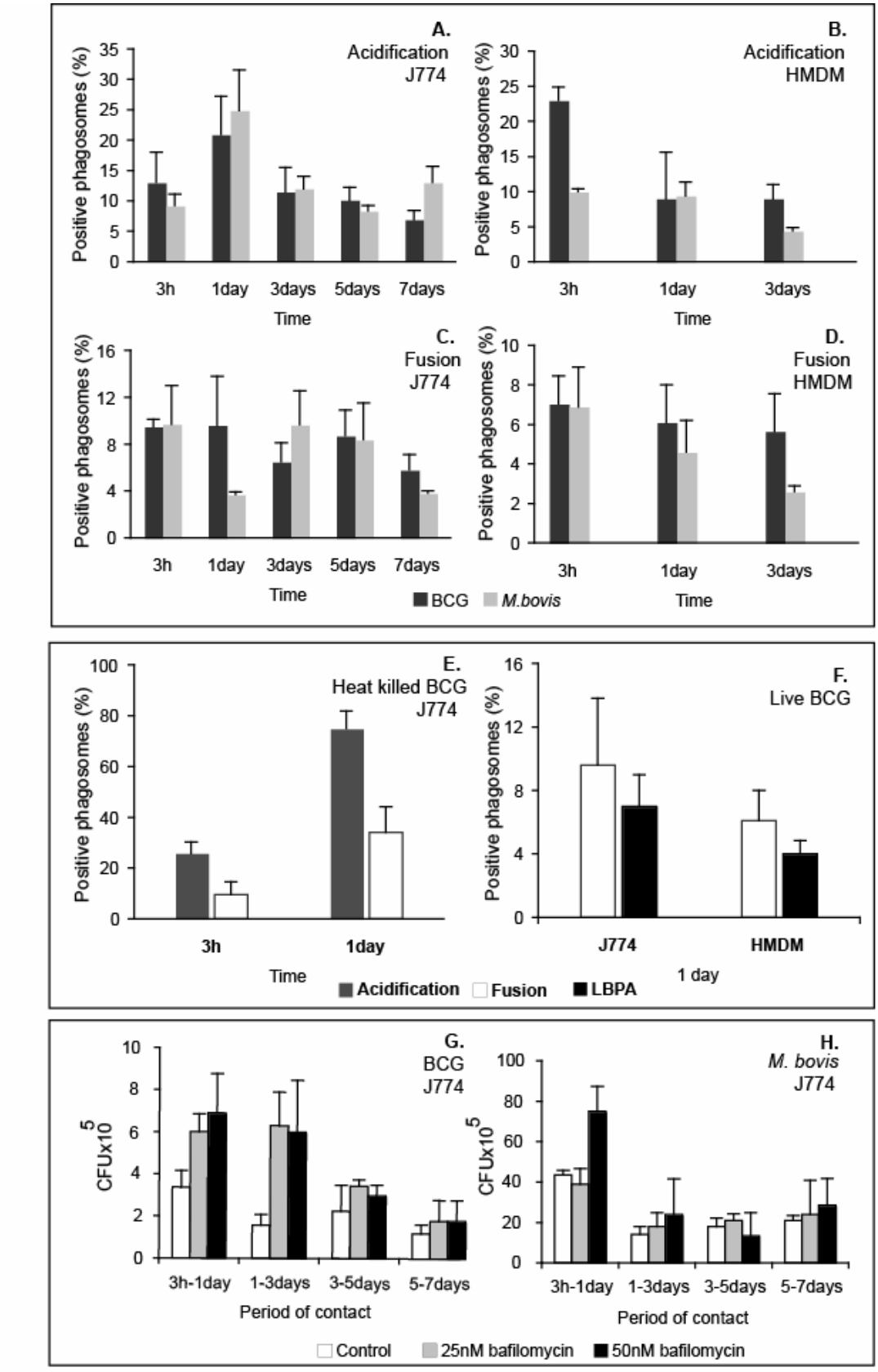

Figure 5. Phagosome acidification and fusion with late endosomes and lysosomes

Acquisition of lysotracker and rhodamine gold by live BCG or *M. bovis* phagosomes in J774 (A and C) or HMDM (B and D) and heat killed BCG phagosomes in J774 (E). Shown in (F) is the

acquisition of LBPA and gold by live BCG phagosomes either in J774 or HMDM. The effects of bafilomycin A1 in macrophages infected with BCG are seen in (G) and with *M. bovis spp* (H).

When one compares the overall pattern of phagosome maturation over the infection period with the growth of BCG or *M. bovis* (Figs. 2G and H) it was difficult to observe any clear correlations.

In our earlier study on *M. smegmatis* in J774 cells we showed that a low pH in the phagosome contributes to the killing of these bacteria since the V-ATPase inhibitor bafilomycin A1 reduced the extent of killing [18]. Given that even the early phagosome stage has a pH around 6.2 [13,47], that will not be detected by lysotracker we asked whether lowering the pH had any effect on the survival of BCG or *M. bovis in vitro*. An early study [48] had shown that *M. tuberculosis* has an optimal pH for growth *in vitro* at pH 6.2 but there was significant less growth as the pH was reduced. In contrast, *M. smegmatis* is highly robust and can grow well in a wide pH range (from 4.5 to above 8), as might be expected for an organism found naturally in soil. As observed in Table 2, while *M. bovis* was not affected in our experiments by pH down to 5.5 BCG was more susceptible, with 20 % even being killed at pH 6.5. At pH 4.5 however, 40 % of *M. bovis* and over 80 % of BCG were killed.

Table 2. Effects of pH on BCG and *M. bovis in vitro*

pH	CFU compared to the control (%)			
	M. bovis		BCG	
	1 day	7 days	1 day	7 days
6.5	---	---	20	10
5.5	---	---	20	10
4.5	40	40	84	84

CFU estimate of BCG and *M. bovis* incubated at different pH values. The data are presented as the percentage of bacteria killed relative to comparing the control (bacteria grown in standard medium) after 1 and 7 days. In this table (---) means no difference relative to the control.

If we extrapolate these pH values to those found in the different phagosomes in macrophages -early phagosomes around pH 6.2 and late phagosomes down to pH 4.5 [47]

these data predict that in 'non-matured' early phagosomes BCG could be exposed to a partial bactericidal effect of pH whereas *M. bovis* would not be affected by the mild acidity. In contrast, should either bacteria find themselves in fully matured phagosomes (pH 4.5-5) both would be susceptible to low pH killing. In order to test this hypothesis we used the V-ATPase inhibitor bafilomycin A1 to neutralize the pH of all endocytic compartments. We showed earlier that this treatment significantly reduced the killing of *M. smegmatis* in J774 cells [18].

J774 cells infected with BCG or *M. bovis* were treated with bafilomycin A1 at the different time windows indicated in Figs. 5G and H. The treatment with 25 or 50 nM of the drug led to a significant increase in growth of BCG between the 3 and 24 h time points and at the 1-3 day period but it had no effect at subsequent times up to day 7 (Fig. 5G). For *M. bovis* a similar result was seen with bafilomycin (at 50 but not 25 nM) between 3 and 24 h whereas no effect was seen at later times (Fig. 5H). These data show that (i) a low pH does contribute significantly to killing of both BCG and *M. bovis* but this effect is restricted to the early phases of the infections and (ii) the period (up to day 1) in which BCG is resistant to pH is significantly longer (up to 3 days) than for *M. bovis* (up to 1 day). As shown below these periods coincide precisely with initial strong bacteriocidal stages in macrophages that are different for the two mycobacteria.

All mycobacteria are exclusively in phagosomes

Although it is generally accepted that intracellular mycobacteria in macrophages are always enclosed by membranes of phagosomes or phago-lysosomes, two earlier EM studies suggested that *M. tuberculosis* could under some conditions escape out of the phagosome [49,50]. This idea, received with scepticism in the field was recently re-awakened by a more convincing EM study by Peters and collaborators [51]. Using the Tokuyasu cryo section EM method following chemical fixation, these authors provided a striking scenario in which *M. tuberculosis* H37Rv-enclosing phagosomes in human blood macrophages and dendritic cells fused significantly with lysosomes after 2 days infection (as monitored via acquisition of LAMP-1, CD63 and cathepsin D). After this period the phagosomes were found to lyse and *M. tuberculosis* escaped into the cytoplasm, where bacterial growth was observed. In contrast BCG remained within phagosomes at all times after infection. This result fits well with the behaviour of the closely related pathogen *M. marinum* [52,53], that was even able to move actively through the cytoplasm by actin comets, similar to *Listeria* and other pathogens [54].

The possibility that *M. bovis* in particular could escape into the cytoplasm in our experiments offered an attractive alternative hypothesis to explain the lack of obvious correlation between its intracellular growth/killing and the fraction of fully matured phagosomes. We found no conditions in this study (even after treatment with γ-IFN- Results not shown) in which BCG, *M. bovis* or *M. tuberculosis* -containing phagosomes showed an index of phago-lysosome fusion much above the 10 % value, at least up to 7 days. Similar conclusions were drawn by Armstrong and Hart (1971) [19] after monitoring the infection with *M. tuberculosis* up to 15 days in primary macrophages. Nevertheless, perhaps this abrupt maturation of pathogen-containing phagosomes seen by Van der Wel *et al.* (2007) [51] might have occurred too rapidly in our cell systems. If the bacteria were in the cytoplasm they could not be expected to contain any lysosomal marker. Clearly, this question could only be addressed using electron microscopy. An obvious worry for any EM study using conventional fixation is the question of fixation artefacts, a problem that can be particularly difficult in preserving membranes [55]. Only by use of cryo-immobilization methods such as freeze substitution or cryo electron microscopy of vitrified sections (CEMOVIS) [56] can one be sure to avoid all chemically-induced artefacts. However, if pathogens are to be investigated by these more modern technologies it requires the combination of a high pressure freezer machine in a bio-safety level 3 facility, a combination that we currently do not have.

There is, however one proviso for using conventional chemical embedding that makes this approach suitable for analysing pathogen phagosomes. While there is always the possibility that phagosomal membranes can lyse, or even perhaps disappear in response to fixation, we consider it highly unlikely that a bacterium free in the cytoplasm can acquire a membrane artifactually as a result of this procedure. This discussion is highly relevant to interpretation of EM images of chemically fixed specimens, and to the data we now present.

We chemically fixed J774 or HMDM infected with BCG, *M. bovis* or *M. tuberculosis* with glutaraldehyde, post-fixed in osmium and uranyl acetate and embedded the samples in epoxy resin. Alternatively, after only glutaraldehyde fixation the cells were infused with sucrose and prepared for cryo-sectioning [57]; these were contrasted either with uranyl acetate or ammonium molybdate in combination with methyl cellulose [55].

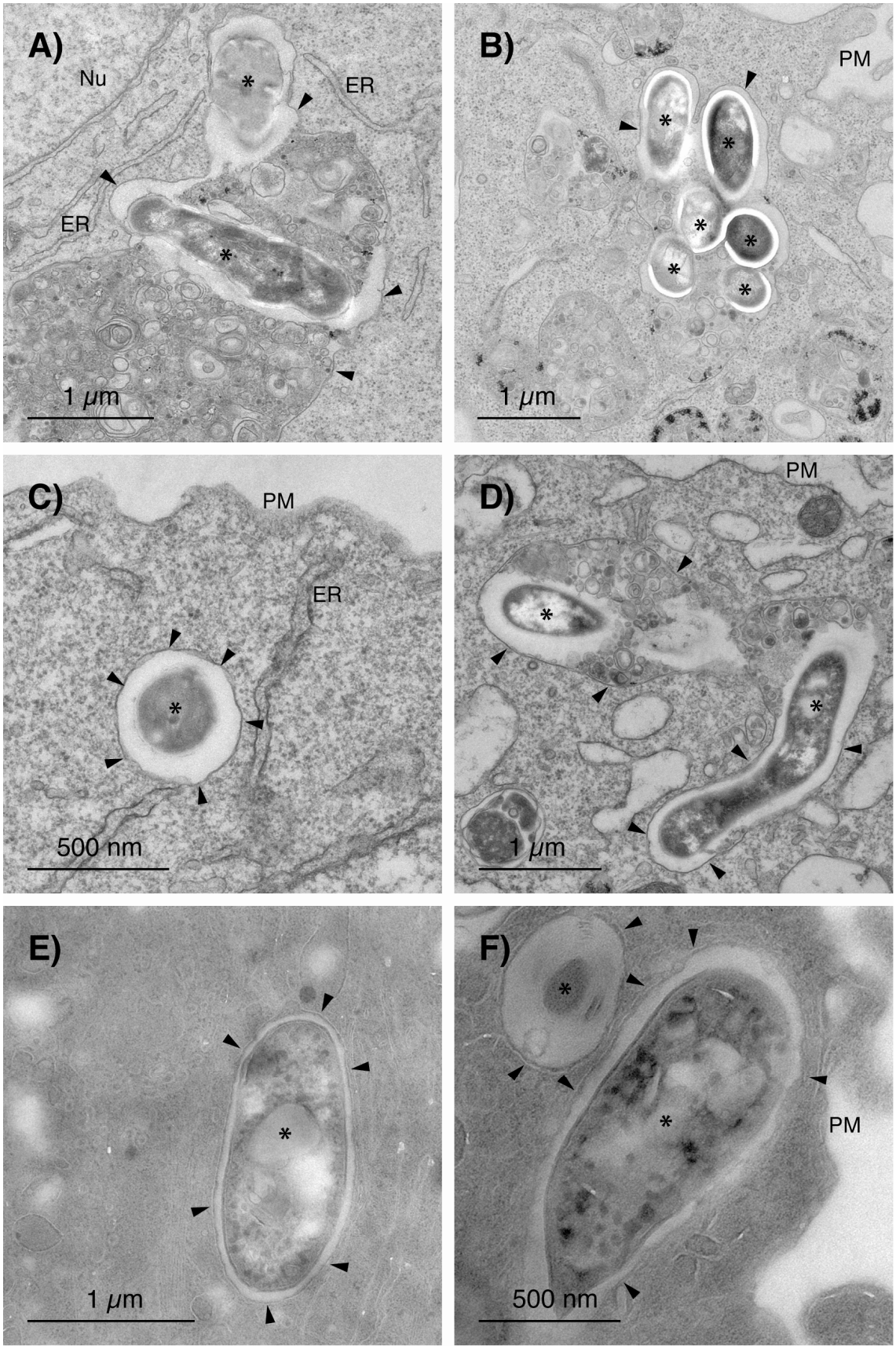

Figure 6. *Mycobacterium spp* reside in a phagosome compartment at all infection times

A-D. Epoxy resin plastic section of J774 macrophages infected after 3 days infection with *M. bovis* (A, B) or *M. tuberculosis H37Rv* (C, D). E and F show thawed cryo-sections of HMDM

infected for 3 days (E) and 5 days (F) with *M. bovis*; sections stained with ammonium molybdate and methyl cellulose. In all Figs Mycobacteria are marked with an asterisk (*) and arrow-heads indicate the membrane of phagosomes that enclose the mycobacteria. Plasma membrane (PM), nucleus (Nu) and endoplasmic reticulum (ER) are also indicated.

Using both approaches thin section EM analysis showed unequivocally that all of the bacteria we observed within the macrophages were invariably surrounded by a phagosome membrane at all times up to 6 days infection. Examples of these images are shown in Fig. 6. Thus rules out the possibility that any cytoplasmic mycobacteria exist under our conditions and supports the observations of Armstrong and D'Arcy Hart (1971) [19] who found *M. tuberculosis* to be enclosed by a phagosomal membrane at all times over two weeks of infection.

Killing of mycobacteria occurs in mature and non-mature phagosomes

From the above results both BCG and *M. bovis* reside in macrophages in phagosomes that we can operationally separate into 'early' or non-matured phagosomes (not fused with 'lysosomes' and lyso-tracker negative) and 'late' or mature phagosomes (fused with lysosomes and lysotracker positive). The vast majority (90 %) of both BCG and *M. bovis* phagosomes were in early (non-mature) phagosomes. We wanted to distinguish between the two extreme models presented in the Introduction, first, killing occurs only *after* a live bacterium finds itself in a matured phagosome and, second, killing occurs in early phagosomes and is perhaps a pre-requisite for some of these phagosomes to mature into a hydrolytic compartment that degrades the pathogens.

To address this issue we set up an experiment in which we could distinguish between live and dead bacteria per cell, using an approach similar to that described by Anes *et al.* (2006) [18] and Barker *et al.* (1997) [58]. For this, we infected J774 cells with *M. bovis* that had been surface-stained with Oregon green or with GFP-BCG. Subsequently, the cells were lysed and the recovered bacteria were stained with propidium iodide, a red dye that is unable to cross intact bacterial membranes but stains nucleic acid in dead bacteria. This allowed us to distinguish between dead (red or yellow) and live bacteria (green) and by separately counting the number of macrophages we could relate the numbers of bacteria to the numbers of cells. Importantly, the viability and the total number of macrophages during the time of the experiment remained constant. Less than 1 % of macrophages could be stained with trypan blue in infected cultures for 7 days.

The quantitative analysis of this experiment was quite revealing (Fig. 7A). With both BCG and *M. bovis* the number of green (live) bacteria dropped at a similar initial rate giving a total killing of around 40 % during the first day of infection (Table 3). From the data in Figs. 3C, 3D and 5G it seems likely that RNI and a low pH are the major factors responsible for this early killing of both bacteria. In the case of *M. bovis* day 1 was the start of a continuous growth period whereas for BCG killing proceeded until day 3 when a static condition was reached. The initial decrease in the number of green bacteria, up to day 3, was however, not correlated with an increase in the number of red/yellow bacteria, as we expected. Rather, this number was kept at a consistently low value of around 0.5- 1 bacteria per cell, for both *M. bovis* and BCG. Our interpretation at this point is that we have dead bacteria in different stages of digestion and only the best-preserved ones would be recovered after macrophages lysis and propidium iodide staining. Clearly, these killed bacteria must be cleared relatively fast, and at a similar rate for both bacteria. Taking this into account we consider that the rate of disappearance of the green bacteria provides the best independent estimate of the killing rate. This assumption was supported by the excellent correlation between CFU (Fig. 7B) and the different kinetics of disappearance of BCG and *M. bovis* green bacteria (Fig. 7A).

During the first 24 hours, the rate of killing for BCG and *M. bovis* was similar (Table 3). Thus, both BCG and the pathogenic *M. bovis* are subjected to a similar macrophage killing potential early in infection. After 1 day *M. bovis* strikingly switched to a state of growth, with the number of green (live) bacteria increasing to give an average of 8 bacteria per cell after 7 days, as seen by direct microscopy counts and by CFU estimations (Figs. 7A and B). So the major difference between BCG and *M. bovis* is that BCG continuously suffers a net loss until a steady state is reached after three days, whereas *M. bovis* is able to switch to a growth phase after 1 day- we presume that this involves a signalling switch from a pro-inflammatory signalling state of macrophages to an anti-inflammatory one (Jordao *et al*-submitted). Nevertheless, since a constant number of dead bacteria are seen at all times for *M. bovis* (Figs. 7 A, B) it argues that the net growth seen for *M. bovis* reflects a balance between growth and a constant rate of killing; a similar conclusion was made for *M. marinum* in phagosomes [58]. Although no net growth is seen for BCG at any time, the constant ratio of live to dead bacteria also argues that this bacterium is also at a steady state with continuous growth and killing. Since roughly half the BCG population in these late infection period is dead,

and only 5-10 % are in phagosomes that have fused with lysosomes we interpreted these data to mean that some bacteria must be killed in non-matured phagosome.

We also analysed the rate of disappearance of heat killed GFP-BCG and *M. bovis* taken up by phagocytosis by J774 cells. The rate of clearance was identical for both bacteria (Table 3) with 67 % of these killed bacteria having disappeared from cells between 3 h and 1 day. Between 1 and 3 days almost all remaining bacteria were eliminated (n.b. for this experiment we used a low number of bacteria for infection in order to more clearly visualise the bacteria; see below).

A comparison of Figs. 7A and B with Figs. 5G and H reveals an interesting correlation. For both BCG (with net killing until day 3) and *M. bovis* (killed until day 1) these periods of killing coincided precisely with the times that blocking phagosomal acidification prevents killing. This provides more compelling evidence that low pH is directly involved in the initial net killing period, but not thereafter.

Under some conditions particles within phagosomes can exit cells by exocytosis of the phagosomes [59]. We therefore hypothesized that the potential live (green) bacteria that were 'lost' from cells might be exocytosed after (or even before) killing. However, extensive microscopy and CFU counts of live and killed bacteria on the surface of cells or released into medium showed no significant release of bacteria to the extra-cellular space (results not shown). This indicates that the digestion and clearance of bacteria must occur in the lumen of the early or late phagosomes.

Modeling intracellular transport and killing of BCG

We then assessed whether the data in Figs. 7A and B for BCG could be fitted to a simple model considering two compartments (early and late) and the rates of bacterial growth, killing, disappearance, and transport between compartments (i. e, phagosome maturation). We described the system by defining the seven different reactions shown in Fig. 7D, each having a rate constant, k1-7. A set of differential equations were generated in the COPASI modelling program (see Experimental procedures and Fig. 7C). This elegant program allows one to change each constant independently and then the program is run to see what pattern of curves emerge for the number of bacteria over time. COPASI can be instructed to find the set of constants that best reproduce the observed values. For this exercise we used all available experimental evidence we had. The data for dead and live bacteria at different times after internalization were taken from Fig. 7A (BCG). The values for the fraction of bacteria in early compartments

were taken from Fig. 5C (BCG). The dynamics of transport to late compartments (along with phagosome maturation) and the disappearance from macrophages of dead BCG were those shown in Fig. 5E and Table 3.

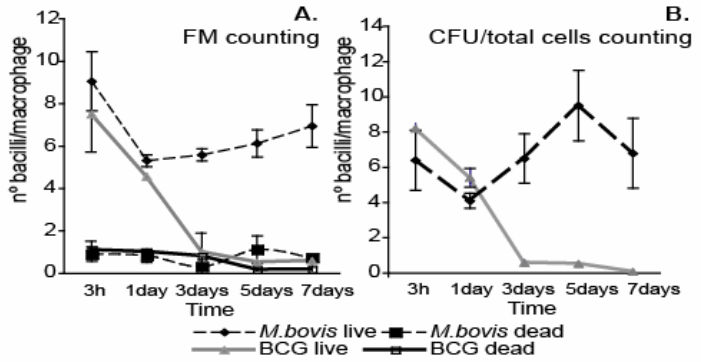

Table 3. Live *versus* dead intracellular bacteria

Time post-infection	*Numbers of bacilli per macrophage*		
	live BCG	live *M.bovis*	dead BCG or *M.bovis*
3 h	7.50	9.10	2.00
1 day	4.56	5.32	0.65
3 days	1.00	5.59	0.17
5 days	0.52	6.13	0.00
7 days	0.58	6.94	0.00

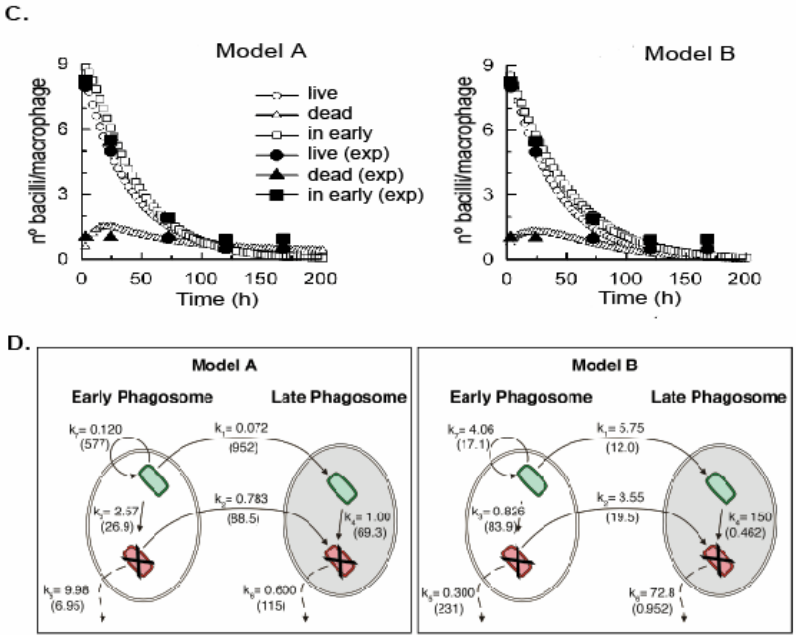

Figure 7. Evaluation of mycobacteria growth/survival by different methods and the COPASI models for BCG transport and killing in J774 macrophages.

Evaluation of live and dead *M. bovis spp* in J774 macrophages over 7 days by microscopy (A) or by CFU (B). Table 3 shows a numerical summary of parameters calculated from Fig 7A and B. Fig 7 C shows the results of two modelling scenarios, A and B. The different reaction

constants that were necessary for the curve fitting in A and B are given in Fig D that shows schematically the seven reactions modelled for the two models -for more details see Supplementary information (COPASI file). In C the open symbols show the experimental data from Fig 7A while the filled symbols indicate the values obtained by modeling. The first numerical value for each constant (K) gives the average rate (number of bacteria per hour) while the number in parentheses give the average time in hours that each reaction takes. In the model two phagosomal compartments are considered (early or non-matured, and late or matured). The bacteria can divide, be killed, or transported from early to late compartments. Kinetics constants in C are: k1, rate of transport (by maturation) from early to late compartments for live BCG; k2, rate of transport from early to late compartments for killed BCG; k3, rate of killing of BCG in early compartments; k4, rate of killing of BCG in late compartments; k5, rate of disappearance of BCG from early compartments; k6, rate of disappearance of BCG from late compartments; k7, rate of duplication of BCG in early compartments.

The general features for BCG intracellular transport and survival in J774 macrophages i.e., most bacteria present in early compartments at all times after infection, a stable amount of dead microorganisms, and an exponential decrease of live bacteria could be reproduced quite well by two totally different scenarios (Figs. 7C, D). In the first (Model A) the majority of the bacteria is killed in, and disappears from early compartments whereas in the second (Model B) the majority of the bacteria is first transported to late compartments where they are quickly killed and degraded (Fig. 7D). It is interesting to notice that both models require killing in the early compartments -as postulated by Armstrong and D´Arcy Hart (1971) [19] in order to fit the experimental data. However, whereas this process is the main player in model A it plays a quantitatively less important role in model B. The time-limiting step for BCG disappearance in the first model is the killing and degradation in the early compartments whereas for the second, it is the transport to late compartments. It is worth mentioning that we could not find any other set of parameters that fit the experimental data, although calculations were started from 8 different initial conditions.

At first glance model A was attractive since it seems to be consistent with the low fraction of bacteria in phago-lysosomes and the low rate of killed bacteria. If the majority of the bacteria are cleared from an early compartment (a phenomenon that has never been observed) it might explain why we detected such apparent low values for phago-lysosome fusion as well as the relatively low numbers of dead bacteria. However, a deeper analysis makes us favour much more the second model B in which

an important small fraction of bacteria are killed in early phagosomes. Both live and killed bacteria phagosomes have a relatively low chance of undergoing full maturation, but when they do they face a compartment where the live bacteria are rapidly killed (30 min) and both this pool, and the bacteria already killed in early phagosomes, are rapidly digested and disappear (60 min). In model B the almost perfect fitting of theoretical values to our experimental data is observed with a duplication time for BCG (k7 in Fig. 7D) of 17 h. This value, which was important for the curve fitting, is within the range estimated for the cell division time of 23 h for BCG growing *in vitro* [60]. In contrast, in model A the fitting of theory to experimental data necessitated a k7 value of over 500 h, a value that is totally unrealistic.

DISCUSSION

Here, we addressed those factors that were believed to contribute to killing mycobacteria in macrophages and investigated the interactions between three mycobacteria, *M. smegmatis*, *BCG* and *M. bovis* in up to six different cell types. We started our analysis by further investigating *M. smegmatis,* that we have recently characterized in great detail in J774 cells [18]. In these cells *M. smegmatis* is exposed to a first killing phase (1-4 h) a subsequent growth phage (4-8/9 h) and two further killing stages with different kinetics (9-24 h). It was striking that the three other cell types we tested (RAW, mouse BMM and human HMDM) all showed the same kinetics of efficient killing between 1 and 4 h; this argues that the bacteria bind receptors which induce the same dynamics of early signalling in all the cells. At subsequent times the pattern of *M. smegmatis* growth in BMM cells was almost identical to J774 cells whereas different patterns were seen with RAW and HMDM, although all the cells effectively cleared *M. smegmatis* by 48 h.

Differences between cells became much more apparent when we compared six different macrophage types following infection with *M. bovis* BCG (GFP). No easily discernable pattern emerges from this analysis, arguing that each combination of cell-mycobacterium tends to behave differently. Further, the ability of a cell type to kill BCG or *M. bovis* could not easily be correlated with their ability to kill *M. smegmatis*.

Extensive literature argues that NO produced by iNOs in macrophages is a crucial killing factor for mycobacteria in macrophages [26,61-63]. Our data lend support to this hypothesis and to the notion that the pathogenic *M. bovis* is more resistant to the killing effects of NO *in vitro* than is BCG. There is also significantly less NO produced from *M. bovis* - relative to BCG-infected mouse macrophages although these levels could be increased dramatically in both infections with γ-IFN treatment; this resulted in a slight increase in killing of BCG and a significant increase in killing *M. bovis* after one day, but not at later days of infection. Effects of γ-IFN in killing mycobacteria in macrophages have been described earlier [10,36,64]. In mouse cells there was a good correlation between the levels of NO and the killing of mycobacteria, with both higher levels of NO and iNOS-dependent killing being restricted to the first 1-2 days infection. A similar pattern was seen earlier with *M. smegmatis* in J774 cells in which the NO production and iNOS-dependent killing was restricted to the first 2 h of infection. That RNI is not the only killing mechanism is also seen by the fact that human macrophages

are unable to show iNOS activity but are still capable of killing mycobacteria. Here, HMDM produced undetectable levels of NO but were nevertheless capable of killing *M. smegmatis* in the first 4 h infection at the same rate as the three types of mouse cells (Figs. 1A-D).

An additional factor that was important for the early killing potential of macrophages was a low pH. When BCG or *M. bovis*-infected J774 macrophages were treated with the V- ATPase inhibitor bafilomycin A1 there was a significant increase in bacterial growth at the 3-24 h period for *M. bovis* and between 3-24 h and 1 and 3 days for BCG. However, this drug had no effect at later times of infection for either bacteria up to 7 days (Fig. 5G). The early infection period where a low pH facilitates killing coincides with the period of iNOS activity and it is known that a low pH synergizes with the RNI system to induce more potent killing activity [29]. It is striking that the period where a low pH is needed for net killing of both bacteria coincides precisely with the early infection period in which the bacterial counts were decreasing strongly (the pro-inflammatory phase), as accessed both by direct microscopy estimates and CFU (Figs. 7A and B). We propose that the combination of RNI and a lowered compartment pH synergise to provide the first killing process. The early mycobacterial phagosomes have a pH of around 6.2 while the late ones are at 5 or slightly below [14,32,47]. Since NO and its relatives are freely diffusible it is conceivable that its combination with a lowered pH in early or late endocytic organelles could induce killing in either compartment; our data do not allow us to distinguish between these options. The observation that blocking phagosome acidification at days 3-7 had no effect on the survival of BCG or *M. bovis* was especially surprising. Since both these bacteria must be continually killed, even after the RNI wave it, argues that whatever mechanism that kills them is not dependent on a low pH.

The interpretation of our data was not straightforward, given the many different potential reactions that operate in the highly dynamic system- in which a variable fraction of the pathogens can divide and a different, variable fraction can be killed at any time by the macrophage. We therefore carried out a more detailed analysis of the BCG and *M. bovis* infections by estimating the total numbers of live and killed bacteria in the cells at different times of infection. Both bacteria were initially killed rapidly until day 1 (*M. bovis*) or day 3 (BCG). Thereafter *M. bovis* switched to a robust net growth phase while BCG retained a constant low level of live bacteria per cell until day 7. Surprisingly, the fraction of bacteria that were rod-shaped but accessible to propidium

iodide, and therefore presumed to be dead, remained at a constant value of around one dead bacterium per cell at all infection times for both BCG and *M. bovis*. Clearly the killed bacteria must be digested and the number of dead ones identified at any stage represents the balance between the rate of killing and the rate of digestion.

The use of the COPASI program to model our data turned out to be a very powerful tool. When one deals with complex multi-step processes such as phagosome maturation, pathogen growth and killing processes it is very difficult to make an intuitive interpretation of the data. In fact, without such modelling we would have concluded that the quantitatively most significant killing of the bacteria occurs in an early compartment, in agreement with the classical study by Armstrong and D'Arcy (1971) [19]. However, the theoretical modelling led to us a different conclusion. In this exercise the overall process of infection is separated into seven distinct reactions with their own rate or activity constants. The COPASI program then allows on to find estimates for these seven parameters that gives the best fit of the dynamics of the bacterial growth/killing with the observed experimental data (Figs. 7A and B). We found two quite different potential 'solutions' that accurately mimicked the experimental data (Fig. 7D). The main difference between the two models is that in model A, the majority of bacteria are killed and cleared from early phagosomes whereas in model B these processes predominantly occur in late compartments. As already pointed out, the latter model makes more sense, for example because it assumes a reasonable doubling time for BCG in the macrophage of 17 h whereas model A predicts a totally unrealistic value for this parameter of over 500 h. Moreover, the input value of 17 h in model A was essential for the good fit between theory and experiment; with slightly higher or lower values there was poor agreement between theory and experimental data.

Of course a model that accurately fits the data is far from guaranteeing that its assumptions are correct; after all model A, that we believe is unrealistic, also gives an excellent concordance between theory and experiment. Nevertheless, a model can lead to predictions that can be tested in further experiments. The preferred model B predicts that: (1) A small but significant degree of BCG killing (and presumably *M. bovis*) must occur in early phagosomes. (2) A rate-limiting step of maturation of phagosomes containing both live and killed bacteria occurs. (3) Once phagosomes have matured the live bacteria are killed very rapidly, on average in 30 min. (4) The bacteria that were killed in early phagosomes and those that are killed in late phagosomes are rapidly digested, and disappear from the system within 1 h. A recent study by Majlessi *et al.*

(2007) [22] provides support for the hypothesis that both the early and late mycobacterial phagosome can show hydrolytic activity since the same level of mycobacterial antigen presentation was seen irrespective of whether the bacteria resided in early or late phagosomes. We are currently setting up experiments to test some of these predictions, most notably the idea that the bacteria are killed and removed from the late compartments in a relatively short period, using live cell imaging methods.

Our data collectively argue that for BCG and *M. bovis* the killing by macrophages occurs in two distinct phases, the first, an early low pH- and RNI-dependent process, the second independent of both. The hypothesis emerges that multiple bacteriocidal factors must be delivered into the pathogenic mycobacterial phagosome. The first, early phase may be explained by the combination of a pH below neutrality and RNI. The second, later phase that occurs for sure after (and perhaps also before) the RNI wave evidently occurs independently of a low pH. We presume that two sets of hydrolytic enzymes or factors must contribute to the small degree of killing postulated to occur in early phagosomes and to the more extensive killing that likely occurs in late phagosomes. Factors such as cathelicidin, that has recently been implicated in killing *M. tuberculosis* [65] can be expected to contribute to the overall killing process. Although hydrolases are generally more active at lowered pH the late killing factors that we observed in this study were not affected by blocking the proton pump with bafilomycin. However, some lysosomal enzymes have an optimal activity at neutral pH [66], and even some enzymes with a low pH optimum may still retail significant activity at neutral pH. The identification of all the factors within both early and late phagosomes that have the potential to kill pathogenic mycobacteria, especially *M. tuberculosis* is now crucial to our understanding of the macrophage killing potential, and to evolve therapies that could boost this process.

Acknowledgements

We are grateful to Antonio Pedro Matos and Curry Cabral Hospital for his support in providing access to EM facilities and to Michael Niederweis for the GFP-recombinant strain of BCG, Helena Ferronha for the virulent strain of *M. bovis*, Isabel Portugal and Marta Simoes for the characterization of the virulent strain of *M. bovis* and technical support, respectively. We are also grateful for the reagents provided by the Centralised Facility for AIDS Reagents (NISB) and by Jean Gruenberg (LBPA antibody). This work was financed by a grant of the National Foundation for Science-FCT with co-

participation of FEDER project POCI/BIA-BCM/55327/2004. Luisa Jordao was funded as a PhD fellow from FCT (SFRH/BD/14284/2003). The sabbatical visit of Luis Mayorga to the EMBL was generously supported by a Research award from the Alexander von Humboldt Stiftung.

MATERIAL AND METHODS

Bacterial culture conditions: *M. tuberculosis* H37 Rv, *M. bovis* BCG Pasteur (ATCC35734), *M. bovis* BCG harbouring a pMN437 plasmid and a strain of *M. bovis* genetically characterized isolated from a bovine were grown on Middlebrook's 7H9 broth Medium (Difco) supplemented with 10 % OADC (v/v) and 0.05 % Tween 80 (v/v) until exponential phase at 37ºC / 5 % CO_2 . Media were supplemented with 50 µg/ml hygromycin (Roche) for selection of recombinant mycobacteria.

Cell line culture conditions: The mouse macrophage cell lines J774.A1 and RAW 264.7 were cultured as described previously. Two days before infection macrophages were seeded onto 24 wells culture dishes and left for 2 days in a 5 % CO_2 incubator at 37ºC (10^5 macrophages/ml).

THP-1 cells were grown in RPMI 1640 (Gibco) supplemented with 10 % fetal bovine serum (FBS: Gibco), 1 % Hepes (Gibco), penicillin and streptomycin (Gibco). The cells were seeded onto 24 well cultures dishes at a density of 5 x 10^5 cells/ml and treated overnight with 5 nM phorbol myristate acetate (PMA: Sigma). Then cells were washed three times with PBS and incubated for one more day.

Human monocyte derived macrophages (HMDM) isolation and culture: HMDM were prepared from venous blood from healthy volunteers donors using density gradient centrifugation as described before [67]. Cells were platted at a density of 2 x 10^6 cells/ml and incubated for 3 days with RPMI 1640 supplemented with 30 % FCS and 10 % human type AB serum (Sigma). Then cells were washed three times with warm 1 % FCS in PBS and cultured for 7 days before infection.

Bovine monocyte derived macrophages (BMDM) isolation and culture: BMDM were prepared from venous blood from healthy 8-9 months old male Holstein Friesian bovines using density gradient centrifugation. The protocol used was similar to the described above for HMDM. The density gradient used was different (NycoPrep 1.077A from AXIS-SHIELD) and the 10 % of human type AB serum added to RPMI medium was replaced by 10 % homologous bovine serum.

Bone marrow derived macrophages (BMM) isolation and culture: Experiments were performed with 3 weeks old C57BL/6 male mice from Jackson Laboratory. Mice were killed by cervical dislocation, and the femur and tibia bones were removed. The bones were trimmed at both ends, and the marrow was flushed out with 5 to 10 ml of RPMI containing 10 % FCS using a 23 gauge needle. The cell suspension was centrifuge for 4 minutes at 900 g and the pellet was gently ressuspended in RPMI supplemented with 10 % FCS, 1 % penicillin/streptomycin, 1 % non-essencial amino acids (Gibco) and 15 % L929 supernatant and plate into bacterial Petri dishes. After 3 days monolayers were washed with warm 1 % FCS in PBS and incubated for more 3 days. At this point more than 95 % of the cells were CD14 (BD Pharmigen) positive by flow citometry. Cells were scrapped and platted at a density of 2.5 x 10^5 cells/ml and incubated overnight before infection.

Macrophage infection: Bacterial cultures on exponential grown phase were pellet, washed twice in PBS pH 7.4 and resuspended in PBS to a final concentration of 5-10 x 10^9 cells/ml. Single cell suspensions were generated by 2 min pulse in a water-bath sonicator (room temperature) followed by passage through a 23-gauge needle to disrupt remaining bacterial clumps. Before infection, residual bacterial aggregates were removed by low speed centrifugation (120 x *g*) for 2 min. Single cell suspension was verified by light microscopy.

Before infection, non adherent cells were removed by wash with PBS and the medium replaced by antibiotic free medium supplemented with 10 % FBS. For achieve 2 to 8 bacilli per macrophage after 3 h uptake, an OD_{600nm}~0.1 was used for all the macrophages used except HMDM. For these macrophages an OD_{600nm}~0.01 was used instead. The cells were washed twice with PBS to remove free mycobacteria. At infection time (3 h) and after several days (3, 5 and 7 days) infected macrophages were washed with PBS and lysed with 1 % Igepal (Sigma) solution in water. Serial dilutions of the lysate were prepared in water and platted at Middlebrook 7H10 medium supplemented with OADC. After about 3 weeks of incubation at 37ºC colonies were counted.

For M. smegmatis a similar protocol was used with the following differences: (i) an OD_{600nm}~0.1 was used for all the macrophages and (ii) cells were allowed to uptake bacteria only for 1 h.

Treatment with γ-IFN, inhibitors and NOC-18: When required cells were treated with murine γ-IFN (50 IU) overnight before infection. γ-IFN was a kind gift from the Centralised Facility for AIDS Reagents.

When treated with iNO inhibitor N-(G)-nitro-L-arginine methyl ester hydrochloride (500 µg/ml L-NAME; Sigma) this compounds was added to the medium 1h before infection and left until the end of the experience. When treated with NOC-18 (0.1 or 1 µM; Calbiochem) this compound was added to the medium at time zero and left until the end of the experience. Chemicals were renewed during the course of the experiments according to their half-lives.

The V-ATPase inhibitor, bafilomycin A1, 25 nM or 50 nM (Sigma) was added to the medium in the following time windows: 3 h-1day, 1-3 days, 3-5days and 5-7days.

Nitric oxide: Culture supernatants were collect at several time points for determination of nitrite contents. Nitrite concentration indicating the NO production was performed using the standard Griess reaction adapted to microplate.

M. bovis spp in vitro sensitivity to NO was determined using serial dilutions of an 1000 µM NOC-18 solution in DMEM supplemented with 10 % FCS. After 1, 7 and 14 days serial dilutions of control and samples were platted on 7H10 supplemented with OADC supplement. After about 3 weeks of incubation at 37ºC colonies were counted.

Epifluorescence and Confocal Fluorescence Microscopy: Macrophages grown on glass coverslips were allowed to uptake *M. bovis* BCG harbouring a pMN437 plasmid (live / heat killed) or *M. bovis* stained with Oregon green (Molecular Probes). Cells were fixed with 3 % paraformaldehyde at room temperature for 15 min.

Lysotracker Red DND-99 (Molecular Probes) staining of acidic organelles was carried out by adding a 1:10.000 dilution in DMEM that was added for the last 30 min of the experiments. Cell permeabilization, when required, was achieved with 20 min treatment with 0.1 % Triton X100 (Sigma) in PBS. After 30 min blocking with 5 % goat serum (Sigma) in 0.1 % BSA/PBS, cells were incubated for 1 h with primary antibody, followed for further 30 min by secondary antibody. For LBPA staining and blocking were made with 0.1 % BSA/PBS, followed by simultaneous permeabilization /incubation with primary antibody diluted in a 0.05 % saponin (Sigma) solution in PBS, followed for further 30 min incubation with secondary antibody.

Confocal microscopy images were collected using the LSM510 from Zeiss and the percentage of co-localisation was calculated using either the Image J software system or manually. Fluorescence labelling and viability of mycobacteria was performed as described [30].

The following antibodies were used for immunofluorescence microscopy: The mouse iNOS antibody was purchased from BD Pharmigen and the LBPA antibody was a kind gift from Jean Gruenberg. The secondary antibodies used were linked to Cy3 (Molecular Probes).

Fusion assay: Analysis of phagosome lysosome fusion was carried out using 7 nm gold particles as describe before [18]. Macrophages were pulsed for 1 h with these gold particles, washed three times with PBS. Then one of two treatments was done: (a) chase for 1 h in complete culture medium, infection with mycobacteria 3 h in complete medium without antibiotics or (b) chase for 4 h in medium without antibiotics. The first treatment was applied for 3 h time point and the second for all the others. Macrophages were fixed with 3 % PFA in PBS and processed for microscopy.

Dead *vs* live bacteria determination: 3 h, 1, 3, 5 and 7 days post-infection macrophages were scrapped, stained with trypan blue (Sigma) and counted in a Neubauer chamber. Infected macrophages were then lysed with 1 % Igepal in water. Dead mycobacteria were stained with PI as described in Anes *et al.* (2006) [18]. Mycobacteria pellets were ressuspended in PBS and dead (red or yellow) and live (green) bacteria were counted in a Neubauer chamber by fluorescence microscopy.

Preparation of whole cell extracts and immunoblot analysis: Whole cell extracts were prepared as previously described [18]. Equal amounts of protein were loaded on a 6 % SDS-PAGE, transferred to nitrocellulose membrane and probed with a mouse anti-iNOS (BD Pharmigen) and mouse anti-actin (BD Pharmigen) antibodies. Enhanced chemi-luminescence (Pierce biotechnology) was used to visualize antibody binding. Actin was used to assess the amount of total protein in the different membrane isolates.

Electron microscopy: Macrophages (J774.A1, HMDM) infected with *M. bovis spp* as described previously in this section were fixed with 1 % glutaraldehyde (EM grade Sigma) in cell culture medium without serum during 10 minutes at 37ºC. Cell cultures

were washed several times with 200 mM Hepes pH 7.4 and incubated overnight at room temperature with 1 % glutaraldehyde in 200 mM Hepes 7.4. Samples were processed for cryo-sectioning as described by Tokuyasu (1973) [57]. Negative staining using ammonium molybdate was done as described before by Griffiths *et al* (1993) [55].
After fixation some samples were post-fixed in osmium and uranyl acetate and embedded in epoxy resin as described previously [68,68]. Thin sections were stained with lead citrate and uranyl acetate and analysed by transmission electron microscopy.

Modelling the intracellular transport and killing of *M. bovis* BCG: A set of 7 differential equations were generated in the COPASI 4.0.20 modelling program (http://www.copasi.org) [69] describing the duplication, killing in early and late compartments, transport of live and dead bacteria from early to late compartments (= phagosome maturation) and disappearance (digestion) of bacteria in early and late compartments . Simple mass action reactions were used for the kinetics of all steps. The same program was used to find a set of parameters that minimize the weighted sum of square differences between values predicted for the model and the experimental data. The COPASI file is available in the following webpage http:// www.ff.ul.pt/paginas/eanes/COPASI**.**

REFERENCE LIST

1. Baker,M.G., Lopez,L.D., Cannon,M.C., de Lisle,G.W. & Collins,D.M. Continuing *Mycobacterium bovis* transmission from animals to humans in New Zealand. *Epidemiol. Infect.* 1-6 (2006).

2. Wedlock,D.N., Skinner,M.A., de Lisle,G.W. & Buddle,B.M. Control of *Mycobacterium bovis* infections and the risk to human populations. *Microbes Infect.* **4**, 471-480 (2002).

3. Biet,F., Boschiroli,M.L., Thorel,M.F. & Guilloteau,L.A. Zoonotic aspects of *Mycobacterium bovis* and *Mycobacterium avium*-intracellulare complex (MAC). *Vet. Res.* **36**, 411-436 (2005).

4. Pollock,J.M. & Neill,S.D. *Mycobacterium bovis* infection and tuberculosis in cattle. *Vet. J* **163**, 115-127 (2002).

5. Hedvalle,E. Some cases of pulmonary tuberculosis treated with streptomycin. *Acta Med. Scand.* **134**, 311-34, illust (1949).

6. Gandhi,N.R. *et al.* Extensively drug-resistant tuberculosis as a cause of death in patients co-infected with tuberculosis and HIV in a rural area of South Africa. *Lancet* **368**, 1575-1580 (2006).

7. Clemens,D.L. Characterization of the *Mycobacterium tuberculosis* phagosome. *Trends Microbiol.* **4**, 113-118 (1996).

8. Stewart,G.R., Patel,J., Robertson,B.D., Rae,A. & Young,D.B. Mycobacterial mutants with defective control of phagosomal acidification 1. *PLoS. Pathog.* **1**, 269-278 (2005).

9. Vergne,I., Chua,J., Singh,S.B. & Deretic,V. Cell biology of mycobacterium tuberculosis phagosome. *Annu. Rev. Cell Dev. Biol.* **20**, 367-394 (2004).

10. Via,L.E. *et al.* Effects of cytokines on mycobacterial phagosome maturation. *J Cell Sci* **111 (Pt 7)**, 897-905 (1998).

11. Hart,P.D., Armstrong,J.A., Brown,C.A. & Draper,P. Ultrastructural study of the behavior of macrophages toward parasitic mycobacteria. *Infect. Immun.* **5**, 803-807 (1972).

12. Pethe,K. *et al.* Isolation of *Mycobacterium tuberculosis* mutants defective in the arrest of phagosome maturation. *Proc. Natl. Acad. Sci. U. S. A* **101**, 13642-13647 (2004).

13. Russell,D.G. *Mycobacterium tuberculosis*: here today, and here tomorrow. *Nat. Rev. Mol. Cell Biol.* **2**, 569-577 (2001).

14. Sturgill-Koszycki,S. *et al.* Lack of acidification in *Mycobacterium* phagosomes produced by exclusion of the vesicular proton-ATPase. *Science* **263**, 678-681 (1994).

15. Kusner,D.J. Mechanisms of mycobacterial persistence in tuberculosis. *Clin. Immunol* **114**, 239-247 (2005).

16. Silva,M.T., Appelberg,R., Silva,M.N. & Macedo,P.M. *In vivo* killing and degradation of *Mycobacterium aurum* within mouse peritoneal macrophages. *Infect. Immun.* **55**, 2006-2016 (1987).

17. Cohn,Z.A. The fate of bacteria within phagocytic cells. II. The modification of intracellular degradation. *J Exp. Med.* **117**, 43-53 (1963).

18. Anes,E. *et al.* Dynamic life and death interactions between *Mycobacterium smegmatis* and J774 macrophages. *Cell Microbiol.* **8**, 939-960 (2006).

19. Armstrong,J.A. & Hart,P.D. Response of cultured macrophages to *Mycobacterium tuberculosis*, with observations on fusion of lysosomes with phagosomes. *J Exp. Med.* **134**, 713-740 (1971).

20. Gomes,M.S. *et al.* Survival of *Mycobacterium avium* and *Mycobacterium tuberculosis* in acidified vacuoles of murine macrophages. *Infect. Immun.* **67**, 3199-3206 (1999).

21. MacGurn,J.A. & Cox,J.S. A genetic screen for *Mycobacterium tuberculosis* mutants defective for phagosome maturation arrest identifies components of the ESX-1 secretion system. *Infect. Immun.* **75**, 2668-2678 (2007).

22. Majlessi,L. *et al.* Inhibition of phagosome maturation by mycobacteria does not interfere with presentation of mycobacterial antigens by MHC molecules. *J Immunol* **179**, 1825-1833 (2007).

23. Webb,J.L., Harvey,M.W., Holden,D.W. & Evans,T.J. Macrophage nitric oxide synthase associates with cortical actin but is not recruited to phagosomes. *Infect. Immun.* **69**, 6391-6400 (2001).

24. Chan,E.D. *et al.* Induction of inducible nitric oxide synthase-NO* by lipoarabinomannan of *Mycobacterium tuberculosis* is mediated by MEK1-ERK, MKK7-JNK, and NF-kappaB signaling pathways. *Infect. Immun.* **69**, 2001-2010 (2001).

25. Morris,K.R. *et al.* Role of the NF-kappaB signaling pathway and kappaB cis-regulatory elements on the IRF-1 and iNOS promoter regions in mycobacterial lipoarabinomannan induction of nitric oxide 1. *Infect. Immun.* **71**, 1442-1452 (2003).

26. Long,R., Light,B. & Talbot,J.A. Mycobacteriocidal action of exogenous nitric oxide. *Antimicrob. Agents Chemother.* **43**, 403-405 (1999).

27. Long,R. *et al.* Inhaled nitric oxide treatment of patients with pulmonary tuberculosis evidenced by positive sputum smears. *Antimicrob. Agents Chemother.* **49**, 1209-1212 (2005).

28. O'Brien,L., Carmichael,J., Lowrie,D.B. & Andrew,P.W. Strains of *Mycobacterium tuberculosis* differ in susceptibility to reactive nitrogen intermediates *in vitro*. *Infect. Immun.* **62**, 5187-5190 (1994).

29. Rhoades,E.R. & Orme,I.M. Susceptibility of a panel of virulent strains of *Mycobacterium tuberculosis* to reactive nitrogen intermediates. *Infect. Immun.* **65**, 1189-1195 (1997).

30. Anes,E. *et al.* Selected lipids activate phagosome actin assembly and maturation resulting in killing of pathogenic mycobacteria. *Nat. Cell Biol.* **5**, 793-802 (2003).

31. Kuehnel,M.P. *et al.* Characterization of the intracellular survival of *Mycobacterium avium ssp*. paratuberculosis: phagosomal pH and fusogenicity in J774 macrophages compared with other mycobacteria. *Cell Microbiol.* **3**, 551-566 (2001).

32. Clemens,D.L. & Horwitz,M.A. Characterization of the *Mycobacterium tuberculosis* phagosome and evidence that phagosomal maturation is inhibited. *J Exp. Med.* **181**, 257-270 (1995).

33. Bonecini-Almeida,M.G. *et al.* Induction of in vitro human macrophage anti-*Mycobacterium tuberculosis* activity: requirement for IFN-gamma and primed lymphocytes. *J Immunol* **160**, 4490-4499 (1998).

34. Carpenter,E., Fray,L. & Gormley,E. Antigen-specific lymphocytes enhance nitric oxide production in *Mycobacterium bovis* BCG-infected bovine macrophages. *Immunol Cell Biol.* **76**, 363-368 (1998).

35. Nozaki,Y., Hasegawa,Y., Ichiyama,S., Nakashima,I. & Shimokata,K. Mechanism of nitric oxide-dependent killing of *Mycobacterium bovis* BCG in human alveolar macrophages. *Infect. Immun.* **65**, 3644-3647 (1997).

36. Schaible,U.E., Collins,H.L. & Kaufmann,S.H. Confrontation between intracellular bacteria and the immune system. *Adv. Immunol* **71**, 267-377 (1999).

37. Miller,B.H. *et al.* Mycobacteria inhibit nitric oxide synthase recruitment to phagosomes during macrophage infection. *Infect. Immun.* **72**, 2872-2878 (2004).

38. Deretic,V. *et al. Mycobacterium tuberculosis* inhibition of phagolysosome biogenesis and autophagy as a host defence mechanism. *Cell Microbiol.* **8**, 719-727 (2006).

39. Kusner,D.J. & Barton,J.A. ATP stimulates human macrophages to kill intracellular virulent *Mycobacterium tuberculosis* via calcium-dependent phagosome-lysosome fusion. *J Immunol* **167**, 3308-3315 (2001).

40. Malik,Z.A., Denning,G.M. & Kusner,D.J. Inhibition of Ca(2+) signaling by *Mycobacterium tuberculosis* is associated with reduced phagosome-lysosome fusion and increased survival within human macrophages. *J Exp Med.* **191**, 287-302 (2000).

41. Russell,D.G. *Mycobacterium tuberculosis* and the four minute phagosome. *ASM News* **71**, 459-463 (2005).

42. Vieira,O.V., Botelho,R.J. & Grinstein,S. Phagosome maturation: aging gracefully. *Biochem. J* **366**, 689-704 (2002).

43. Vergne,I. *et al.* Mechanism of phagolysosome biogenesis block by viable *Mycobacterium tuberculosis*. *Proc. Natl. Acad. Sci. U. S. A* **102**, 4033-4038 (2005).

44. Griffiths,G., Hoflack,B., Simons,K., Mellman,I. & Kornfeld,S. The mannose-6-phosphate receptor and the biogenesis of lysosomes. *Cell* **52**, 329-341 (1988).

45. Xu,S. *et al.* Intracellular trafficking in *Mycobacterium tuberculosis* and *Mycobacterium avium*-infected macrophages. *J Immunol* **153**, 2568-2578 (1994).

46. Schmid,S.L. & Cullis,P.R. Membrane sorting. Endosome marker is fat not fiction. *Nature* **392**, 135-136 (1998).

47. Yates,R.M., Hermetter,A. & Russell,D.G. The kinetics of phagosome maturation as a function of phagosome/lysosome fusion and acquisition of hydrolytic activity. *Traffic.* **6**, 413-420 (2005).

48. Chapman J S & Bernard,J.S. The tolerances of unclassified mycobacteria. I. Limits of pH tolerance. *Am. Rev. Respir. Dis.* **86**, 582-583 (1962).

49. McDonough,K.A., Kress,Y. & Bloom,B.R. Pathogenesis of tuberculosis: interaction of *Mycobacterium tuberculosis* with macrophages. *Infect. Immun.* **61**, 2763-2773 (1993).

50. Myrvik,Q.N., Leake,E.S. & Wright,M.J. Disruption of phagosomal membranes of normal alveolar macrophages by the H37Rv strain of *Mycobacterium tuberculosis*. A correlate of virulence. *Am. Rev. Respir. Dis.* **129**, 322-328 (1984).

51. van der Wel,N. *et al. M. tuberculosis* and *M. leprae* Translocate from the Phagolysosome to the Cytosol in Myeloid Cells. *Cell* **129**, 1287-1298 (2007).

52. Stamm,L.M. *et al. Mycobacterium marinum* escapes from phagosomes and is propelled by actin-based motility. *J Exp. Med.* **198**, 1361-1368 (2003).

53. Stamm,L.M. *et al.* Role of the WASP family proteins for *Mycobacterium marinum* actin tail formation. *Proc. Natl. Acad. Sci U. S. A* **102**, 14837-14842 (2005).

54. Cossart,P. & Sansonetti,P.J. Bacterial invasion: the paradigms of enteroinvasive pathogens. *Science* **304**, 242-248 (2004).

55. Griffiths,G. Fine Structure Immunocytochemistry. Berlin (1993).

56. Al Amoudi,A. *et al.* Cryo-electron microscopy of vitreous sections. *EMBO J* **23**, 3583-3588 (2004).

57. Tokuyasu,K.T. A technique for ultracryotomy of cell suspensions and tissues. *J Cell Biol.* **57**, 551-565 (1973).

58. Barker,L.P., George,K.M., Falkow,S. & Small,P.L. Differential trafficking of live and dead *Mycobacterium marinum* organisms in macrophages. *Infect. Immun.* **65**, 1497-1504 (1997).

59. Di,A. *et al.* Quantal release of free radicals during exocytosis of phagosomes. *Nat. Cell Biol.* **4**, 279-285 (2002).

60. Beste,D.J. *et al.* Compiling a molecular inventory for *Mycobacterium bovis* BCG at two growth rates: evidence for growth rate-mediated regulation of ribosome biosynthesis and lipid metabolism. *J Bacteriol.* **187**, 1677-1684 (2005).

61. Jagannath,C., Actor,J.K. & Hunter,R.L., Jr. Induction of nitric oxide in human monocytes and monocyte cell lines by *Mycobacterium tuberculosis*. *Nitric. Oxide.* **2**, 174-186 (1998).

62. Macmicking,J.D. *et al.* Identification of nitric oxide synthase as a protective locus against tuberculosis. *Proc. Natl. Acad. Sci. U. S. A* **94**, 5243-5248 (1997).

63. Rich,E.A. *et al. Mycobacterium tuberculosis* (*MTB*)-stimulated production of nitric oxide by human alveolar macrophages and relationship of nitric oxide production to growth inhibition of *MTB*. *Tuber. Lung Dis.* **78**, 247-255 (1997).

64. Denis,M. Involvement of cytokines in determining resistance and acquired immunity in murine tuberculosis. *J Leukoc. Biol.* **50**, 495-501 (1991).

65. Liu,P.T. *et al.* Toll-like receptor triggering of a vitamin D-mediated human antimicrobial response. *Science* **311**, 1770-1773 (2006).

66. Butor,C., Griffiths,G., Aronson,N.N., Jr. & Varki,A. Co-localization of hydrolytic enzymes with widely disparate pH optima: implications for the regulation of lysosomal pH. *J Cell Sci* **108 (Pt 6)**, 2213-2219 (1995).

67. Mendez-Samperio,P., Ayala,H., Trejo,A. & Ramirez,F.A. Differential induction of TNF-alpha and NOS2 by mitogen-activated protein kinase signaling pathways during *Mycobacterium bovis* infection. *J Infect.* **48**, 66-73 (2004).

68. Bozzola JJ, Johnson MC & Shechmeister IL. In situ multiple sampling of attached bacteria for scanning and transmission electron microscopy. *Stain Technol.* **48**, 317-325 (1973).

69. Hoops,S. *et al.* COPASI--a COmplex PAthway SImulator. *Bioinformatics.* **22**, 3067-3074 (2006).

Chapter 4

PUFAs and ceramide regulation of inflammatory states during macrophage infection with intracellular pathogens

Lipid regulation of inflammatory states during macrophage infection with *Mycobacterium*.

Luisa Jordao[1], Carlos Guzman[2], Pablo D. Becker[2], Andreas Lengeling[2], Yann Bordat[3], Frederic Boudou[3], Brigitte Gicquel[3], Olivier Neyrolles[3,4], Gareth Griffiths[5*] and Elsa Anes[1*]

[1] Molecular Pathogenesis Centre, Unit of Retrovirus and Associated Infections, Faculty of Pharmacy, University of Lisbon, Av. Forcas Armadas, 1600-083 Lisbon, Portugal.

[2] Department of Vaccinology, Helmholtz Centre for Infection Research, Inhoffenstrasse 7, 38124 Braunschweig, Germany.

[3]Unité de Génétique Mycobactérienne, Institut Pasteur, Paris

[4] Genetics and Biochemistry of Microorganisms, Centre National de la Recherche Scientifique (CNRS) Paris, France.

[5] EMBL, Postfach 102209, 69117 Heidelberg, Germany.

[*]Corresponding Authors

Submitted for publication.

ABSTRACT

Recently we showed that treatment of mycobacteria-infected macrophages with pro-inflammatory lipids, especially the omega-6 lipid, arachidonic acid (AA) and ceramide (Cer) enhanced bacterial killing whereas the anti-inflammatory, omega-3 lipid eicosapentanoic acid (EPA) stimulated bacterial growth. The latter result agreed with earlier studies with *M. tuberculosis* and another intracellular pathogen in mouse infection models. We therefore tested the effects of diets enriched in omega-3 and omega-6 lipids on these pathogens in mice. In contrast to the results with macrophages, the omega-6 supplemented diets tended to increase survival of both pathogens, while the omega-3-rich diet tended to increase pathogen killing. Given these unpredictable results we focused in more detail at the macrophage level. We recently showed that *M. smegmatis* in macrophages is subjected to alternate cycles of pro-inflammatory killing and anti-inflammatory survival/growth responses. Here in macrophages infected with *M. smegmatis* and *M. tuberculosis* H37Rv the three lipids could switch the system between pro- and anti-inflammatory signalling states. In general, the effects of Cer and/or AA were opposite to those of EPA, but in many infection stages all three lipids could be either pro-inflammatory (more killing of bacteria) or anti-inflammatory (more growth). These results argue against the idea of considering a simple recommended lipid-based diet to treat mycobacteria-infected individuals.

INTRODUCTION

An important part of the life cycle of *M. tuberculosis* and related pathogens in infected animals is spent within phagosomes inside macrophages. These cells will take up all mycobacteria but a striking difference is seen between the non-pathogenic types, such as *M. smegmatis*, that are killed by macrophages, and the pathogens, such as *M. tuberculosis* that can survive and multiply in macrophages [1-3]. After phagocytic uptake of *M. smegmatis* into phagosomes, these organelles undergo a maturation process involving multiple fusion events with early endosomes and the late endocytic organelles that are generally classified as late endosomes and lysosomes or, often simply 'lysosomes'. As a consequence of the late fusion events, the phagosomes acquire hydrolytic enzymes and the proton ATPase that acidifies the lumen, the phagosomes thereby undergo complete maturation. Collectively, these factors together with free radicals, may contribute to killing *M. smegmatis*, that is cleared by macrophages within 24-48 h [4-6]. In contrast, the pathogenic mycobacteria block late fusion events allowing *M. tuberculosis* and related pathogens to grow and divide within an arrested early phagosome [7-11].

In recent studies, we provided evidence for links between the ability of phagosomes to assembly actin filaments *de novo* on the cytoplasmic surface to the late fusion events between phagosomes and late endocytic organelles. Indeed, under an increasing set of conditions that stimulate macrophages, the ability of phagosomes to assemble actin correlates well with both their increased fusion with later endocytic organelles and their acidification as well as with an increased ability of infected macrophages to kill non-pathogenic and pathogenic mycobacteria. In contrast, conditions that inhibit phagosomal actin assembly are correlated with less fusion/acidification but more growth of the mycobacteria [4,5,12-14]. This leads us to hypothesize that the nucleation of actin on membranes is part of the pro-inflammatory response. The MAP Kinase p38 was found to be a key regulator of many of the processes relevant for the macrophage-phagosome interactions. Whereas some functions regulated by p38 seemed to favour the macrophage infected with *M. smegmatis* other functions appeared to favour the bacteria, at some particular stages of the life cycle [5].

A striking effect of stimulating phagosomal-actin assembly activity, and consequently late fusion and killing of mycobacteria was seen after adding to J774 macrophages infected with *M. smegmatis* and pathogenic strains of *M. tuberculosis* spp complex a

number of pro-inflammatory lipids, especially arachidonic acid (AA) and Cer. In contrast, the anti-inflammatory lipid eicosapentanoic acid (EPA) induced an increase in mycobacterial growth in macrophages [4]. These results were exciting because they fitted nicely into a general pattern seen with these classes of lipids in whole organisms. In fact, two earlier studies showed that a high omega-3 diet indeed led to significant increases in growth of *Salmonella* in mice [15] and *M. tuberculosis* in guinea pigs [16,17].

An omega-3 enriched diet was correlated over 30 years ago with a higher incidence of tuberculosis in Eskimos and Inuits, whose diet is rich in fish oil, the best-characterized source of omega-3 lipids [18,19]. Parallel studies by Bang and Dyerberg [20,21] showed the importance of the dietary intake of both omega-3 and omega-6 fatty acids -that are now accepted as being essential constituents of a healthy diet. The modern Western diet tends to be deficient in omega-3 fatty acids and a large number of case studies argue for the beneficial effects of omega-3 supplements, or eating fatty fish [22-25].

Collectively, the above data suggested that a high omega-6 diet might be beneficial against mycobacteria, while a high omega-3 diet might be detrimental. Given the increasing tendency of omega-3 dietary supplements, that are generally beneficial to uninfected people, to be recommended and used [18,21,26-30] it follows that for patients suffering from tuberculosis and other diseases it is important to know whether these lipids influence the course of infection, one way or the other.

However, when one looks at the literature on the effects of omega-3 and -6 lipids on a variety of different pathogens, especially at the level of animal models, the conclusion is more sobering. While these lipids have tremendous effects on many processes related to infections, the results are highly contradictory. In a critical evaluation of all the experiments done to test the effects of omega-3 lipids in the context of infections diseases Anderson and Fritsch [31] concluded that, of the 30 papers they examined there were “an equal number of papers published that report an adverse effect of (n-3) polyunsaturated fatty acids (PUFA) on host infectious disease resistance as those that do not show an effect or show a beneficial effect”. Later in the same article they wrote “It is unclear why so much inconsistency exists”.

Given this situation, we decided to test omega-3 and omega-6 rich diets in mouse models of *Salmonella typhimurium* [15,32,33] and *M. tuberculosis* H37 Rv [17]. The results we obtained and described here were disappointing, in that the opposite effects were seen in the animal to what had been seen in macrophages – but they agreed fully with the assessment of Anderson and Fritsche [31].

We therefore decided to step back in complexity and make a more comprehensive analysis at the macrophage level of two pro-inflammatory lipids, AA and Cer, and the anti-inflammatory lipid EPA. After initial studies in *M. tuberculosis*-infected macrophages, we focussed in more detail on *M. smegmatis* in J774 cells, a system we have recently characterized in great detail [5]. In J774 cells, and in mouse primary bone marrow macrophages (Jordao unpublished results) this bacterium follows a complex dynamics in which periods of killing are interspersed with a transient stage of bacterial growth. Three distinct killing stages were seen between 1and 4 h, 8-12 h and between 12 and 24 h after infection; the second and third killing phases could be separated by the fact that the 8-12 h one was independent of phagosome actin assembly and lysosome fusion whereas both 1-4 h and the 12-24 h correlated with these processes. In between killing phase 1 and 2, the 8-12 h phase is a period conducive for *M. smegmatis* growth [34]. An identical pattern was seen in *M. smegmatis* infection in mouse bone marrow macrophages. However, with monocyte derived macrophages from human blood and RAW macrophages, while the 1-4 h killing was identical, thereafter a period of stasis was seen (Jordao unpublished results).

These data suggest that the macrophage can alternate between cytoplasmic states that are beneficial to the host and to the bacteria. That different macrophage states exist was also shown by analysis of latex bead phagosomes; whereas 2-4 h LBP are active in actin assembly, high in phosphatidylinositol biphosphate (PIP_2), and in total kinase activity the 8-12 h stages are low in these parameters. Strikingly, at 24 h the phagosomes are again active [35-37]. The cyclical pattern of actin assembly was also seen with isolated *M. smegmatis* phagosomes [5].

We therefore took advantage of these different macrophage cytoplasmic states and tested the addition of AA, Cer and EPA, that were added at restricted times of infection, on *M. smegmatis* survival in J774 cells. Strikingly, all the lipids can stimulate either bacteria killing or survival depending on when they are added during the time course of infection. Cer has been shown to stimulate p38 in many studies [38-40]. We provide more evidence for links between Cer and p38 in the context of *M. smegmatis* and *M. tuberculosis* infection of macrophages.

RESULTS

Effects of omega-3 and omega-6 enriched diets on the infection of mice with *Salmonella* and *M. tuberculosis*.

We first tested the effect of Omega-3 and Omega-6 enriched diets on the survival of *S.typhimurum* in order to extend the earlier studies of Chang *et al* [15]. For this, we investigated the ability of *Salmonella* to colonize and persist *in vivo* in mice receiving one of three different diets: control (soy), omega-3 rich (menhaden oil) or omega-6 rich (Safflower oil). Balb/C mice were fed with these diets one week before and during infection. The animals were infected by the oral route with the virulent strain ATCC 14028. The number of bacteria recovered from Peyer's patches, mesenteric lymph-nodes, spleen and liver were determined at different time intervals. On day 3 post-infection, similar numbers of bacteria were recovered in Peyer's patches and mesenteric lymph nodes from mice under all treatment conditions (Fig.1A). This argued that the bacterial capacity to infect, invade and survive within the host was not affected by any of the lipid diets. However, when liver and spleen were considered, bacterial loads seemed to be higher in animals receiving the omega-6 enriched diet. This pattern was even more striking on day 7 post infection (Fig.1A), since in all tested organs the number of bacteria per gram of tissue was significantly higher ($P<0.05$) than in the groups receiving the standard (soy) and omega-3-enriched (i.e., menhaden) diets.

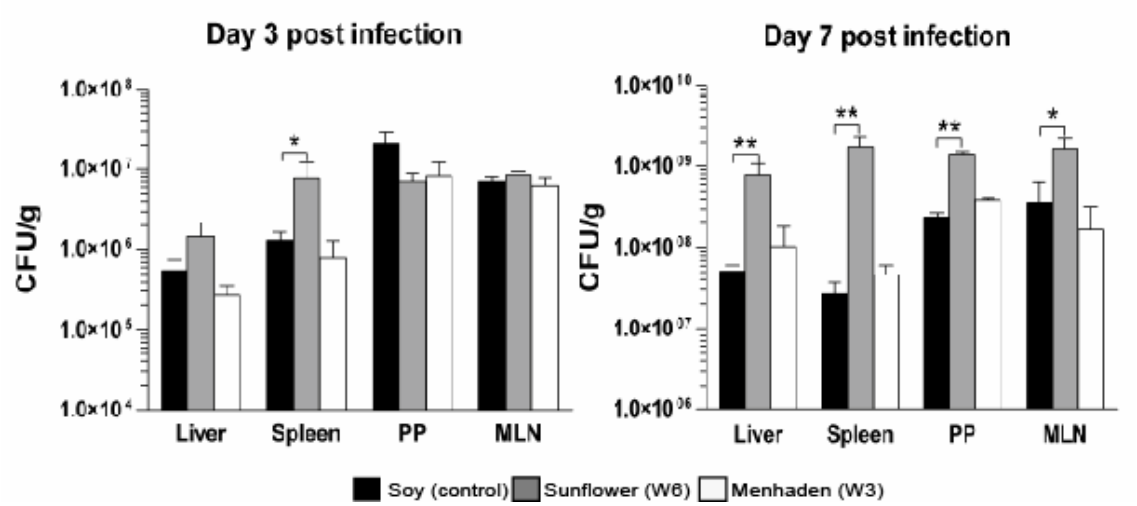

Figure 1A. Persistence of *S. enterica serovar Typhimurium* in organs from mice receiving diets enriched in specific fatty acids

After 5 weeks on the diets enriched in specific fatty acids, mice were challenged with $5x10^6$ cells of the virulent *S. enterica* strain ATCC 14028 by oral route. On day 3 and 7 post infection,

mice were sacrificed (n=3) and the number of viable bacteria present in Peyer's patches (PP), mesenteric lymph nodes (MLN), spleen and liver was determined by plating serial dilutions. Results are expressed as colony forming units (CFU) per gram of tissue. The standard error of the mean is indicated by vertical lines. The differences between experimental groups were statistically significant at $P < 0.05$ (*) or 0.01 (**).

These results suggest that in animals receiving the omega-6 enriched diet, the non specific clearance mechanisms were less efficient in controlling bacterial spread and dissemination. However, despite the fact that the omega-3 diet conferred a better edge to control infection, in the long term none of the diets was able to confer full-protection against a lethal challenge. Although mice receiving soy and menhaden enriched diets survived longer than those on the omega-6 diet (9 versus 11 days), the differences were not statistically significant (P>0.05).

We next carried out a similar strategy to test the effects of the lipids on *M. tuberculosis* infection (done in a separate laborarory). Balb/C mice were fed with a basal low fat diet supplemented or not with 10% safflower oil (rich in omega-6) or 10% Ropufa fish oil (rich in omega-3), and were infected intra-nasally with 10^3 *M. tuberculosis* H37Rv colony forming units (CFUs). Diets were given two weeks prior to infection, and were continued during the infection. One, 21 and 56 days after inoculation, lungs and spleens were recovered, homogenized and plated onto agar medium for CFU scoring (Fig. 1B).

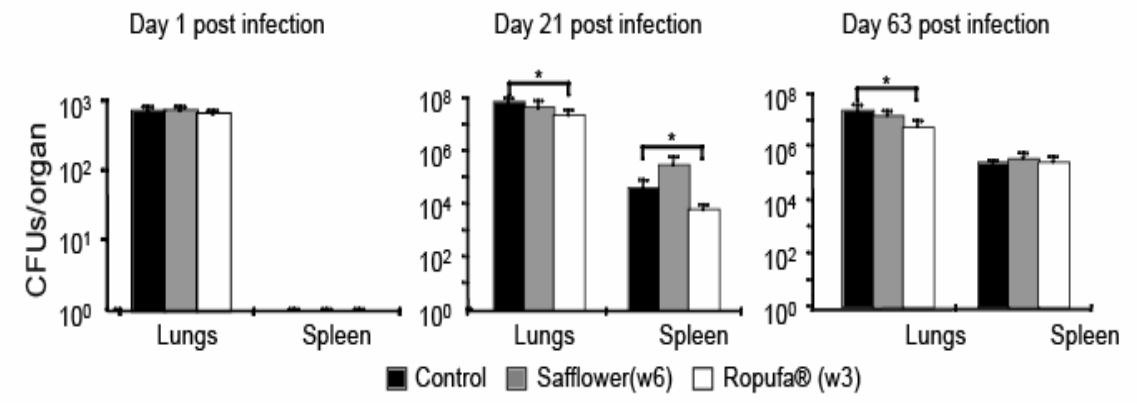

Figure 1B. Persistence of *M. tuberculosis* in organs from mice receiving diets enriched in specific fatty acids

Mice where divided in two groups, one receiving a normal lipid containing diet and the other receiving a low fat regimen. Both groups were then submitted to diets enriched in specific fatty acids. After 2 weeks on these regimens, mice were challenged with 10^3 cells of the virulent *M.*

tuberculosis H37Rv by intranasal route. On day 1 and 21 and 56 post infection, mice were sacrificed (n=3) and the number of viable bacteria present in the lung and spleen was determined by plating serial dilutions. Results are expressed as colony forming units (CFU) per gram of tissue. The standard error of the mean is indicated by vertical lines. The differences between experimental groups were statistically significant at $P < 0.05$ (*) or 0.01 (**).

While the omega-6 regimen had only a weak and statistically non-significant effect on progression of the infection in the lungs and the spleen of the animals, omega-3 treatment led to a slight, but statistically significant reduction in mycobacterial loads in the lungs and spleen both after 21 and 56 days after inoculation (Fig. 1B- Low fat regimen). This result suggest that, if anything, the omega-3 had an antimycobacterial effect *in vivo* rather than being conducive to pathogen survival, as we had predicted.

Effect of EPA, Ceramide and AA on *M. tuberculosis* growth in J774 macrophages

Given the fact that the effects of the pro and anti-inflammatory lipids were the opposite at the animal level to what we observed at the *in vitro* macrophage level we decided to go back to the macrophage level for further analysis. We started to investigate the effect of pre or co-infection treatment with pro-inflammatory (AA) or the anti-inflammatory (EPA) lipid on the survival of *M. tuberculosis* H37Rv (Fig. 2).

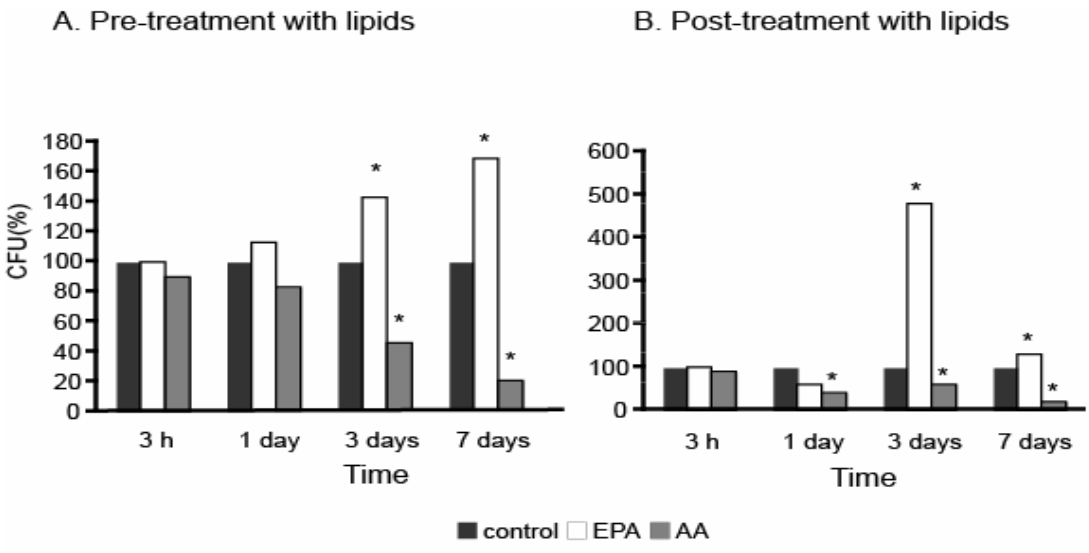

Figure 2. Effects of EPA or AA during the course of *M. tuberculosis H37Rv* infection in J774 macrophages (A)

Cultures of J774 macrophages were pre-treated from 3 days before infection with EPA or AA. After uptake DMEM medium was replaced without adding more lipids **(B)** Infected cultures were put in contact with EPA or AA after 3 h of bacteria uptake. Bacteria were recovered for CFU counting during the course of the infection. *P<0.05* (*)

In accordance with our previous data [4] *M. tuberculosis* survival in J774 macrophages was enhanced by EPA and decreased by AA addition. These general effects could be observed for both kinds of lipid treatments, as seen in Fig. 2A (pre-treatment) and Fig. 2B (Co-treatment) although some differences could be observed. The magnitude of the observed effects was higher after co-treatment with both lipids (Fig. 2B) than with pre-treatment (Fig. 2A).

We next tested another lipid, Cer that we had also found to be effective in killing *M. tuberculosis* in J774 macrophages. This lipid is generated from sphingomyelin by the action of sphingomyelinase, whose activity is stimulated by AA [41,42]. Thus, Cer may be a downstream effector of AA. Many of the effects of Cer can be considered pro-inflammatory [43]. When added after infection (3h) to J774 cells Cer significantly enhanced *M. tuberculosis* killing, with the effects increasing from day 3 to day 7 when 80 % of bacterial killing was achieved (Fig. 3).

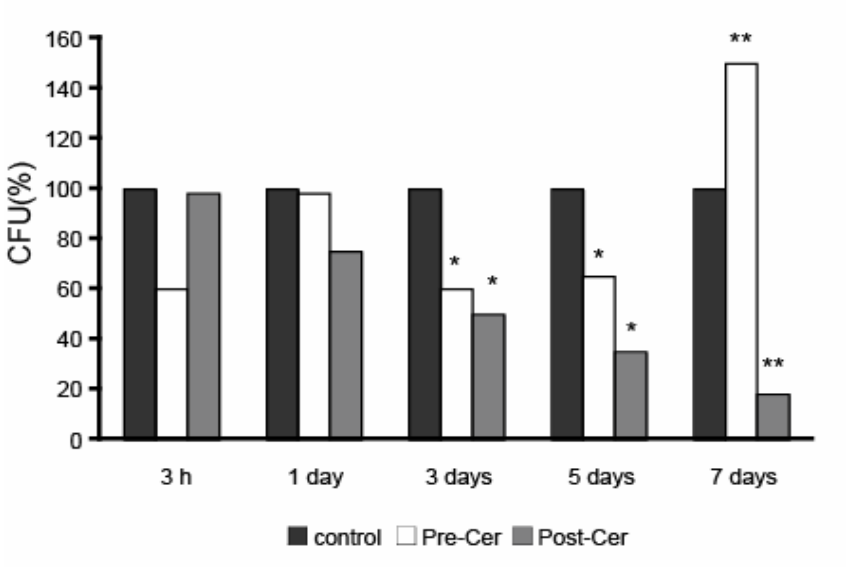

Figure 3. Effects of ceramide during the course of *M. tuberculosis H37Rv* infection in J774 macrophages

Cultures of J774 macrophages were pre-treated from 3 days before infection with Cer and after uptake DMEM medium was replaced without adding more lipids (Pre-Cer). Infected cultures were put in contact with ceramide after 3 h of bacteria uptake (Post-Cer). Bacteria were recovered for CFU counting during the course of the infection. *P<0.05* (*), *P<0.01* (**).

When cells were pre-treated with Cer for 3 days before infection and the lipid were left on the culture there was also a tendency for increasing killing at days 3 and 5. However, at day 7 a significant increase in *growth* was seen (Fig. 3). So at this particular time, the pre-treatment with Cer seems to switch the system from a pro-inflammatory to an anti-inflammatory state.

Pro- and anti-inflammatory lipids regulate TNF-α secretion

In macrophages infected with pathogenic mycobacteria TNF-α is known to be an important cytokine whose extra-cellular levels correlate strongly with the ability of macrophages to kill mycobacteria both *in vitro* studies and in animal models [44-47]. In response to the non-pathogenic, *M. smegmatis* macrophages secrete high amounts of TNF-α whereas *M. tuberculosis*-infected cells secrete much less [48]. In *in vitro* macrophage infection the secreted TNF-α has the potential to activate the TNF-α receptor to induce an autocrine signalling cascade. In the case of non-pathogenic mycobacteria these cascades somehow induce more killing of the bacteria, whereas the pathogens have the ability to block these signalling events [49]. Here, we asked whether EPA, Cer or AA could modulate the levels of TNF-α secretion. We therefore asked whether any of the three lipids had any effect on the secretion of TNF- α in J774 cells infected with *M. tuberculosis* H37Rv.

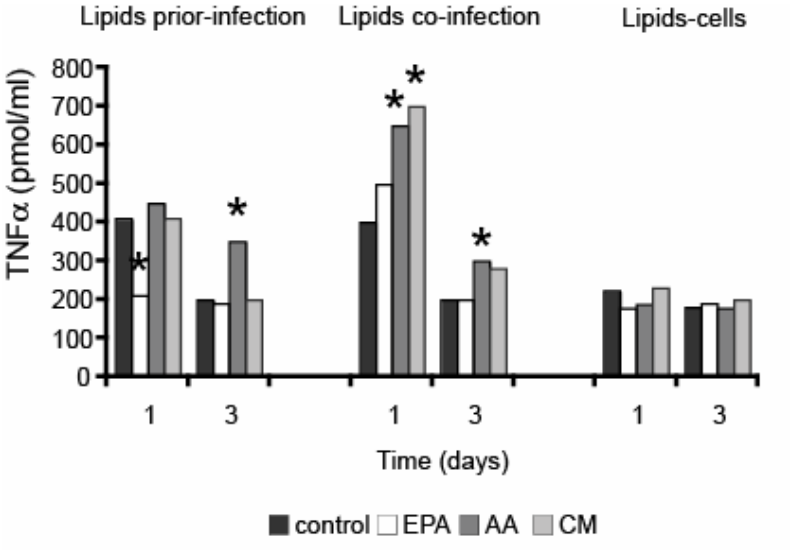

Figure 4. Effects of lipids on TNF-α pro inflammatory response in J774 cell cultures infected with *M. tuberculosis H37Rv*

The supernatants of the infected cultures either treated before infection with EPA, AA or Ceramide mix (CM) (preT) or treated post-tinfection with these lipids (postT) was assessed for

TNF alpha production. There's no effect of lipids observed in non-infected cells (cells) *P<0.05* (*).

In uninfected cells, a basal secretion level of TNF-α was detected (200 pmol/ml) and lipid treatment did not affect this level (Fig. 4 shown: Lipids control:cells). *M. tuberculosis* infection of macrophages treated with lipids induced secretion under specific conditions. Co-treatment with Cer, increased secretion of this pro-inflammatory cytokine while pre-treatment of macrophages prior infection with Cer had no effect. A similar increase in TNF-α was observed using AA. In contrast macrophages treatment with EPA prior to infection with *M. tuberculosis* had reduced TNF-α secretion (Fig. 4). In general these results support the notion that the pro-inflammatory lipids tend to increase TNF- α levels in the medium whereas the anti-inflammatory lipid EPA had the opposite effect. Moreover kinetics of TNF-α release was in good agreement with the killing pattern induced by these lipids in J774 infected macrophages (Figs. 2 and 3).

The links between lipids (ceramide and EPA) and p38 MAP kinase activity during *M. tuberculosis* infection.

Pro-inflammatory TNF-α downstream signalling events could lead to MAP Kinase activation. We and others had previously showed that p38 MAP Kinase is a crucial player in mycobacterial infections [4,50,51]. For this reason we decided to investigate a possible connection between *M. tuberculosis* survival profiles modulated by Cer, AA or EPA with p38 activation. When phosphorylated on serine residues this kinase becomes activated, a process that can be evaluated by immunoblotting against an antibody that recognises the phospho-p38. In uninfected cells, without lipid treatment or treated with EPA p38 activation was not detected during 5 days but both AA and Cer were able to activate this kinase. As early as 3h after addition of AA a strong activation of p38 in uninfected cells was detected. This signal persisted until 5days. The activation of p38 induced by Cer was slower, than with AA, showed a peak of activity after 3 days and a significant reduction after 5 days (Fig. 5A).

Interestingly, when J774 cells were infected with *M. tuberculosis* H37Rv and treated with these lipids coincidental with infection, there was no activation of p38 by AA or EPA. In contrast, Cer induced a significant activation of p38 after 3h, but by 3 days no activity could be detected. These data argue that the presence of *M. tuberculosis* in these

macrophages strongly inhibited the ability of AA and (after 3h) also Cer to activate p38 MAP Kinase (Fig. 5B). Collectively these data argue that the ability of Cer and AA to induce killing of *M. tuberculosis* [4] is independent of its ability to activate p38. Looked at from the perspective of the pathogen, although it completely blocks p38 under all conditions, it is still susceptible to killing by Cer and AA.

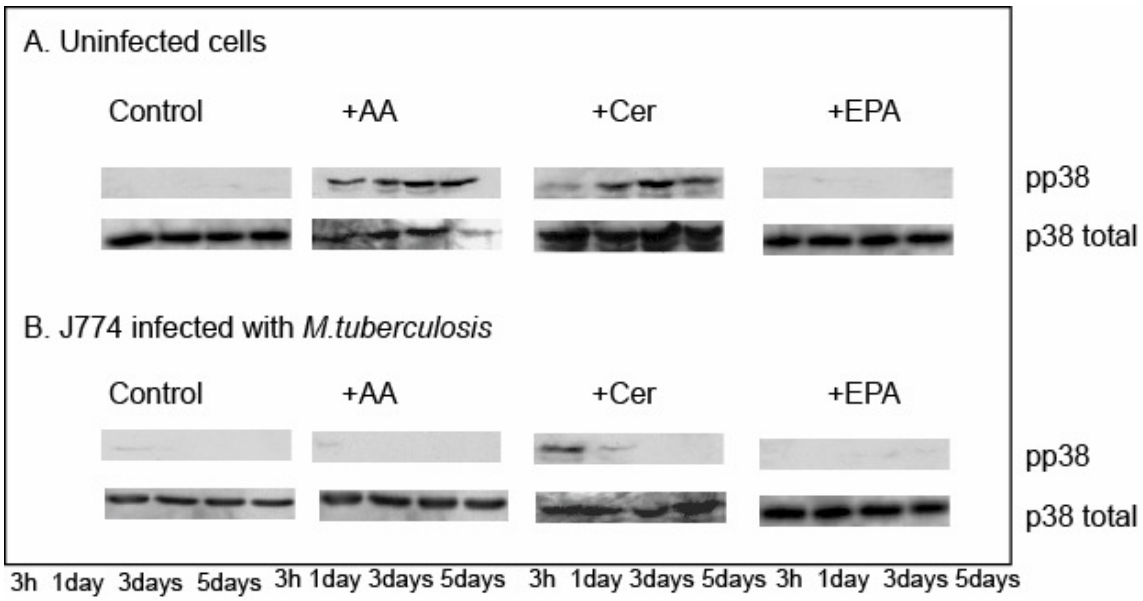

Figure 5. Lipid-induced phosphorylation of p38 in J774 macrophages during *M. tuberculosis* infection

(A) Western-blot for phospho-p38 and total p38 for uninfected macrophage not treated with lipids during 5 days (B) Western-blot for phospho-p38 and total p38 for macrophage infected with *M. tuberculosis* not treated with lipids up to 5 days

Effect of EPA, ceramide and AA on *M. smegmatis* growth in J774 macrophages

Given the complex effects of the three lipids on the infection with *M. tuberculosis* we decided to focus in more detail on the *M. smegmatis* model, in which the pro- and anti-inflammatory phases have been described in more detail [5].

Since our previous study with J774 cells and *M. smegmatis* had revealed the alternate phases of killing (1-4 h), growth (4-8 h) and then two distinct consecutive stages of killing (8-12 h; 12-24 h), we decided to test the effects of the pro-inflammatory lipids AA and Cer and the anti-inflammatory lipid EPA by adding them at those specific

stages of the infection. The rationale here being that a pro-inflammatory lipid might accentuate the effects of a pro-inflammatory phase (increasing killing) while it might reduce the rate of growth seen in the anti-inflammatory phases (and vice-versa for an anti-inflammatory lipid). In addition, a pro-inflammatory lipid might reverse a 'natural' anti-inflammatory phase while an anti-inflammatory one might dampen the pro-inflammatory phase killing.

We first added these lipids, at concentration optimised previously [4], at different time windows starting 1 h before infection, with the last period being from 16-24 h, a time in which the vast majority of bacteria are normally killed [5]. We then estimated CFU of bacteria after isolating them from cells after 24 h in all experiments. A highly heterogeneous response was seen for all lipids, with the same overall tendency seen earlier: EPA tended to stimulate growth and AA and Cer tended to induce killing of the bacteria (Fig. 6A).

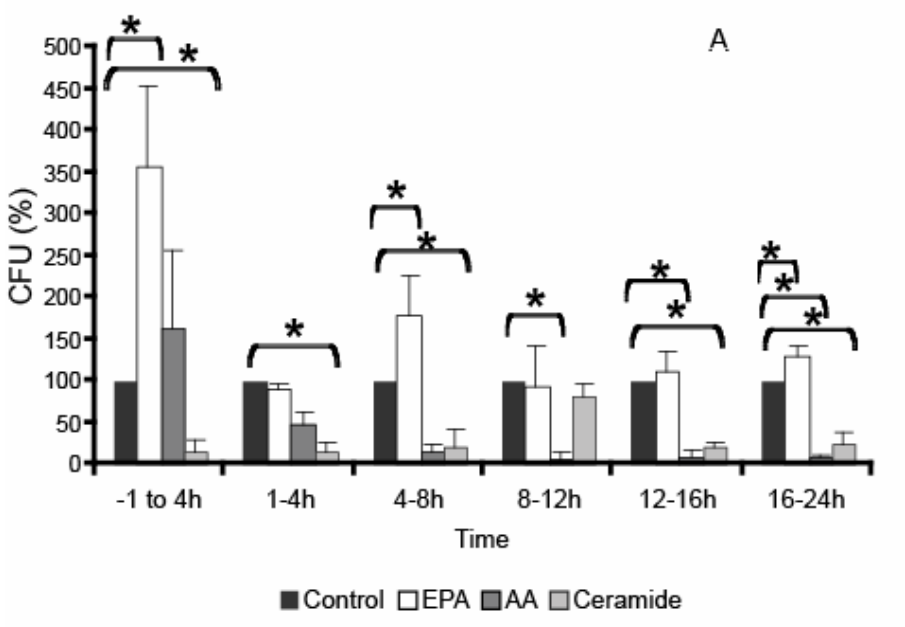

Figures 6 A. Persistence of *M. smegmatis* in J774 macrophages in culture supplemented whit specific fatty acids during distinct phases of intracellular killing cycles Effects of Arachidonic Acid (AA: 125 µM), Eicosapentaenoic Acid (EPA 15µM), or ceramide from a mix of brain ceramides (5 µg/ml) on killing of intracellular Mycobacterium. **(A)**

When the lipids were added 1 h before infection and left on the cultures until 4 h, EPA gave a 3.5 fold increase in CFU (after 24 h). When added only in a restricted time window corresponding to two killing phases, 4-8 h and 16-24 h, the addition of EPA

also increased bacterial growth, therefore suggesting that this lipid can reverse these pro-inflammatory stages into a bacterial growth stage. However, the addition of EPA at 1-4 h, 8-12 h and 12-16 h had no effect on the growth of bacteria by 24 h (Fig. 6A).

The striking effect seen in Fig. 6.A is the enormous increase in growth after 24 h when EPA is present only from -1 to 4 h. Since the 1-4 h addition had no effect, we conclude that one hour "priming" of the macrophages prior to infection has a strong anti-inflammatory effect on the cell. AA showed an effect only when added at time windows coincident with the second and third killing phases (8-12 h, 12-16 h and 16-24 h). This lipid significantly induced bacterial killing at this stages (Fig. 6A). In contrast the addition of Cer significantly increased killing at all stages *except* the 8-12 h stage. Notable was the inability of Cer to affect killing during 8-12 h, whereas AA was also effective during this period.

The same set of experiments was repeated by estimating CFU at the end of the period of adding the lipids; for example, if AA was added between 4 and 8 h, the bacterial growth *in vitro* was estimated after 8 h. With this experimental approach we tried to relate the changes in signalling due to the lipids with *M. smegmatis* survival in a time window of approximately one division time.

When EPA was tested in this way we saw a significant increase in bacterial growth at -1 to 4 h, a slight increase between 1- 4 h and between 16- 24 h but a significant increase in killing was seen between 12 and 16 h (Fig. 6B). This result provides evidence that in the 12-16 h period the cells are in a different signalling state to the 16-24 h period. When AA was tested a surprising result was that this lipid could significantly increase bacterial growth between -1 and 4 h and even more dramatically between 8 and 12 h (Fig. 6C). This latter result was highly paradoxical: AA added between 8 and 12 h significantly decreased total CFU estimated after 24 h (Fig. 6A) but, within this time window it stimulated the rate of bacterial growth five-fold (Fig. 6B).

The treatment of infected cells at the different times with Cer led to less dramatic effect in this assay (Fig. 6D). However, also here an unexpected result was seen. Whereas the treatment with Cer between 4-8 h led to a significant increase in killing after 24 h (Fig. 6A), it had no killing effect within this time-frame (Fig. 6D). These results unexpectedly argued that the tested lipids can all induce pro- or anti-inflammatory effects - depending on the cellular state of the macrophages during the infection cycle.

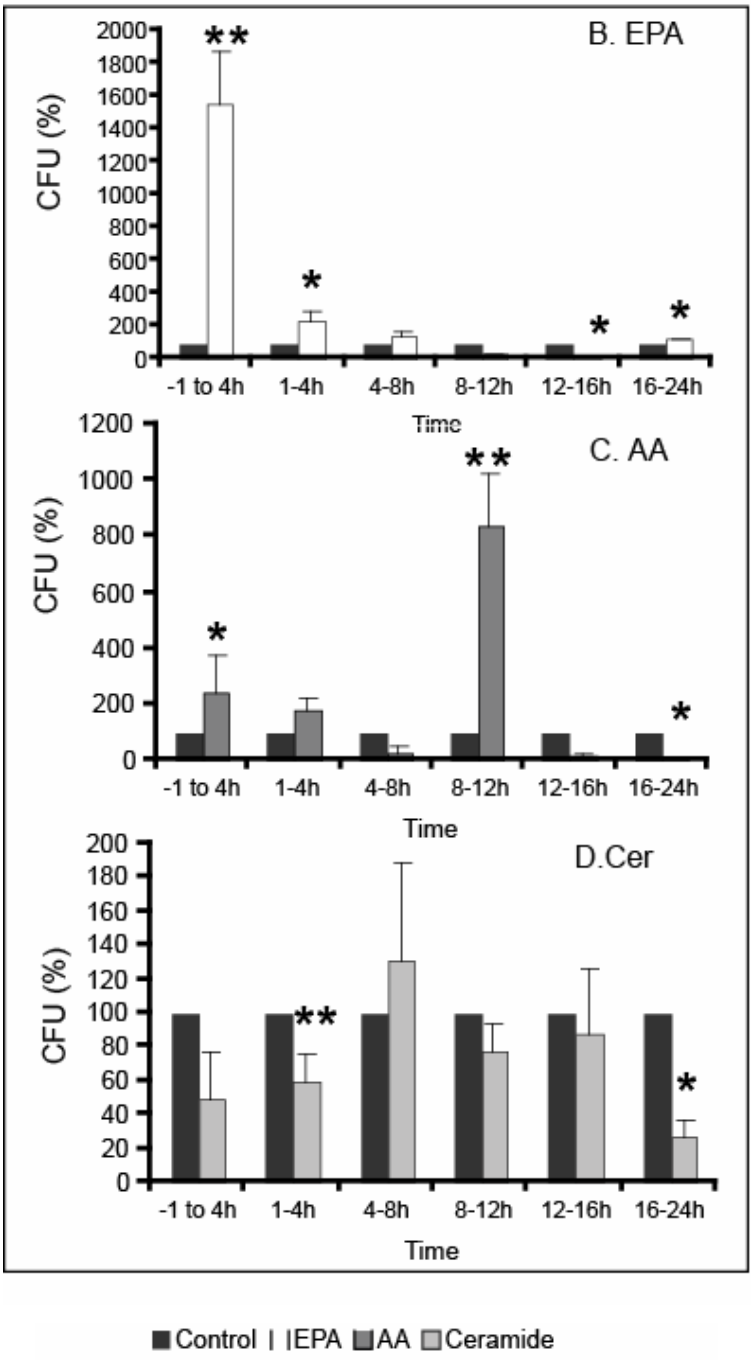

Figures 6 B-D. Persistence of *M. smegmatis* in J774 macrophages in culture supplemented whit specific fatty acids during distinct phases of intracellular killing cycles

(B) EPA, (**C**) AA, or (**D**) Cer were added in specific time windows to macrophages and bacteria were recovered for CFU plating at the end of lipid treatment, namely 4 h, 8 h, 12 h, 16 h and 24 h post-infection.

Pre-treatment of cells with EPA

Given that pre-treatment with EPA of cells for 1 h strongly facilitates *M. smegmatis* growth between 1-4 h and up to 24 h we asked what would happen if we pre-treated the

macrophages with EPA for 3 days before infection, as we had done for *M. tuberculosis*. We first followed bacterial survival during 24 h following the 3 days pre-treatment with EPA. As shown in Fig. 7A this treatment strengthened the first killing phase (1-4 h) but completely abolished the second (8-12 h) and third killing phases (16-24 h).

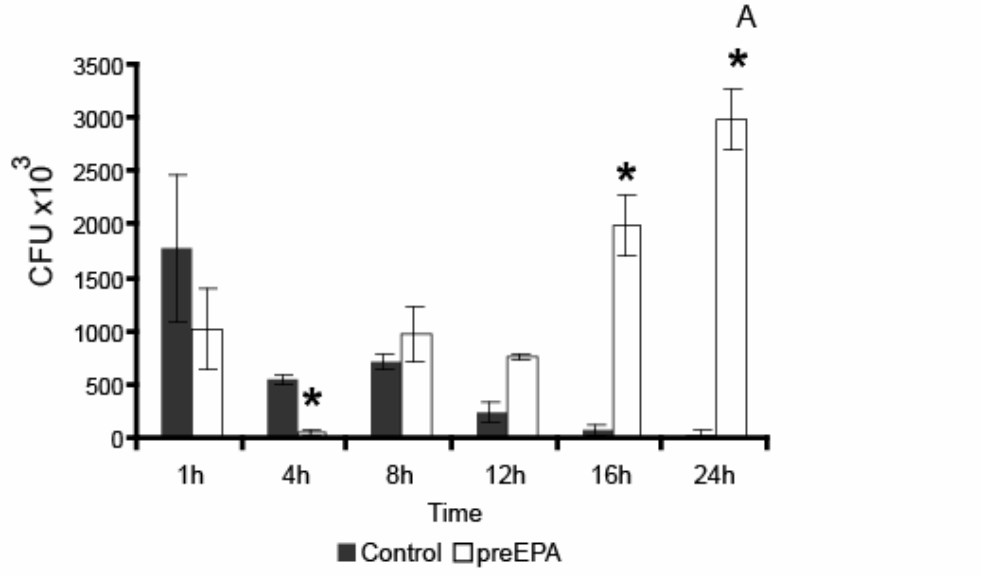

Figure 7A. Effects of EPA pre-treated macrophages prior to infection on the intracellular survival of *M. smegmatis*

Cultures of J774 macrophages were pre-treated from 3 days before infection with EPA. **(A)**

Since cells pre-treated with EPA for 1 h or 3 days behaved quite differently to untreated cells we next repeated the experiment in which Cer and EPA were also added at different time windows during bacteria infection after the 3 day pre-treatment with EPA. In the first experiments the CFU was estimated only after 24 h (Fig. 7B). Under this condition the addition of EPA between -1 and 4 h and 4-8 h significantly increased growth by 24 h, whereas the other time points showed no significant differences compared to the control (macrophages infected with *M. smegmatis* treated with EPA during 3 days before infection). For Cer an unexpected result was the finding that its addition in the 8-12 h period, that was refractory to Cer in cells not pre-treated with EPA (Fig. 6A), was now able to induce a significant killing of *M. smegmatis* (Fig. 7B). In contrast, at the 16-24 h stage, when Cer normally induces killing in the pre-EPA treated cells this stage was now refractory to killing by this lipid.

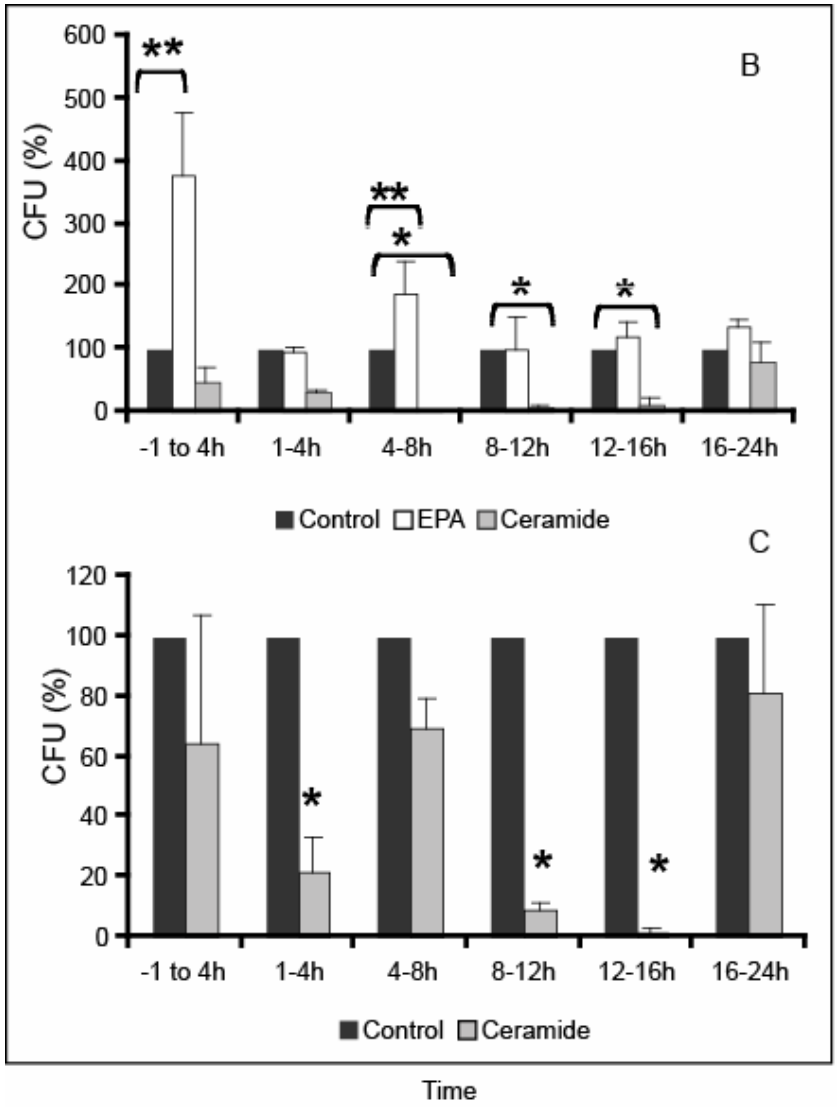

Figures 7 B and C. Effects of EPA pre-treated macrophages prior to infection on the intracellular survival of *M. smegmatis*

After infection DMEM medium was replaced without any supplement of lipids. Bacteria were recovered from infected macrophages for CFU counting following the time post-infection. **(B)** After infection DMEM medium was replaced supplemented either with more EPA or with ceramide. Bacteria were recovered for CFU counting 24 h post infection. **(C)** Effects of ceramide added at specific time windows to macrophages. Bacteria were recovered for CFU plating at the end of lipid treatment namely 4 h, 8 h, 12 h, 16 h and 24 h post-infection.

Another set of experiments was conducted as before, with the CFU estimated at the end of the period of lipid addition (Fig. 7C). Thus, after pre-treatment with EPA, Cer would be added for example between 1 and 4 h and the CFU estimated after 4 h. A striking result that emerged was that Cer treatment significantly increased the effectiveness of the 8-12 h (second) killing period whereas it had no effect when added without the EPA

pre-treatment (Fig. 7C and Fig. 6D). Conversely, whereas Cer induced killing between 16 and 24 h in the absence of pre-EPA treatment (Fig. 6D) the pre-treatment with EPA prevents Cer from having an effect during this period (Fig. 7C). Pre-treatment of cells for three days with EPA therefore completely re-programs the macrophage response to Cer in the context of *M. smegmatis* infection.

These experiments make it clear that the different time windows we analysed must represent functionally distinct macrophage signalling states, each with its own specific response to each lipid. Pre-treatment with EPA seems to set a different 'clock' in the macrophage.

The links between lipids (ceramide and EPA) and p38 Map kinase activity during *M. smegmatis* infection.

Since Cer mediated p38 activation could be linked to *M. tuberculosis* killing we decided to investigate this MAP kinase in the context of *M. smegmatis* infection. The above results show that Cer induced killing of *M. smegmatis* could be modulated by pre-treatment of the infected macrophages with EPA. In earlier published data we compared the kinetics of activation of p38 in cells infected with live or heat-killed *M. smegmatis* [52]. An intriguing difference was seen in that the killed bacteria induced a rapid activation of p38 that was essentially turned off by 1 h. In contrast, with the live bacteria the first activation was not seen until 2h. At 4 h, a period in which the system switches from a killing phase to a bacterial growth phase the p38 activity was repressed. However, a strong re-activation was seen at 8 h, followed by a low signal at the 24 h time point Fig. 8A [5].

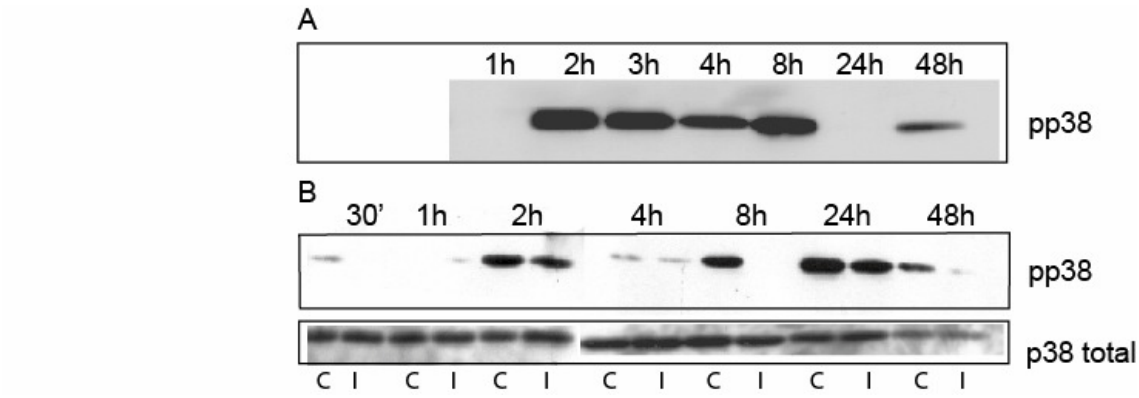

Figure 8. Ceramide-induced phosphorilation of p38 in J774 macrophages

(A) Western-blot for phospho-p38 for macrophage infected with *M. smegmatis* over the time

course. (B) After treatment with ceramide of non-infected cells (C: ceramide) or infected cells (I: infected) total proteins were probed anti phospho p38 and, after stripped reprobed with anti-tubulin antibody. Note the blocking on p38 phosphorilation at 8 h post infection in cells treated with ceramide. Every group of C I corresponds to ceramide treated cells vs ceramide treated cells and infected. The results shown are from three independent experiments.

Here, we first compared the kinetics of activation of p38 in response to Cer in uninfected cells and in cells infected with live *M. smegmatis* (Fig. 8B). In uninfected cells the addition of Cer induced a remarkable oscillatory pattern of p38 activation and de-activation. There was no activity until 2h, when the p38 activity peaked, followed by lower activity of the kinase at 4 h. A strong activation followed at 8 h, as well as at the 24 h time point, with a weak signal also at 48 h. A similar pattern was seen when Cer was added to *M. smegmatis*-infected cells with one notable exception: the p38-active 8 h time point seen in uninfected cells treated with Cer, as well as in untreated cells infected with *M. smegmatis,* was completely switched off when Cer was added to infected macrophages. The latter result suggested that one of the switches in the system, between the generally bacterial friendly 4-8 h phase and the bacteriocidal 8-12 h are controlled by p38, in such a way that it can be regulated by Cer. In agreement with this hypothesis was the observation that an inhibitor of p38 strongly inhibited the killing period 2 (8-12 h) [5].

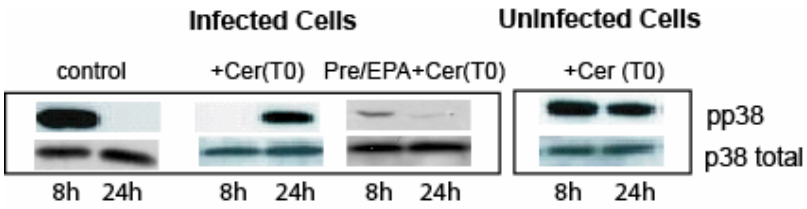

Figure 9. Differential lipid induced phosphorylation of p38 in J774 macrophages during *M. smegmatis* infection

Western-blot for phospho-p38 and total p38 of macrophages infected with *M. smegmatis* after 8 h and 24 h is shown. These macrophages did not receive lipid treatment (control) or received co-treatment with Cer in different conditions. Ceramide was either added to untreated macrophages (+Cer T0) or macrophages treated during 3 days with EPA (Pre/EPA+Cer T0). Western-blot for uninfected cells treated with ceramide after 8 and 24 h for phosphorylated and total forms of p38 is also shown.

In both uninfected and infected cells p38 phosphorylation was not induced by EPA addition (Results not shown). We next investigated Cer induced p38 activation in cells pre-treated for 3 days with EPA. In uninfected cells, EPA-pre-treatment allowed Cer to activate p38 at 8 h as well as at the 24 h time point. In contrast, in infected cells the ability of Cer to activate p38 was blocked after 8 h, and completely inhibited after 24 h (Fig. 9). This result argues that the anti-inflammatory effect of pre-treatment with EPA is in part due to its ability to antagonise the effect of Cer on p38 MAP Kinase activation.

DISCUSSION

In an earlier study [4] we found a striking effect whereby adding AA or Cer to cells infected with non-pathogenic and pathogenic mycobacteria significantly enhanced bacterial killing. Conversely, the fish oil lipids (especially EPA) significantly enhanced the intracellular growth of virulent strains of *M. tuberculosis*. The latter experiment leads to the interesting conclusion that even in (not classically activated) macrophages (in the absence of EPA), although the pathogen multiplies, its ability to do so is still repressed to some extent by the innate pro-inflammatory mechanisms of the macrophage. The overall anti-inflammatory properties of EPA tend to suppress these mechanisms, leading to more growth of the pathogen. The availability of human and animal data showing the same effect with *Salmonella* and *M. tuberculosis* (see Introduction) made it an attractive hypothesis that EPA, increasingly used as a human nutritional supplement, should be something avoided in humans infected with tuberculosis and other diseases. Dietary lipids are absorbed directly into the body (unlike proteins, polysaccharides and nucleic acids). This also made the alternative hypothesis, that pro-inflammatory lipids might have therapeutic effects against tuberculosis and related diseases, a more interesting hypothesis from a therapeutic perspective.

Our data with both *Salmonella* and *M. tuberculosis* in infected mice provided no support whatsoever for these hypotheses, with a trend seen towards the opposite results to what was predicted. These mice experiments are obviously open to many criticisms, including the debate as to whether mouse is, or is not a good model to study tuberculosis [53,54] and the fact that we used crude, rather than pure lipids. Due to the time-consuming aspect, and expense of these experiments, our data can only be considered as preliminary, in that only a limited set of conditions were tested. Nevertheless, our data fit nicely into a general pattern of unpredictable results with omega-3 lipids in animal models, as comprehensibly discussed by Anderson and Fritche [31].

Our macrophage level experiments provide a strong rationale for expecting the unpredictability of EPA, as well as for the pro-inflammatory AA and Cer. While the overall trend of the effects of these lipids were similar to our earlier study [4] by adding the lipids for more restricted periods all these lipids could induce a pro- or anti-inflammatory effect, depending on how and when they were added.

A recent, detailed analysis of the infection cycle of *M. smegmatis* in J774 cells gave us the first indication that, even with a mycobacterium that can eventually be briefly killed by macrophages the interaction between the live bacteria and its host induced a dynamic cycle of killing (pro-inflammatory) and growth (anti-inflammatory) phases. Theoretical modelling of the infection provided a plausible explanation why cyclical on/off killing phases can be more effective for killing than a one-shot program [5]. Having defined the periodicity of these phases in this system, our goal here was to ask how the pro-inflammatory AA and Cer, and the anti-inflammatory EPA could influence the system when added only at the pro- or the anti-inflammatory phases seen earlier [5], namely 1-4 h (pro) 4-8 h (anti), 8-12 h (pro) 12-24 h (pro). Our data here are fully consistent with the notion that these phases represent different signalling states of the macrophages. They also reveal that the 12-16 and 16-24 h periods are functionally distinct from each other, and in general pro-inflammatory (e.g. see Figs. 6A-D and 7B-C).

By adding the lipids only for a window of time corresponding to the above periods we found a striking effect on total killing/survival after 24 h. This first experiment (Fig. 6A) revealed that EPA only significantly increases *M. smegmatis* growth when added at 4-8 h. However, when EPA was added 1 h before infection, until 4 h, it induced a massive growth of the bacteria by 24 h. A comparison of Fig. 6A, with Fig. 6B, in which the lipids were added as for Fig. 6A but CFU were estimated directly at the end of the period of interest, revealed that the only time in which EPA could significantly induce growth was during the 1-4 h period (that was strictly dependent on the 1 h pre-addition of EPA). So, the 1-4 h period that normally represents a strong killing phase is switched to a strongly anti-inflammatory state by a 1 h pre-treatment with EPA. A longer pre-treatment with EPA was also able to stimulate growth at 4-8 h (Fig. 7A).

AA showed a pattern of effects that were quite different to EPA. When added only at the different stages and CFU collected after 24 h, it had potent killing-inducing properties at all times. However, if added from 1-4 h it did *not* induce killing, and showed a tendency to increase growth (Fig. 6A). This latter effect was more evident when the CFU were estimated at the end of the time period when AA was added (Fig. 6C). This experiment revealed two surprising findings. First, AA could not induce more killing during the first 1-4 h killing period (in contrast to Cer). More strikingly, the addition of AA during the second killing period (8-12 h) induced a striking increase in bacterial *growth* in this period (Fig. 6C). Thus, although AA addition at 8-12 h led to an overall increase in killing at 24 h it induced a 5-fold increase in growth between 8-12 h

relative to the un-treated control. This figure shows clearly that the killing effects of AA are restricted to 4-8 h, 12-16 h and 16-24 h.

The effects of the second pro-inflammatory lipid Cer were quite different to what was seen with AA. In Fig. 6A Cer induced a significant increase in killing after 24 h when it was added at any of the time periods tested, with one notable exception. When added during the 8-12 h period it had no effect on overall growth over 24 h. However, when the CFU were estimated at the end of the period of Cer addition, (Fig. 6D), there was a striking difference to what was observed with AA (Fig. 6C). Only when added 1-4 h or 16-24 h could it induce significantly more killing with a trend to reverse the killing between 4 and 8 h.

Given the striking effect of pre-treatment of cells with EPA it was interesting to ask how this treatment affected the response to Cer (Fig. 7B). Under this condition, the addition of Cer between 8-12 h, that had no effect without EPA pre-treatment (Fig. 6A) was able to induce a strong killing effect during this period, in effect enhancing the innate killing ability of the macrophage during this period. So the pre-treatment with EPA that strongly favours bacterial growth between 8 and 12 h (as well as between 12-16 and 16-24 h) induces Cer to become more pro-inflammatory. This experiment is one of many that we would cite in support of the utter unpredictability of the effects of these lipids, which are even more striking when used in combination.

The cyclical phase of killing/growth seen with *M. smegmatis* can also be seen during infection with *M. tuberculosis* and *M. bovis* (Jordao unpublished results). Here the length of the phases is longer than with *M. smegmatis*, observable over days, rather than hours, and presumably related to the longer doubling time of these bacteria (24 h) relative to *M. smegmatis* (3h). For these bacteria we carried out a more limited set of experiments to see how the addition of lipids during these different phases affected the pattern of growth or killing of *M. tuberculosis*. We first compared the effect of pre-treatment of cells with EPA, AA (Fig. 2A) or Cer (Fig. 3). Pre-treatment with EPA led to increased growth of *M. tuberculosis* up to 9 days infection whereas pre-treatment with AA had a striking effect in increasing killing. In contrast, pre-treatment with Cer showed no effects until after 3 days, with continued increase in killing until day 5. However, by day 7 a paradoxical increase in growth, relative to the untreated control was seen, again a striking example of unpredictability of the effects and the ability of lipid treatment to switch the inflammatory state of the macrophage.

When the lipids were added at the end of the 3 h infection period and left on the cultures, the pattern of effects was completely different to the pre-treatment. EPA showed a tendency to increase killing of *M. tuberculosis* after day 1 but it led to a five-fold increase in bacteria by day 3, with little effect thereafter (Fig. 2B). When AA was added post-infection it had a striking killing effect at all times (Fig. 2B). In this experiment Cer behaved similarly to AA, with a tendency for killing at all times.

Our data revealed that one of the key regulators of a number of the switches between the pro- and anti-inflammatory response that were influenced by EPA and Cer was p38 MAP Kinase. We had earlier described activity of these enzyme cycles in relation to *M. smegmatis* infection phases [48] and, using a p38 inhibitor, we provided evidence that the activity of p38 could facilitate either macrophage killing capacity, or the growth of *M. smegmatis* (8-12 h), depending on when the inhibitor was added. Our data here show that Cer inhibited the normal 8 h activation of p38 by *M. smegmatis*-infected cells. They also show that the pre-treatment of cells by EPA allows some activation of p38 by Cer, relative to cells only treated with Cer. More strikingly, the pre-EPA treatment blocks the ability of Cer to activate the system over 24 h (Fig. 1C). AA was also a potent stimulator of p38 in uninfected macrophages at periods from 3h to 5 days (Fig. 4).

The ability of pathogenic mycobacteria to block MAP Kinase, including p38 activity has been well documented [55-58] for *M. tuberculosis* and *M.avium*. We could confirm this result for *M. tuberculosis* at 24 h (Fig. 4). This inhibition could not be overcome by AA treatment at the start of infection nor, after 3 days infection when Cer was added; Cer could, however, transiently overcome the block transient between the 3h and 1day period. Since both AA and Cer are potent inducers of *M. tuberculosis* (and *M.avium*) killing over a 7-14 day period [4], when p38 is switched off, this argues clearly that p38 activation is not essential for these killing events. Thus, while p38 plays a crucial role in the killing and growth phases of *M.smegmati*s (up to 48 h) in macrophages, it deos not regulate the longer-term killing growth phases in the *M. tuberculosis*-infected macrophages.

We could, however, make a more positive molecular connection between the effects of EPA, AA and Cer to the pro-and anti-inflammatory responses in *M. tuberculosis*-infected macrophages when we investigated TNF-α release. As mentioned, the synthesis and release of this cytokine tends to correlate with pathogenicity, with non-pathogens inducing higher release than the pathogens. High TNF-α secretion leads to the activation of signalling by its receptor that somehow facilitates killing. We found that after pre-

treatment with EPA, there was less TNF-α released whereas pre-treatment with AA, but not Cer, induced more secretion of TNF-α after day 3. Post-infection treatment with EPA had no effect while post-treatment with both AA and Cer significantly increased TNF-α level at day 1. These data argue that synthesis or secretion of TNF-α is one mechanism that is targeted by EPA, AA and Cer. The mechanism by which TNF-α facilitates mycobacterial killing is still to be defined.

An interesting picture emerges from this work. The infection of macrophages with live non-pathogenic (or pathogenic) mycobacteria induces a dynamical system that switches, clock-like from pro-to-anti-to-pro-inflammatory signalling states, including two consecutive, but differently regulated killing phases (12-16 h and 16-24 h). Overall, the pro-state facilitates host killing while the anti-state facilitates pathogen survival and growth. Specific and reproducible albeit unpredictable and often counter-intuitive effects of EPA, Cer and AA could be observed in switching one state into the other. We will need to understand the networking properties of the signalling networks in order to interpret these switches, which is currently beyond our means. Given the complexity of the responses at the macrophage level, it seems difficult to imagine a clear rationale for suggesting a lipid-diet that could lead to a potential therapy against *M. tuberculosis*, or for making any conclusions as to whether the omega-3 lipids should be avoided in the diet.

Acknowledgements

We thank Cecília Rodrigues group for technical assistance and Maximilliano Gutierrez, Luiz Mayorga and Sabrina Marion for their constructive discussion. This work was financed by a grant of the National Foundation for Science-FCT with co-participation of FEDER project POCI/BIA-BCM/55327/2004. Luisa Jordao was funded as a PhD fellow by FCT SFRH/BD/14284/2003.

MATERIALS AND METHODS

Bacterial strain and growth conditions: The virulent *Salmonella enterica* serovar Typhimurium strain ATCC 14028 was routinely grown at 37°C in brain heart infusion (BHI) broth or agar (Difco). For challenge studies, bacteria were grown in 250 ml Erlenmeyer flasks at 37°C with gentle shaking (50 rpm) until they reach an OD_{600} of approximately 0.8 (middle exponential growth phase). Then, they were harvested by centrifugation (3,000 x *g*) and resuspended in 5% bicarbonate buffer. The number of viable bacteria was evaluated by plating serially diluted samples on BHI agar plates.
M. smegmatis mc^2155 was grown in medium containing Middlebrook's 7H9 broth Medium (Difco), Nutrient broth (Difco) (4.7 g and 5 g per litre, respectively), supplemented with 0.5% glucose and 0.05% Tween 80 at 37°C on a shaker at 220 r.p.m. Bacteria were subcultured every day in fresh medium for 7–10 days before use in infection studies. *M. tuberculosis* H37Rv was grown in Middlebrock 7H9 medium (Difco) and was maintained as described before [4]. For CFU experiments bacteria was platted on Middlebrook's 7H10. All *M. tuberculosis* culture conditions where supplemented with 10% OADC (Difco).

Animals and diets: All investigations involving animals were conducted in conformity with Public Health Service Policy on Human Care and Use of Laboratory Animals, incorporated in the Institute for Laboratory Animal Research Guide for Care and Use of Laboratory Animals. All investigations were approved by appropriate National Institutional Committees.
For *Salmonella* infection, female BALB/c ($H\text{-}2^d$) mice (10 weeks old) were purchased from Harlan-Winkelmann GmbH (Borchen, Germany) and treated according to local and European Community guidelines. Animals received a fat-free diet for one week, then, they were divided into three groups, which received the following diets: (i) 3.5 % of soy oil (normal fat content), (ii) 10 % of sunflower oil (i.e., omega 6), and (iii) 10 % of menhaden oil (i.e., omega 3). Food lots were fractioned and conserved at 4°C, and the food pellets were changed daily to preserve lipid content and properties.
For *M. tuberculosis* infection, 6-8 week old female BALB/c mice were fed with low fat diet supplemented or not with 10 % safflower oil (i.e., omega 6), or 10 % Ropufa (i.e., omega 3). Special diets started 2 weeks before infection and were maintained during the course of infection.

Challenge experiments: After five weeks on the fat-specific diets, mice were gently feed with a suspension of the *S. enterica* serovar Typhimurium strain ATCC 14028 in bicarbonate buffer (20 µl containing $5x10^6$ bacteria/mouse; lethal dose 50 (LD_{50}) by oral route $4.2x10^5$). To evaluate bacterial invasion, survival and *in vivo* dissemination, three mice from each group were sacrificed by CO_2 inhalation on days 3 and 7. Spleen, liver, Peyer's Patches and mesenteric lymph nodes were aseptically removed, weighed and homogenized in sterile PBS. The number of viable bacteria present in the organs was determined by plating appropriate dilutions on BHI agar plates. The results were expressed as number of CFU/g of tissue.

For *M. tuberculosis* H37Rv experiments, after two weeks receiving fat specific diets, mice were infected intranasally with 10^3 CFU of bacilli. Five mice were used per time-point. One, 21, and 63 days after infection, mice were sacrificed and lungs and spleen were collected, homogenized and serial dilutions of homogenates were plated onto 7H11 agar medium. Plates were incubated for at 37°C for 3 weeks and CFU were scored.

For *M. tuberculosis* H37Rv experiments, after two weeks receiving fat specific diets, mice were infected intranasally with 10^3 CFUs of bacilli. Five mice were used per time-point. One, 21, and 63 days after infection, mice were sacrificed and lungs and spleen were collected, homogeneized and serial dilutions of homogeneates were plated onto 7H11 agar medium. Plates were incubated for at 37°C for 3 weeks and CFUs were scored.

Cell line, macrophage infection and survival experiments: The mouse macrophage cell line J774A.1 was cultured as described previously [4]. Bacterial cultures in exponential growth phase were pelleted, washed twice in PBS pH 7.4 and re-suspended in DMEM medium. Clumps of bacteria were removed by ultrasonic treatment of bacteria suspensions in a ultrasonic water bath for 15 min followed by a low speed centrifugation (120 *g*) for 2 min. Single cell suspension was verified by light microscopy.

J774 cells were seeded onto 24 well tissue culture plates at a density of $0.5x10^5$ cells per well and were incubated for 2 days until 90% confluency and infected with bacteria. To achieve more than five bacilli per macrophage after 1 h uptake, a multiplicity of

infection of 100:1 was used (OD600 □0.1). In each experiment using *M. smegmatis*, after 1 h infection gentamicin (10 µg ml−1) was added in order to prevent extracellular multiplication of the remaining non-uptaked bacteria (Anes et al., 2006). Intracellular viable bacteria were recovered from infected macrophages as described in Anes *et al*., 2006 [5]. A similar procedure was used *for M. tuberculosis* but instead of 1 h uptake we used 3h uptake.In all experiments described the errors reported are the standard deviations from at least three separate experiments. For all lipid treatments the stock lipids were dissolved in ethanol (1mg/ml). In all experiments the lipid at the following empirically determined optimal final concentrations: 125µM AA, 15µM EPA, 5µM Cer (mixture of bovine brain ceramides; all from Sigma) Solvent without lipids was routinely tested. TNF-α was assessed in culture supernatants following the mouse Quantitine TNF-α kit instructions from R&D.

Preparation of whole cell extracts and immunoblot analysis: When needed lipid treatment was performed as described under *Cell line, macrophage infection and survival experiments.* Cells where washed twice with PBS and lysed in IP buffer (50 mM Tris pH 7.5, 150 mM sodium chloride, 1 mM EDTA, 1 mM EGTA, 1% NP-40 and protease inhibitors) at 4°C for 30 min. The extracts were sonicated in 5 s bursts until complete homogenization and centrifuged at 13000 *g* for 10 min to remove cell debris. Equal amounts of protein were loaded on a 12% SDS-PAGE, transferred to nitrocellulose membrane and probed with a rabbit antiphospho p38 and anti total p38 (Cell Signaling Technology). Enhanced chemi-luminescence (Pierce biotechnology) was used to visualize antibody binding. Total p38 was used to assess the amount of total protein in the different membrane isolates.

Statistical analysis: The statistical significance of the differences observed in bacterial loads was analyzed by the Student's *t*-test, whereas those from the mice survival studies were analyzed using the logrank test. Differences were considered significant at $P<0.05$.

REFERENCE LIST

1. Kusner,D.J. Mechanisms of mycobacterial persistence in tuberculosis. *Clin. Immunol* **114**, 239-247 (2005).

2. Russell,D.G. *Mycobacterium tuberculosis*: here today, and here tomorrow. *Nat. Rev. Mol. Cell Biol.* **2**, 569-577 (2001).

3. Vergne,I., Chua,J., Singh,S.B. & Deretic,V. Cell biology of mycobacterium tuberculosis phagosome. *Annu. Rev. Cell Dev. Biol.* **20**, 367-394 (2004).

4. Anes,E. *et al.* Selected lipids activate phagosome actin assembly and maturation resulting in killing of pathogenic mycobacteria. *Nat. Cell Biol.* **5**, 793-802 (2003).

5. Anes,E. *et al.* Dynamic life and death interactions between *Mycobacterium smegmatis* and J774 macrophages. *Cell Microbiol.* **8**, 939-960 (2006).

6. Kuehnel,M.P. *et al.* Characterization of the intracellular survival of *Mycobacterium avium ssp*. paratuberculosis: phagosomal pH and fusogenicity in J774 macrophages compared with other mycobacteria. *Cell Microbiol.* **3**, 551-566 (2001).

7. Armstrong,J.A. & Hart,P.D. Response of cultured macrophages to *Mycobacterium tuberculosis*, with observations on fusion of lysosomes with phagosomes. *J Exp. Med.* **134**, 713-740 (1971).

8. Clemens,D.L. & Horwitz,M.A. Characterization of the *Mycobacterium tuberculosis* phagosome and evidence that phagosomal maturation is inhibited. *J Exp. Med.* **181**, 257-270 (1995).

9. Russell,D.G. *Mycobacterium tuberculosis* and the four minute phagosome. *ASM News* **71**, 459-463 (2005).

10. Sturgill-Koszycki,S. *et al.* Lack of acidification in *Mycobacterium* phagosomes produced by exclusion of the vesicular proton-ATPase. *Science* **263**, 678-681 (1994).

11. Yates,R.M., Hermetter,A. & Russell,D.G. The kinetics of phagosome maturation as a function of phagosome/lysosome fusion and acquisition of hydrolytic activity. *Traffic.* **6**, 413-420 (2005).

12. Jahraus,A. *et al.* ATP-dependent membrane assembly of F-actin facilitates membrane fusion. *Mol. Biol. Cell* **12**, 155-170 (2001).

13. Kalamidas,S.A. *et al.* cAMP synthesis and degradation by phagosomes regulate actin assembly and fusion events: consequences for mycobacteria. *J Cell Sci* **119**, 3686-3694 (2006).

14. Kjeken,R. *et al.* Fusion between phagosomes, early and late endosomes: a role for actin in fusion between late, but not early endocytic organelles. *Mol. Biol. Cell* **15**, 345-358 (2004).

15. Chang,H.R. *et al.* Fish oil decreases natural resistance of mice to infection with *Salmonella typhimurium*. *Metabolism* **41**, 1-2 (1992).

16. Mayatepek,E. *et al.* Influence of dietary (n-3)-polyunsaturated fatty acids on leukotriene B4 and prostaglandin E2 synthesis and course of experimental tuberculosis in guinea pigs. *Infection* **22**, 106-112 (1994).

17. Paul,K.P. *et al.* Influence of n-6 and n-3 polyunsaturated fatty acids on the resistance to experimental tuberculosis. *Metabolism* **46**, 619-624 (1997).

18. Kaplan,G.J., Fraser,R.I. & Comstock,G.W. Tuberculosis in Alaska, 1970. The continued decline of the tuberculosis epidemic. *Am. Rev. Respir. Dis.* **105**, 920-926 (1972).

19. Kromann,N. & Green,A. Epidemiological studies in the Upernavik district, Greenland. Incidence of some chronic diseases 1950-1974. *Acta Med. Scand.* **208**, 401-406 (1980).

20. CHRISTENSEN,P.E. *et al.* An epidemic of measles in southern Greenland, 1951; measles in virgin soil. III. Measles and tuberculosis. *Acta Med. Scand.* **144**, 450-454 (1953).

21. Dyerberg,J. & Bang,H.O. Haemostatic function and platelet polyunsaturated fatty acids in Eskimos. *Lancet* **2**, 433-435 (1979).

22. Calder,P.C. Dietary modification of inflammation with lipids. *Proc. Nutr. Soc.* **61**, 345-358 (2002).

23. Calder,P.C. Use of fish oil in parenteral nutrition: Rationale and reality. *Proc. Nutr. Soc.* **65**, 264-277 (2006).

24. La Guardia,M. *et al.* Omega 3 fatty acids: biological activity and effects on human health. *Panminerva Med.* **47**, 245-257 (2005).

25. Suchner,U., Kuhn,K.S. & Furst,P. The scientific basis of immunonutrition. *Proc. Nutr. Soc.* **59**, 553-563 (2000).

26. He,K. & Song,Y. Risks and benefits of omega 3 fats: a few thoughts on systematic review. *BMJ* **332**, 915-916 (2006).

27. He,K. *et al.* Risks and benefits of seafood consumption. *Am. J Prev. Med.* **30**, 440-441 (2006).

28. Horrobin,D., Fokkema,M.R. & Muskiet,F.A. The effects on plasma, red cell and platelet fatty acids of taking 12 g/day of ethyl-eicosapentaenoate for 16 months: dihomogammalinolenic, arachidonic and docosahexaenoic acids and relevance to Inuit metabolism. *Prostaglandins Leukot. Essent. Fatty Acids* **68**, 301-304 (2003).

29. Mori,T.A. & Beilin,L.J. Omega-3 fatty acids and inflammation. *Curr. Atheroscler. Rep.* **6**, 461-467 (2004).

30. Siddiqui,R.A. *et al.* Omega 3-fatty acids: health benefits and cellular mechanisms of action. *Mini. Rev. Med. Chem.* **4**, 859-871 (2004).

31. Anderson,M. & Fritsche,K.L. (n-3) Fatty acids and infectious disease resistance. *J Nutr.* **132**, 3566-3576 (2002).

32. Blok,W.L., Katan,M.B. & van der Meer,J.W. Modulation of inflammation and cytokine production by dietary (n-3) fatty acids. *J. Nutr.* **126**, 1515-1533 (1996).

33. Clouva-Molyvdas,P., Peck,M.D. & Alexander,J.W. Short-term dietary lipid manipulation does not affect survival in two models of murine sepsis. *JPEN J Parenter. Enteral Nutr.* **16**, 343-347 (1992).

34. Anes,E. *et al.* Dynamic life and death interactions between *Mycobacterium smegmatis* and J774 macrophages. *Cell Microbiol.* **8**, 939-960 (2006).

35. Defacque,H. *et al.* Involvement of ezrin/moesin in de novo actin assembly on phagosomal membranes. *EMBO J* **19**, 199-212 (2000).

36. Defacque,H. *et al.* Phosphoinositides regulate membrane-dependent actin assembly by latex bead phagosomes. *Mol. Biol. Cell* **13**, 1190-1202 (2002).

37. Emans,N., Nzala,N.N. & Desjardins,M. Protein phosphorylation during phagosome maturation. *FEBS Lett.* **398**, 37-42 (1996).

38. Medvedev,A.E., Blanco,J.C., Qureshi,N. & Vogel,S.N. Limited Role of Ceramide in Lipopolysaccharide-mediated Mitogen-activated Protein Kinase Activation, Transcription Factor Induction, and Cytokine Release. *J. Biol. Chem.* **274**, 9342-9350 (1999).

39. Sirkar,M. & Majumdar,S. Lipoarabinomannan-induced cell signaling involves ceramide and mitogen-activated protein kinase. *Clin. Diagn. Lab Immunol* **9**, 1175-1182 (2002).

40. Westwick,J.K., Bielawska,A.E., Dbaibo,G., Hannun,Y.A. & Brenner,D.A. Ceramide activates the stress-activated protein kinases. *J Biol. Chem.* **270**, 22689-22692 (1995).

41. Marchesini,N. & Hannun,Y.A. Acid and neutral sphingomyelinases: roles and mechanisms of regulation. *Biochem. Cell Biol.* **82**, 27-44 (2004).

42. Yaqoob,P. Lipids and the immune response. *Curr. Opin. Clin. Nutr. Metab Care* **1**, 153-161 (1998).

43. Baumruker,T., Bornancin,F. & Billich,A. The role of sphingosine and ceramide kinases in inflammatory responses. *Immunol Lett.* **96**, 175-185 (2005).

44. Flesch,I.E., Hess,J.H., Oswald,I.P. & Kaufmann,S.H. Growth inhibition of *Mycobacterium bovis* by IFN-gamma stimulated macrophages: regulation by

endogenous tumor necrosis factor-alpha and by IL-10. *Int Immunol* **6**, 693-700 (1994).

45. Hirsch,C.S., Ellner,J.J., Russell,D.G. & Rich,E.A. Complement receptor-mediated uptake and tumor necrosis factor-alpha-mediated growth inhibition of *Mycobacterium tuberculosis* by human alveolar macrophages. *J Immunol* **152**, 743-753 (1994).

46. Kindler,V., Sappino,A.P., Grau,G.E., Piguet,P.F. & Vassalli,P. The inducing role of tumor necrosis factor in the development of bactericidal granulomas during BCG infection. *Cell* **56**, 731-740 (1989).

47. Manca,C. *et al. Mycobacterium tuberculosis* CDC1551 induces a more vigorous host response in vivo and in vitro, but is not more virulent than other clinical isolates. *J Immunol* **162**, 6740-6746 (1999).

48. Lee,S.B. & Schorey,J.S. Activation and mitogen-activated protein kinase regulation of transcription factors Ets and NF-kappaB in *Mycobacterium*-infected macrophages and role of these factors in tumor necrosis factor alpha and nitric oxide synthase 2 promoter function. *Infect Immun.* **73**, 6499-6507 (2005).

49. Faldt,J., Dahlgren,C. & Ridell,M. Difference in neutrophil cytokine production induced by pathogenic and non-pathogenic mycobacteria. *APMIS* **110**, 593-600 (2002).

50. Roach,S.K. & Schorey,J.S. Differential regulation of the mitogen-activated protein kinases by pathogenic and nonpathogenic mycobacteria. *Infect. Immun.* **70**, 3040-3052 (2002).

51. Yadav,M., Roach,S.K. & Schorey,J.S. Increased Mitogen-Activated Protein Kinase Activity and TNF-{alpha} Production Associated with *Mycobacterium smegmatis*- but Not *Mycobacterium avium*-Infected Macrophages Requires Prolonged Stimulation of the Calmodulin/Calmodulin Kinase and Cyclic AMP/Protein Kinase A Pathways. *J Immunol* **172**, 5588-5597 (2004).

52. Anes,E. *et al.* Dynamic life and death interactions between *Mycobacterium smegmatis* and J774 macrophages. *Cell Microbiol.* **8**, 939-960 (2006).

53. Flynn,J.L. Lessons from experimental *Mycobacterium tuberculosis* infections. *Microbes Infect* **8**, 1179-1188 (2006).

54. Pozos,T.C. & Ramakrishnan,L. New models for the study of *Mycobacterium*-host interactions. *Curr. Opin. Immunol* **16**, 499-505 (2004).

55. Anes,E. *et al.* Dynamic life and death interactions between *Mycobacterium smegmatis* and J774 macrophages. *Cell Microbiol.* **8**, 939-960 (2006).

56. Roach,S.K. & Schorey,J.S. Differential regulation of the mitogen-activated protein kinases by pathogenic and nonpathogenic mycobacteria. *Infect. Immun.* **70**, 3040-3052 (2002).

57. Yadav,M., Roach,S.K. & Schorey,J.S. Increased mitogen-activated protein kinase activity and TNF-alpha production associated with *Mycobacterium smegmatis*- but not *Mycobacterium avium*-infected macrophages requires prolonged stimulation of the calmodulin/calmodulin kinase and cyclic AMP/protein kinase A pathways. *J Immunol* **172**, 5588-5597 (2004).

58. Yadav,M., Clark,L. & Schorey,J.S. Macrophage's proinflammatory response to a mycobacterial infection is dependent on sphingosine kinase-mediated activation of phosphatidylinositol phospholipase C, protein kinase C, ERK1/2, and phosphatidylinositol 3-kinase. *J Immunol* **176**, 5494-5503 (2006).

Chapter 5

Final remarks

A better understanding of mycobacteria interaction with the host cell could provide valorous tools for TB treatment. Although mycobacteria interference with host defence is well documented the molecular mechanisms underlying it are poorly elucidated. Our knowledge of the exact position occupied by mycobacteria phagosome in the endosomal continuum as well as its luminal and membrane composition is also scarce.

While it is consensual that mycobacteria uptake triggers several defence mechanisms the relevance of each one in infection resolution is not. For example, phagosome maturation into phagolysosome is pointed as a key mechanism in pathogen clearance so the ability of pathogenic mycobacteria to avoid it is seen as crucial for their success. Nevertheless, other mechanisms such as RNI and ROI production are regarded as minor players in mycobacterial infection clearance.

All together our data show that mycobacteria uptake triggers a complex macrophage defence program in which different bactericidal mechanisms are sequentially activated. The mechanisms and the order in which they are activated are independent of the mycobacteria uptaken. In the early stage of infection NO plays a crucial role in mice macrophages but it is absent both in human and bovine macrophages. Although mycobacteria killing can occur in immature phagosomes it is more efficient in acidified compartments probably due to synergistic effects with proteases and RNI. Since all mycobacteria are exposed to the same defence program and have different fates their pathogenicity play an important role. Pathogenic mycobacteria are more resistant to effectors molecules as NO and protons.

When macrophages were fed with heat killed mycobacteria we faced a completely different scenario. Although these bacteria are more efficiently uptaken they trigger a weaker production of NO and RNI, produce a different pattern of p38 MAP kinase and lack the ability to avoid phagosome maturation into phagolysosome. These results suggest that further studies to elucidate the differential mechanisms of live/dead mycobacteria uptake are needed. The analysis of both host and mycobacteria up and down regulated in both conditions can also provide clues for further elucidation of this enigma.

In the present study we clearly show that intracellular mycobacteria live in membrane surrounded compartments at all stages of infection. This observation is valid for all host macrophage and mycobacteria strains used regardless of host and mycobacteria virulence. Nevertheless, mycobacteria phagosome is a complex and dynamic structure

that acquires and recycles a vast number of phagosome maturation markers during its lifetime. The acquisition of most of these markers is regulated by the p38 MAP kinase. This kinase plays an important role in the regulation of actin assembly by phagosome membrane which is important for phagosome maturation and mycobacteria killing. It was also shown that the activity of this kinase could be modulated by dietary lipids.

All the lipids that enhance p38 activation increase mycobacteria killing and lipids that block this kinase activity enhance mycobacteria survival at the macrophage level. Nevertheless, when we step-forward in complexity moving from a cellular model to an animal (model) we could not confirm our prediction. Several factors such as the use of lipid sources instead of raw lipids, amount of lipid effectively delivered to the target organ and/or cell, genetic background of the animal model, conditions of mycobacteria infection and others contribute for this disappointing result. Nevertheless it also clearly showed us the need to establish a model of intermediate complexicity for example comprising different cells known to play an important role in tuberculosis. The most obvious system would be formed by macrophages and dendritic cells the most important effector and presenting cell in tuberculosis pathogenesis. Another alternative would be a more efficient delivery of lipids to target organs and cells modifying their distribution in the animal model. This goal could be accomplished by using liposome or nanosome formulations of lipids that present as a plus the possibility of enhancing lipid stability by including anti-oxidants.